

การประเมินประสิทธิผลของวิธีการดึงคลอไรด์ออกด้วยวิธีทางไฟฟ้าเคมีในคอนกรีตเสริมเหล็ก

MISS HAI YEN THI NGUYEN

วิทยานิพนธ์นี้เป็นส่วนหนึ่งของการศึกษาตามหลักสูตรปริญญาวิศวกรรมศาสตรมหาบัณฑิต

สาขาวิชาวิศวกรรมโยธา ภาควิชาวิศวกรรมโยธา

คณะวิศวกรรมศาสตร์จุฬาลงกรณ์มหาวิทยาลัย

ปีการศึกษา 2555

ลิขสิทธิ์ของจุฬาลงกรณ์มหาวิทยาลัย

บทคัดย่อและแฟ้มข้อมูลฉบับเต็มของวิทยานิพนธ์ตั้งแต่ปีการศึกษา 2554 ที่ให้บริการในคลังปัญญาจุฬาฯ (CUIR)

เป็นแฟ้มข้อมูลของนิสิตเจ้าของวิทยานิพนธ์ที่ส่งผ่านทางบัณฑิตวิทยาลัย

The abstract and full text of theses from the academic year 2011 in Chulalongkorn University Intellectual Repository(CUIR)
are the thesis authors' files submitted through the Graduate School.

EFFECTIVENESS EVALUATION OF ELECTRO-CHEMICAL
CHLORIDE EXTRACTION IN REINFORCED CONCRETE

MISS HAI YEN THI NGUYEN

A Thesis Submitted in Partial Fulfillment of the Requirements
for the Degree of Master of Engineering Department of Civil Engineering

Faculty of Engineering

Chulalongkorn University

Academic Year 2012

Copyright of Chulalongkorn University

HAI YEN THI NGUYEN:

การประเมินประสิทธิผลของวิธีการดึงคลอไรด์ออกจากด้วยวิธีทางไฟฟ้าเคมีในคอนกรีตเสริมเหล็ก

(EFFECTIVENESS EVALUATION OF ELECTROCHEMICAL CHLORIDE EXTRACTION IN REINFORCED CONCRETE). อ.ที่ปรึกษาวิทยานิพนธ์หลัก: ผศ. ดร.วิฑิต ปานสุข,

อ.ที่ปรึกษาวิทยานิพนธ์ร่วม: ดร.ภักวดีณ์ แสนเจริญ, 115 หน้า.

การซ่อมแซมโครงสร้างคอนกรีตเสริมเหล็กที่เกิดสนิมเนื่องจากคลอไรด์ถือเป็นปัญหาที่สำคัญปัญหาหนึ่ง การดึงคลอไรด์ออกจากคอนกรีตด้วยวิธีทางไฟฟ้าเคมี (Electrochemical chloride extraction, ECE) ถือเป็นวิธีหนึ่งที่สามารถซ่อมแซมโครงสร้างที่เกิดสนิมเนื่องจากคลอไรด์ได้ อย่างไรก็ตามประสิทธิภาพของวิธีการดังกล่าวยังคงควรได้รับการศึกษาเพิ่มเติม

โดยเฉพาะในการใช้งานกับคอนกรีตที่มีการใช้งานวัสดุผสมเพิ่ม

และคอนกรีตที่มีความคงทนต่อสิ่งแวดล้อมทะเลตามมาตรฐาน ACI 318

เช่นคอนกรีตที่มีอัตราส่วนน้ำต่อวัสดุประสานต่ำ ในการศึกษาได้ทดลองการใช้งาน ECE

กับคอนกรีตที่ใช้ปูนซีเมนต์ล้วน คอนกรีตที่ใช้เถ้าลอยแทนที่ซีเมนต์ร้อยละ 30 โดยน้ำหนัก

และคอนกรีตที่ใช้เถ้าลอยร้อยละ 25 และผงฝุ่นหินปูนร้อยละ 5 แทนที่ซีเมนต์โดยน้ำหนัก

โดยอัตราส่วนน้ำต่อวัสดุประสานจะอยู่ที่ 0.4 และมีกำลังอัดไม่น้อยกว่า 35 MPa

ในการผสมคอนกรีตได้มีการผสมเกลือโซเดียมคลอไรด์เข้มข้นร้อยละ 2 โดยน้ำหนัก

เพื่อเป็นการจำลองการปนเปื้อนของคลอไรด์ในคอนกรีต ผลการทดลองแสดงให้เห็นว่า

เหล็กเสริมในคอนกรีตที่ใช้วัสดุประสานต่างๆ ทั้งสามประเภท

มีความเสี่ยงในการเกิดสนิมลดต่ำลงภายหลังการใช้งาน ECE

แม้ว่าปริมาณคลอไรด์ในคอนกรีตภายหลังการใช้งาน ECE จะอยู่ที่ร้อยละ 30 ถึง 40

ของปริมาณเริ่มต้น และยังมีค่าสูงกว่าค่าคลอไรด์วิกฤติในคอนกรีตก็ตาม

นอกจากนี้ผลการทดลองยังแสดงให้เห็นว่าเคมีเชื่อมอออนมีผลต่อการไหลของกระแสระหว่างการ

ดึงคลอไรด์น้อย เมื่อเทียบกับไฮดรอกซิลอออน ซัลเฟตอออน คลอไรด์อออน โซเดียมอออน

และโพแทสเซียมอออน ซึ่งเป็นอออนหลักที่ส่งผลให้เกิดการไหลของกระแส

ภาควิชา: วิศวกรรมโยธา...

ลายมือชื่อผู้คิด:

สาขาวิชา: วิศวกรรมโยธา...

ลายมือชื่อ อ.ที่ปรึกษาวิทยานิพนธ์หลัก:

Academic year: 2012

ลายมือชื่อ อ.ที่ปรึกษาวิทยานิพนธ์ร่วม:

5470520221: MAJOR CIVIL ENGINEERING

KEYWORDS: ELECTRO-CHEMICAL/CHLORIDE EXTRACTION/ REMOVAL/
REHABILITATION/ REINFORCED CONCRETE

HAI YEN THI NGUYEN: EFFECTIVENESS EVALUATION OF
ELECTROCHEMICAL CHLORIDE EXTRACTION IN REINFORCED
CONCRETE. ADVISOR: ASST. PROF WITHIT PANSUK, Ph. D., CO-
ADVISOR: PAKAWAT SANCHAROEN, Ph.D., 115 pp.

Rehabilitating the reinforced concrete structure contaminated with chloride from the marine environment was always interesting research. Electrochemical chloride extraction (ECE) is one of beneficial options. However, the feasibility and effectiveness of it is still on arguing, especially in concrete using mineral admixtures and concrete satisfied the requirement for using in marine environment according to ACI 318 which has low water to binder ratio.

In this study, ECE was applied in plain OPC concrete, fly ash concrete with 30% of fly ash by weight of binder, limestone fly ash concrete with 25% fly ash and 5% limestone powder by weight of binder, respectively. Water/binder ratio was 0.4, minimum strength 35MPa. Two percentage of sodium chloride by weight of binder was added in mixing water to supply chloride. The results indicated that, all three types of concrete showed that, after extracting 30-40% of initial chloride content in concrete, even though average remained chloride in concrete was still higher than critical value of chloride in concrete, embedded steel in concrete was shown the delete low corrosion risk stage. Moreover, it also indicated that the contribution of calcium ion on the current flow during extracting process electrical current on extracting process was insignificant; meanwhile, hydroxyl, sulfate, chloride, sodium and potassium played the main role on transferring the charge.

Department: Civil Engineering Student's Signature:

Field of Study: Civil Engineering Advisor's Signature:

Academic year: 2012 Co-advisor's Signature:

ACKNOWLEDGEMENT

I would like to thank AUN-SEED/net organization for giving me the opportunity to study in Chulalongkorn University and funded for my project.

I wish to express my deepest gratitude to my advisors, Dr Withit Pansuk and Dr Pakawat Sanchaoren for their help and encouragement throughout my study. I am grateful them for permitting me to pursue this research.

I also want to thank Dr Warankana Saengsoy. The discussions with her gave me great advantage in choosing the appropriate method for testing in my research.

I sincerely thank SIIT and Science Faculty, KIMTL for helping me in ion analysis.

Finally, I would like to thank the panels of my committee, Assoc. Prof. Dr. Boonchai Stitmannathum, Asst. Prof. Dr. Wanchai Yodsudjai and Asst. Prof. Dr. Nattaporn Tonanon.

TABLE OF CONTENT

| | |
|--|----|
| LIST OF TABLES | IX |
| LIST OF FIGURES | IX |
| CHAPTER 1 INTRODUCTION..... | 1 |
| 1.1 Background of study | 1 |
| 1.2 Objectives..... | 2 |
| 1.3 Scope of study | 2 |
| CHAPTER 2 LITERATURE REVIEW | 4 |
| 2.1 Cement hydration and their properties..... | 4 |
| 2.1.1 Hydration of ordinary Portland cement | 4 |
| 2.1.2 Hydration of fly ash cement and properties..... | 5 |
| 2.1.3 Hydration of limestone fly ash cement and properties | 8 |
| 2.2 Corrosion of steel and factors affecting corrosion..... | 11 |
| 2.2.1 Corrosion of steel and types of corrosion..... | 11 |
| 2.2.2 Factors affecting on corrosion | 15 |
| 2.2.3 Types of chloride in concrete and their effects on reinforced concrete | 17 |
| 2.3 Electrochemical re-alkalization (ERA) and electrochemical chloride extraction (ECE) 20 | |
| 2.3.1 Electrochemical re-alkalization (ERA)..... | 20 |
| 2.3.2 Electrochemical chloride extraction (ECE) | 21 |
| CHAPTER 3 METHODOLOGY..... | 29 |
| 3.1 Materials..... | 29 |

| | | |
|--|---|----|
| 3.2 | Specimen preparation..... | 31 |
| 3.3 | Testing..... | 34 |
| 3.4 | Measurement | 36 |
| 3.4.1 | Effects of electrochemical chloride extraction on concrete..... | 36 |
| 3.4.2 | Effect of ECE on steel rod..... | 39 |
| CHAPTER 4 RESULTS AND DISCUSSION | | 40 |
| 4.1 | Resistivity of concrete..... | 40 |
| 4.2 | Chloride removal | 43 |
| 4.2.1 | Release of chloride into electrolyte | 43 |
| 4.2.2 | Remained chloride in concrete | 54 |
| 4.3 | Distribution of water-solubility of sodium, potassium, lithium and calcium... | 59 |
| 4.4 | Microstructure of concrete at interfacial zone..... | 71 |
| 4.5 | Half cell potential of embedded steel..... | 85 |
| CHAPTER 5 CONCLUSION AND RECOMENDATION | | 91 |

LIST OF TABLES

| | | |
|------------|---|----|
| Table 2.1 | Basic differences between cathodic protection, ECE and ECR | 28 |
| Table 3.1 | Chemical compositions of cement (% by weight) | 30 |
| Table 3.2 | Physical criteria of cement | 30 |
| Table 3.3 | Chemical compositions of fly ash (% by weight) | 30 |
| Table 3.4 | Physical criteria of fly ash (FA)..... | 31 |
| Table 3.5 | Chemical compositions of limestone powder (LP) (% by weight)..... | 31 |
| Table 3.6 | Mineral compositions (%), Blain fineness (cm^2/g) and specific gravity (g/cm^3) of limestone powder | 31 |
| Table 3.7 | Specifications of superplasticizer | 31 |
| Table 3.8 | Mix preparatin of concrete (kg/m^3)..... | 33 |
| Table 3.9 | Electrical parameters of specimens..... | 36 |
| Table 4.1 | Resistivity and conductivity of concrete versus embedded steel condition | 42 |
| Table 4.2 | Resistivity of concrete before and after extracted..... | 42 |
| Table 4.3 | Timetable of extraction process | 48 |
| Table 4.4 | Mobility of some ions dissolved..... | 48 |
| Table 4.5 | Extracted chloride content after every week | 49 |
| Table 4.6 | Accumulated chloride content | 50 |
| Table 4.7 | Remained chloride in plain concrete with diameter 15cm..... | 57 |
| Table 4.8 | Remained chloride in plain concrete with diameter 10cm..... | 57 |
| Table 4.9 | Remained chloride in fly ash concrete with diameter 15cm | 58 |
| Table 4.10 | Remained chloride in fly ash concrete with diameter 10cm | 58 |
| Table 4.11 | Remained chloride in limestone fly ash concrete with diameter 15cm | 58 |
| Table 4.12 | Remained chloride in limestone fly ash concrete with diameter 10cm | 58 |
| Table 4.13 | Distribution of sodium in plain concrete 15 cm diameter..... | 62 |
| Table 4.14 | Distribution of sodium in plain concrete 10 cm diameter..... | 62 |
| Table 4.15 | Distribution of sodium in fly ash concrete 15 cm diameter | 62 |
| Table 4.16 | Distribution of sodium in fly ash concrete 10 cm diameter | 62 |
| Table 4.17 | Distribution of sodium in limestone fly ash concrete 15 cm diameter | 63 |

| | | |
|------------|--|----|
| Table 4.18 | Distribution of sodium in limestone fly ash concrete 10 cm diameter | 63 |
| Table 4.19 | Distribution of potassium in plain concrete 15 cm diameter..... | 63 |
| Table 4.20 | Distribution of potassium in plain concrete 10 cm diameter..... | 63 |
| Table 4.21 | Distribution of potassium in fly ash concrete 15 cm diameter | 64 |
| Table 4.22 | Distribution of potassium in fly ash concrete 10 cm diameter | 64 |
| Table 4.23 | Distribution of potassium in limestone fly ash concrete 15 cm diameter | 64 |
| Table 4.24 | Distribution of potassium in limestone fly ash concrete 10 cm diameter | 64 |
| Table 4.25 | Distribution of calcium ion in plain concrete 15 cm diameter | 68 |
| Table 4.26 | Distribution of calcium in plain concrete 10 cm diameter | 69 |
| Table 4.27 | Distribution of calcium ion in fly ash concrete 15 cm diameter..... | 69 |
| Table 4.28 | Distribution of calcium in fly ash concrete 10 cm diameter | 69 |
| Table 4.29 | Distribution of calcium ion in limestone fly ash concrete 15 cm diameter | 69 |
| Table 4.30 | Distribution of calcium in fly ash concrete 10 cm diameter | 70 |
| Table 4.31 | Distribution of lithium ion into concrete 15 cm diameter in case lithium borate buffer as electrolyte | 72 |
| Table 4.32 | Distribution of lithium ion into concrete 10 cm diameter in case lithium borate buffer as electrolyte | 72 |
| Table 4.33 | Result XRD of plain concrete..... | 74 |
| Table 4.34 | Result XRD of fly ash concrete | 74 |
| Table 4.35 | Result XRD of limestone fly ash concrete | 74 |
| Table 4.36 | Half cell potential of steel versus corrosion risk..... | 86 |
| Table 4.37 | Half cell potential of steel rod versus saturated copper sulfate electrode | 90 |

LIST OF FIGURES

| | | |
|-------------|--|----|
| Figure 1.1 | Degradation of reinforced concrete structure in marine environment . | 1 |
| Figure 2.1 | Accumulation of plate-like calcium hydroxide on OPC mortar..... | 7 |
| Figure 2.2 | Decrease of calcium hydroxide on fly ash mortar | 7 |
| Figure 2.3 | C-S-H type I..... | 8 |
| Figure 2.4 | C-S-H type II | 8 |
| Figure 2.5 | C-S-H type III..... | 8 |
| Figure 2.6 | Structure of reinforced concrete | 9 |
| Figure 2.7 | Ettringite | 11 |
| Figure 2.8 | Monosulfate | 11 |
| Figure 2.9 | Plated-like of calcium hexaaluminate hydrate..... | 11 |
| Figure 2.10 | Pourbaix diagram | 12 |
| Figure 2.11 | Corrosion of steel..... | 14 |
| Figure 2.12 | Polarization curves of corrosion process..... | 14 |
| Figure 2.13 | Cathode protection by using sacrificial anode diagram | 14 |
| Figure 2.14 | Cathodic protection by using impressed current diagram..... | 14 |
| Figure 2.15 | Polarization curves of cathodic protection by using impressed current | 15 |
| Figure 2.16 | Corrosion processes of embedded steel in reinforced concrete..... | 16 |
| Figure 2.17 | Scanning electron microscope (SEM) of Fiedel's salt..... | 17 |
| Figure 2.18 | Corrosion process in chloride environment..... | 17 |
| Figure 2.19 | Evans diagram..... | 18 |
| Figure 2.20 | Modified Evan diagram..... | 18 |
| Figure 2.21 | Modified Pourbaix diagram..... | 18 |
| Figure 3.1 | Particle size distribution of coarse aggregate | 27 |
| Figure 3.2 | Particle size distribution of sand..... | 28 |
| Figure 3.3 | Cross-section and preparing specimens for experimental testing..... | 30 |
| Figure 3.4 | Specimens for experimental testing..... | 30 |
| Figure 3.5 | Installation for testing specimen..... | 31 |
| Figure 3.6 | Installation for experimental testing specimen | 31 |
| Figure 3.7 | Installation of fly ash concrete in 15cm diameter and 10cm diameter | 32 |
| Figure 3.8 | Installation of limestone fly ash concrete in 15cm diameter and 10cm diameter..... | 32 |

| | | |
|-------------|---|----|
| Figure 3.9 | Installation of plain concrete in 15cm diameter and 10cm diameter ... | 33 |
| Figure 4.1 | Enhancement of resistivity of concrete with 10cm diameter | 43 |
| Figure 4.2 | Enhancement of resistivity of concrete with 15cm diameter | 43 |
| Figure 4.3 | Released chloride content (a) and accumulated chloride content (b) in electrolyte of plain concrete with concrete thickness 70 mm..... | 45 |
| Figure 4.4 | Released chloride content (a) and accumulated chloride content (b) in electrolyte of plain concrete with concrete thickness 45 mm..... | 51 |
| Figure 4.5 | Released chloride content (a) and accumulated chloride content (b) in electrolyte of fly ash concrete with concrete thickness 70 mm..... | 51 |
| Figure 4.6 | Released chloride content (a) and accumulated chloride content (b) in electrolyte of fly ash concrete with concrete thickness 45 mm..... | 51 |
| Figure 4.7 | Released chloride content (a) and accumulated chloride content (b) in electrolyte of limestone fly ash concrete with concrete thickness 70 mm | 52 |
| Figure 4.8 | Released chloride content (a) and accumulated chloride content (b) in electrolyte of limestone fly ash concrete with concrete thickness 45 mm | 52 |
| Figure 4.9 | Released chloride and accumulated chloride of different concrete types with saturated calcium hydroxide as electrolyte on specimen diameter 15cm..... | 52 |
| Figure 4.10 | Released chloride and accumulated chloride of different concrete types with lithium borate buffer as electrolyte on specimen 15cm | 53 |
| Figure 4.11 | Released chloride and accumulated chloride of different concrete types with saturated calcium hydroxide as electrolyte on specimen diameter 10cm..... | 53 |
| Figure 4.12 | Released chloride and accumulated chloride of different concrete types with lithium borate buffer as electrolyte on specimen 10cm | 53 |
| Figure 4.13 | Remained chloride content of plain concrete in different electrolyte with diameter 15 cm (a) and 10 cm (b)..... | 54 |
| Figure 4.14 | Remained chloride content of fly ash concrete in different electrolyte with diameter 15 cm (a) and 10 cm (b)..... | 59 |
| Figure 4.15 | Remained chloride content of limestone fly ash concrete in different electrolyte with diameter 15 cm (a) and 10 cm (b)..... | 59 |

| | | |
|-------------|--|----|
| Figure 4.16 | Remained chloride content of plain concrete, fly ash concrete and limestone fly ash concrete with diameter 15cm (a) and 10cm (b) in saturated calcium hydroxide..... | 59 |
| Figure 4.17 | Remained chloride content of plain concrete, fly ash concrete and limestone fly ash concrete with diameter 15cm (a) and 10cm (b) in lithium borate buffer | 60 |
| Figure 4.18 | Distribution sodium ion in plain concrete a) 15cm diameter specimen b) 10cm diameter specimen..... | 60 |
| Figure 4.19 | Distribution sodium ion in fly ash concrete a) 15cm diameter specimen b) 10cm diameter specimen..... | 65 |
| Figure 4.20 | Distribution sodium ion in limestone fly ash concrete a) 15cm diameter specimen b) 10cm diameter specimen | 65 |
| Figure 4.21 | Distribution potassium ion in plain concrete a) 15cm diameter specimen b) 10cm diameter specimen..... | 65 |
| Figure 4.22 | Distribution potassium ion in fly ash concrete a) 15cm diameter specimen b) 10cm diameter specimen | 66 |
| Figure 4.23 | Distribution potassium ion in limestone fly ash concrete a) 15cm diameter specimen b) 10cm diameter specimen..... | 66 |
| Figure 4.24 | Distribution calcium ion in plain concrete a) 15cm diameter specimen b) 10cm diameter specimen..... | 66 |
| Figure 4.25 | Distribution calcium ion in fly ash concrete a) 15cm diameter specimen b) 10cm diameter specimen..... | 70 |
| Figure 4.26 | Distribution calcium ion in limestone fly ash concrete a) 15cm diameter specimen b) 10cm diameter specimen | 70 |
| Figure 4.27 | Distribution calcium ion in limestone fly ash concrete a) 15cm diameter specimen b) 10cm diameter specimen | 71 |
| Figure 4.28 | Distribution calcium ion in limestone fly ash concrete a) 15cm diameter specimen b) 10cm diameter specimen | 71 |
| Figure 4.29 | Diffusion of lithium ion into concrete a) 15cm diameter specimen b) 10cm diameter specimen..... | 71 |
| Figure 4.30 | Diffusion of lithium ion into concrete a) 15cm diameter specimen b) 10cm diameter specimen..... | 72 |
| Figure 4.31 | Specimen for SEM test..... | 73 |

| | | |
|-------------|--|----|
| Figure 4.32 | Scanning electron microscopy (SEM) of Portlandite (CH), C-S-H (CSH) and ettringite (E) and energy dispersive spectroscopy (EDS) at interfacial zone of plain concrete with diameter 10cm before extraction a) CH b) CSH..... | 78 |
| Figure 4.33 | SEM and EDS after extraction with d=10cm of plain concrete in saturated calcium hydroxide a) CSH b) Sodium-rich crystal (N)..... | 78 |
| Figure 4.34 | SEM and EDS after extraction with d=10cm of plain concrete in lithium borate buffer a) CH b) CSH..... | 79 |
| Figure 4.35 | SEM and energy EDS at interfacial zone of plain concrete with diameter 15cm before extraction a) CH b) CSH..... | 79 |
| Figure 4.36 | SEM and EDS after extraction with d=15cm of plain concrete in saturated calcium hydroxide a) CH b) CSH..... | 80 |
| Figure 4.37 | SEM and EDS after extraction with d=15cm of plain concrete in lithium borate buffer a) CSH b) CH..... | 80 |
| Figure 4.38 | SEM and EDS (CSH) at interfacial zone of fly ash concrete with diameter 10cm before extraction | 81 |
| Figure 4.39 | SEM and EDS at interfacial zone of fly ash concrete in saturated calcium hydroxide with diameter 10cm after extraction a) N b) CSH..... | 81 |
| Figure 4.40 | SEM and EDS at interfacial zone of fly ash concrete in lithium borate buffer with diameter 10cm after extraction a) CH b) CSH..... | 82 |
| Figure 4.41 | SEM and EDS (CSH) at interfacial zone of fly ash concrete with diameter 15cm before extraction | 82 |
| Figure 4.42 | SEM and EDS at interfacial zone of fly ash concrete in saturated calcium hydroxide with diameter 15cm after extraction a) N b) CSH..... | 83 |
| Figure 4.43 | SEM and EDS (CSH) at interfacial zone of fly ash concrete in lithium borate buffer with diameter 15cm after extraction | 83 |
| Figure 4.44 | SEM and EDS (CSH) at interfacial zone of limestone fly ash concrete with diameter 10cm before extraction..... | 84 |
| Figure 4.45 | SEM and EDS at interfacial zone of limestone fly ash concrete with diameter 10cm after extraction with saturated calcium hydroxide a) N b) CSH | 84 |
| Figure 4.46 | SEM and EDS (N) at interfacial zone of limestone fly ash concrete with diameter 10cm after extraction with lithium borate buffer | 84 |

| | | |
|-------------|---|-----|
| Figure 4.47 | SEM and EDS (CSH) at interfacial zone of limestone fly ash concrete with diameter 15cm before extraction..... | 85 |
| Figure 4.48 | SEM and EDS at interfacial zone of limestone fly ash concrete with diameter 15cm after extraction with calcium hydroxide a) CH b) CSH | 85 |
| Figure 4.49 | SEM and EDS (CSH) at interfacial zone of limestone fly ash concrete with diameter 15cm after extraction with lithium borate buffer..... | 86 |
| Figure 4.50 | Half cell potential of reinforcing steel after stopped ECE treatment on plain concrete a) 10cm diameter b) 15cm diameter..... | 91 |
| Figure 4.51 | Half cell potential of reinforcing steel after stopped ECE treatment on fly ash concrete a) 10cm diameter b) 15cm diameter | 91 |
| Figure 4.52 | Half cell potential of reinforcing steel after stopped ECE treatment on fly ash concrete a) 10cm diameter b) 15cm diameter | 91 |
| Figure 4.53 | Influence of concrete type to half cell potential in case of saturated calcium hydroxide as electrolyte a) 10cm diameter b) 15cm diameter | 92 |
| Figure 4.54 | Influence of concrete type to half cell potential in case lithium borate buffer as electrolyte a) 10cm diameter b) 15cm diameter..... | 92 |
| Figure 1 | XRD result of PC 10cm before extraction | 97 |
| Figure 2 | XRD result of PC 10cm after extraction in saturate calcium hydroxide | 98 |
| Figure 3 | XRD result of PC 10cm after extraction in lithium borate buffer | 99 |
| Figure 4 | XRD result of FC 10cm before extraction | 100 |
| Figure 5 | XRD result of FC 10cm after extraction in saturate calcium hydroxide | 101 |
| Figure 6 | XRD result of FC 10cm after extraction in lithium borate buffer | 102 |
| Figure 7 | XRD result of LFC 10cm before extraction | 103 |
| Figure 8 | XRD result of LFC 10cm after extraction in saturated calcium hydroxide | 104 |
| Figure 9 | XRD result of LFC 10cm after extraction in lithium borate buffer..... | 105 |
| Figure 10 | XRD result of PC 15cm before extraction | 106 |
| Figure 11 | XRD result of PC 15cm after extraction in saturated calcium hydroxide | 107 |
| Figure 12 | XRD result of PC 15cm after extraction in lithium borated buffer | 108 |

| | | |
|-----------|---|-----|
| Figure 13 | XRD result of FC 15cm before extraction | 109 |
| Figure 14 | XRD result of FC 15cm after extraction in saturated calcium hydroxide | 110 |
| Figure 15 | XRD result of FC 15cm after extraction in lithium borate buffer | 111 |
| Figure 16 | XRD result of LFC 15cm before extraction | 112 |
| Figure 17 | XRD result of LFC 15cm after extraction in saturated calcium hydroxide | 113 |
| Figure 18 | XRD result of LFC 15cm after extraction in lithium borate buffer..... | 114 |

CHAPTER I

INTRODUCTION

1.1 Background of study

Corrosion of steel in reinforced concrete has been studying long time ago. This is very important risk for all reinforced concrete structures; especially structures exposed to the marine environment as shown in figure 1.1. This is also one of main factors responsible for the unexpected collapses due to the sudden decreasing of bearing capacity of structure.



Figure 1.1: Degradation of reinforced concrete structure in marine environment

Nowadays, the role of chloride in corrosion process of embedded steel in reinforced concrete cannot be neglected. Many research have been studied the principle of corrosion process, factor affecting and rehabilitation methods for reinforced concrete structure. Cathodic protection is one of the popular methods to protect steel corrosion. Electrochemical chloride extraction (ECE) or electrochemical re-alkalization (ERA) is currently one of the options studying (Marcotte, 1999). It has been studying.

Although both ECE and ERA are based on the same principle, but meanwhile ERA has been accepted (Redaelli, 2011), ECE has remained many different disputes. Moreover, concrete using low water/cement ratio and mineral admixture such as fly ash, silica fumed, blast furnace slag or limestone powder, etc. have been popular, however, the number of research studying electrochemical chloride extraction on their types of concrete is still very scarce. Although there were some structures applied

ECE to rehabilitate after chloride intrusion, the feasibility of this method is still much uncertainness. Comparably, ECE, if it can be used as a rehabilitation method, it has a lot of advantages about economic, transportation, etc. than cathodic protection.

Nowadays, it has not really be clear yet, but by literature, the feasibility of ECE affected strongly by either condition of structure needed to rehabilitate or applying condition such as, geometry of structure, initial chloride content, impressed current density, etc.

1.2 Objectives

As above mentioned, electrochemical chloride extraction is under studying and still exist many inconsistent results, especial for concrete using blended cement as well as concrete with water/binder ratio and strength satisfied requirement for concrete using in marine environment. Therefore, the main objective of this study is to evaluate the effectiveness of electrochemical chloride extraction (ECE) in reinforced concrete using ordinary Portland cement, fly ash and limestone as a binder with water/binder ratio and strength satisfied requirement for using in marine environment when electrolyte is saturated calcium hydroxide, lithium borate buffer, respectively. To obtain this objective, two sub objectives need to study:

- Investigate the influences of ECE on microstructure of concrete such as released chloride content in concrete into electrolyte during extracting, remained chloride content in concrete after extraction, distribution of positive ions, typical mineral content and the alternation of morphology of mineral after ECE treatment.
- Survey the effects of ECE on the corrosion of steel by half cell potential.

1.3 Scope of study

The feasibility of ECE depended strongly on initial chloride and applying impressed current. Moreover, most of studies on ECE used concrete with average quality. By previous research, 2% sodium chloride by weight of binder and 0.5 A/m^2 with respect to concrete surface were chose to apply and evaluate the effectiveness of ECE on chloride-contaminated reinforced concrete of fly ash concrete and limestone fly ash concrete satisfied the requirement for using in marine environment with:

- Water/binder ratio was 0.4; minimum compressive strength was 35MPa.
- Electrolyte is saturated calcium hydroxide (1.55g/l) or lithium borate buffer with pH is 10 (0.5M LiH₂BO₃).
- In fly ash concrete, fly ash content was 0%, 30% by weight of binder, respectively.
- In limestone fly ash concrete, limestone was 5% and fly ash was 25% by weight of binder.
- Electric current treatment at initial time was 0.5 A/m² (respect to concrete surface area).

1.4 Expected results

By literature review and previous studies, initial condition of structure (including total chloride content and corrosion state of embedded steel) and applying impressed current were chosen; initial total acid soluble chloride content was about 1.5% by weight of cement and applying impressed current was 0.5A/m². With their application, ECE was expected that, after extracting about 30% of initial chloride content in concrete:

- Embedded steel could re-passivate and corrosion state of it could reach to low corrosion risk.
- Portlandite content at interfacial zone increases.
- The decomposition/transformation of adhesive minerals in concrete after extraction was not so severe; then, the strength of concrete might not reduce significant.
- ECE method could be applied for plain concrete, fly ash concrete or limestone fly ash concrete with these qualities satisfied to use in marine environment, such as requirement about thickness cover, water/binder ratio, strength of concrete in according to ACI 318.

CHAPTER II

LITERATURE REVIEW

In this chapter, some knowledge relate to either the hydration of cement, the effect of some types of admixture on microstructure of concrete, corrosion of steel or some main factor affecting on this progress are introduced to give some general overview of these problems. Then, the differences of their properties before and after extraction can be compared to evaluate the effectiveness of ECE

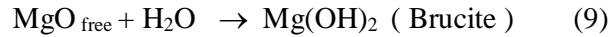
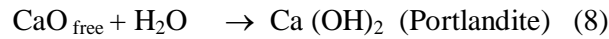
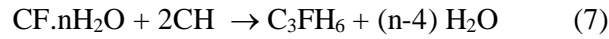
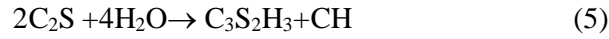
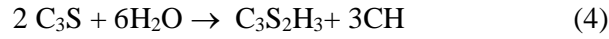
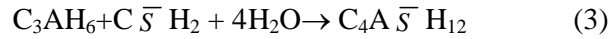
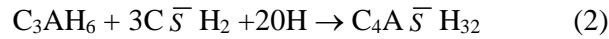
2.1 Cement hydration and their properties

2.1.1 Hydration of ordinary Portland cement

Mechanism of cement hydration was studied long ago. Therefore, many hypothesizes were proposed. Nowadays, by using many modern techniques, mechanism of this process is clearer. In there, two mechanisms are widely accepted (Mehta, 2006). The first mechanism is through-solution hydration which is assumed that the hydration of cement went through three steps. The progress started with the dissolution of anhydrous cement particles and formation of ions solution. Due to the decrease of free water of mixture and the low solubility of cement hydration products, then, ions solution reach quickly to supersaturated solution. At the end of process, the new products are precipitated from oversaturated solution. The second mechanism is solid-stage solution. In this assumption, the hydration progress of cement is to take place on the surface of cement particles. The liberation of ions from cement into solution does not happen. However, from electron microscopy, many studies showed that, at the early stage, as the free water content was still abundant, through-solution played main role in hydration progress. Subsequently, the free water reduced, the movement of ions in the solution was restricted, the second mechanism, solid-stage solution played dominant role.

In chemical standpoint, cement hydration is a series of reactions occurred simultaneously. Depending upon many factors such as chemical content, minerals content, water content, water/cement ratio, temperature ambience, etc. the products of cement hydration might be different. Almost products of cement hydration are not separate. They are usually a series of constituents with difference chemical

components ratio. Nowadays, from many studies, cement hydration can be simplified as shown in equations (1) to (9). When cement contacted with water, calcium aluminates (C_3A) is the first constituent in cement react with water to produce calcium aluminates hydrate (C_3AH_6). However, a part of C_3AH_6 reacts immediately with gypsum $CaSO_4 \cdot 2H_2O$ ($C\bar{S}H_2$), a constituent of cement, to form $C_3A_3CaSO_4H_{32}$ (Ettringite) and $C_3A \cdot Ca(SO_4) \cdot H_{12}$ (monosulfate). Simultaneously, the hydration of C_3S also takes place. In addition, small free content of calcium oxide and magnesium oxide still remained in Portland cement hydrated.



2.1.2 Hydration of fly ash cement and properties

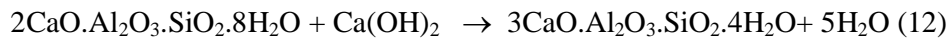
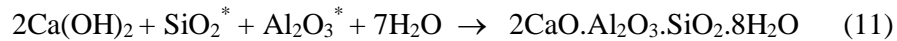
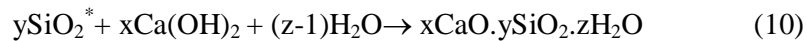
Fly ash has been used as an admixture of cement or concrete long ago to improve their properties, especially when concrete structures are exposed to aggressive medium. In spite of using many advanced method to research, the effects of fly ash on hydration of cement and properties of cement/concrete has been still studying. A full definitive conclusion has not presented yet. And the main reason is due to the heterogeneity of either chemical constituent or mineral component, hydraulic activity of fly ash, even within a single particle. However, the advantages of fly ash in cement and concrete on long-term properties such as strength, porosity or durability of concrete cannot be denied (Ghosh, 1995). In which, the most notable property is the low releasing amount of heat when fly ash cement hydrates.

Mechanism of fly ash cement hydration is proposed by Takemoto and Uchikama (Ghosh, 1995). Their hypothesis assumes that fly ash is formed from anions SiO_4^{4-} and AlO_3^{3-} , AlO_4^{5-} . So, its surface brings negative charge and easy to capture positive charge ions from environmental solution. Meanwhile, free calcium

hydroxide released by cement hydration increase pH of environment that is a favorite condition for fly ash to dissolve and react with Ca^{2+} . In addition, product layer on fly ash surface does not restrict the diffusion of some small molecules or ions as calcium ion or water. Therefore, its hydration progress can be continuing.

Although some researchers did not agreed with this hypothesis because it was over-ideal, but many studies proved that, this model corresponded with the change of zeta potential on the hydration progress.

Due to the complication of fly ash constituents, both chemical and mineral components, hence, the chemical hydration progress of fly ash cement hydration is more complicated. However, to simplify the problem, many researches assumed that, on fly ash cement, fly ash is a pozzolan. At early stage, it plays as a nucleus, and accelerates hydration progress of cement. Hence, fly ash cement hydration, under chemical standpoint is separated to two stages. On first stage, that is the hydration of cement, similar with the hydration of ordinary Portland cement. On second stage, fly ash reacts with calcium hydroxide $\text{Ca}(\text{OH})_2$ (Portlandite) released from cement hydration and that progress can be simplified as shown in equations (10) to (12).



As above mentioned, this study did not deeply investigate the influence of fly ash in cement and concrete, therefore, summarizing some special characteristics is necessary to understand the reason for the using more and more popular of fly ash. Firstly, that is the difference in hydration products of fly ash cement in comparison to OPC cement. Lime content in concrete/mortar using fly ash decreases significantly as shown in Figure 2.2, meanwhile in concrete or mortar without fly ash or mineral admixture, Portlandite accumulated to quite big crystal and formed to the layers as shown in Figure 2.1. Simultaneously, content of Ca^{2+} in calcium silicate hydrates is lower and C-S-H product prefers type II or type III as shown in Figures 2.4 and 2.5 instead of C-S-H type I as shown in Figure 2.3 and content of Ca^{2+} in calcium aluminates hydrates is lower as well. In addition, the content of gehlenite hydrates C_2ASH_8 and garnet hydrates $\text{C}_3\text{AS}_z\text{H}_{6-2z}$ increase significantly. Secondly, there are a lot advantages of fly ash cement when using it on aggressive medium. Due to consuming a large amount of calcium hydroxide by pozzolanic reaction, the

orientation of calcium hydroxide to big plate crystal reduces meaningfully; moreover, C-S-H content at transition zone increases significantly, especially that is the existence of C-S-H in term of low C/S ratio. Besides, because of reducing the heated generation by hydration progress, hence, fly ash can decrease the occurrence of crack due to thermal stress. Concurrently, due to the larger volume of pozzolanic products in comparison with initial components, it can reduce porosity and discontinue pore system. Therefore, the diffusion of ionic harmfulness as chloride, sulfate, etc is prevented. However, the use of fly ash cement in concrete still has some arguing disadvantages. Diminution of pH in concrete due to low content of $\text{Ca}(\text{OH})_2$ may increase the risk for the corrosion of steel in reinforced concrete (Ghosh, 1995). In the other hand, when using fly ash, relative content of OPC is reduced, hence, depending on mixing fly ash content, setting time may increase and strength of concrete at the early stage is usually lower than plain concrete.

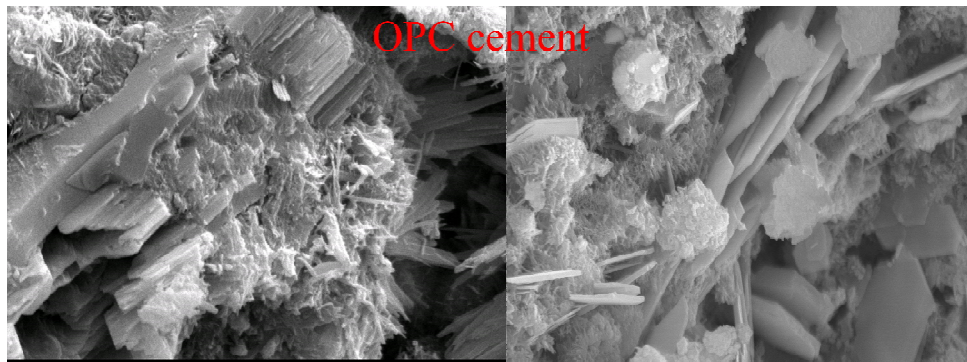


Figure 2.1: Accumulation of plate-like calcium hydroxide on ordinary Portland cement mortar



Figure 2.2: Decrease of calcium hydroxide on fly ash mortar

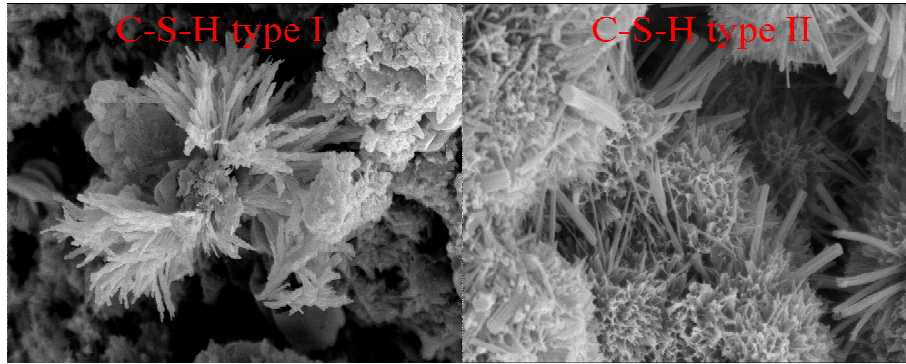


Figure 2.3: C-S-H type I

Figure 2.4: C-S-H type II



Figure 2.5: C-S-H type III

2.1.3 Hydration of limestone fly ash cement and properties

It is clear that, the higher capillary content, the less strength and durability concrete possesses. Transition zone between mortar and coarse aggregate of steel/concrete surface always have higher porosity than at bulk of matrix. The model reinforced concrete and its pore system was shown in Figure 2.6.

That is the reason for occurrence of filler admixtures in concrete. With scratch hardness is 3, limestone is ground and ease to obtain high fineness. Therefore, it may be a good choice to use as a filler admixture. Moreover, the formation of calcium carboaluminate hydrate prevents the decomposition of Ettringite (AFt-Figure 2.7) produced at the early-stage of cement hydration. Hence, the structure of concrete is denser. However, many researches shown that, when limestone content is higher than 5%, the strength of concrete using limestone powder is lower than plain concrete, at all ages (Tsvivilis, 2002) (Kadri, 2010). Nowadays, it can be noticed that limestone

powder concrete may produce higher strength at the early ages but lower strength at mature age in comparison with plain concrete.

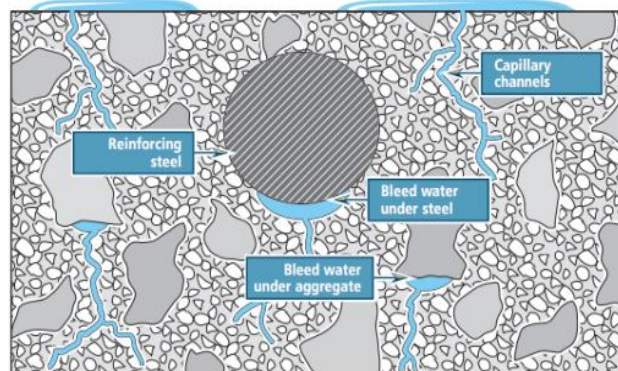


Figure 2.6: Structure of reinforced concrete

Conversely, fly ash concrete in particular or pozzolanic admixture in general except silica fume, it usually produces lower strength at the early strength but higher strength in compared with plain concrete.

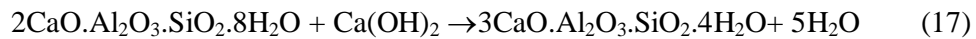
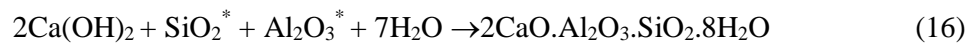
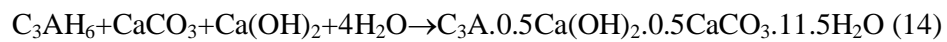
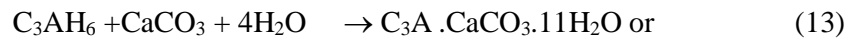
Hence, limestone fly ash cement may remedy the weakness of each others. That was one of main reasons for occurrence of ternary binders. Nowadays, the simultaneous effects of limestone and fly ash on concrete have been still studying, especial theirs benefits on aggressive medium. Their research have usually focused on three fields (Tsivilis, 2002), the effects of limestone on the grinding process of cement, the effects of limestone on hydration of cement and the effects of limestone on properties of concrete, respectively.

Although there were a lot of reseaches, but similarity with fly ash cement, the influence and mechanism of limestion fly ash cement had not been clearly yet. However, some alike results allowed to conclude that, at the early stage, limestone powder and fly ash play as a nucleus for the hydration of cement, they separate cement particles, create favorable condition for cement can easily contact with water and hydrate. Hence, they accelerate the hydration progress of cement. Furthermore, on this stage, with the several smaller than cement size, limestone also can play as a filler element for the mortar matrix.

Recently, some studies showed that, limestone can replace a part of gypsum on the hydration progress. In addition, in this stage, limestone reacts with calcium aluminates hydrates, an hydrated product of cement (Figure 2.9) as shown in equations (13) and (14); then, it prevents the decomposition of Fat, the mineral has

larger size to calcium aluminates monosulfat (AFn-Figure 2.8); the mineral had smaller size. So, it reduced the pore content of concrete at the early stage. Therefore, the strength of concrete at this stage may be improved.

Moreover, by these reactions, limestone can reduce calcium aluminates hydrates content, a harmful mineral when concrete exposes in sulfate attacked medium or marine environment. Therefore, it improves the durability of concrete. At the later stage, the role of limestone was almost stable. The strength of concrete was affected by fly ash in limestone fly ash cement like as fly ash cement as shown in equations (15) to (17).



Similar with fly ash concrete, at that stage, the formation of calcium silicate hydrate has larger volume in comparison with ordinary substances can decrease the pore content as well as discontinue the porosity system.

The properties of limestone fly ash concrete, especially on aggressive environments are still in further research. However, almost studies proved that, it had all benefits of fly ash concrete. In addition, it improved the some disadvantages of it. Although the effects of general admixtures on concrete are still not clear, but the ability prolonged the durability of reinforced concrete in aggressive condition cannot controvert. And some reasons have been accepted to explain those properties such as the density of concrete with blended cement may be higher, the formation of constituents have lower solubility but higher volume, it may discontinue the capillary channel and the new constituents. Therefore, they can prevent the diffusion of harmful ions went further into concrete.

Hence, this can be shown that, in marine environment, blended cement in general and fly ash cement or limestone fly ash cement in particular can reduce the diffusion of sulfate, main agent cracked concrete due to the formation of ettringite, making the favorable condition for the further intrusion of chloride.

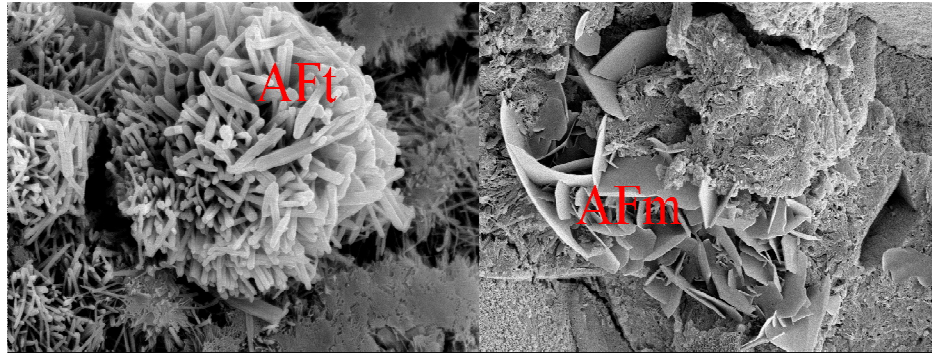


Figure 2.7: Ettringite

Figure 2.8: Monosulfate

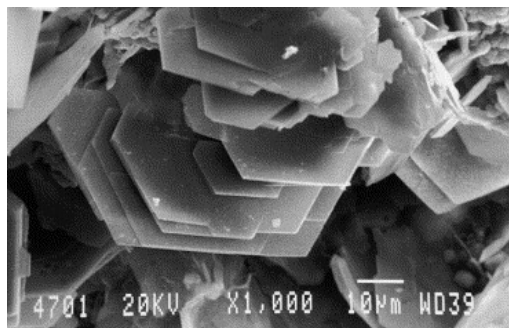


Figure 2.9: Plated-like of calcium hexaaluminate hydrate (Alcocel, 2000)

2.2 Corrosion of steel and factors affecting corrosion

2.2.1 Corrosion of steel and types of corrosion

As standard potential of iron versus standard hydrogen electrode is $-0.447V$, iron and ordinary carbon steel are corroded easily. Nowadays, two methods usually apply to protect steel in particular and metal in general to avoid corrosion, surface coating and electrochemical protection.

For surface coating method, coatings or inhibitors such as zinc, aluminum, alloy, epoxy, sodium nitride, or some organic compound etc. have been covered on the surface of steel. This layer prevents metal contacting with environment outside; therefore, it can prevent the corrosion of steel.

Meanwhile, the principle of electrochemical protection bases on behavior of steel under different environment. For this method, from Pourbaix diagram as shown

in Figure 2.10, which seems that there are two regions where steel may not be corroded when it is put on there, immunity zone and passivity zone. Hence, these are two techniques can be applied to prevent the corrosion progress of steel, anodic protection and cathodic protection. In anodic technique, steel is put on passivity zone. Differently, in cathodic protection, steel is put on immunity zone.

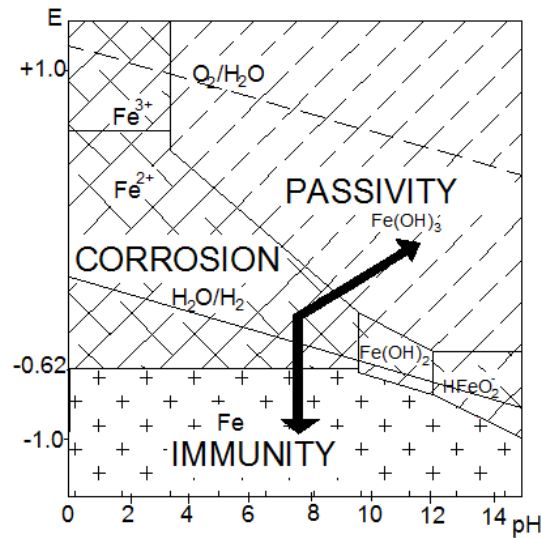
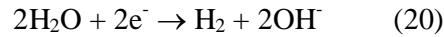
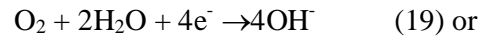
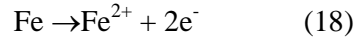


Figure 2.10: Pourbaix diagram

However, Pourbaix diagram have only shown the thermodynamics of process, it does not give any information about kinetics of this corrosion process. Then, kinetics of corrosion process as steel worked in every ambient environment need to be considered. Therefore, corrosion state of embedded steel can be estimated and the maintenance can carry out at right time to prolong the lifetime of structure.

Corrosion of steel is an electrochemical reaction. It involves two reactions occurred simultaneously, anodic reaction, an oxidization of steel as shown in equation (18) and cathodic reaction, a reduction of agents on ambient environment of steel. In concrete, cathodic reaction is the reduction of oxygen or water as shown in equation (19) or equation (20). Usually, the reduction of oxygen is main cathodic reaction. However, while embedded steel is working in some special cases such as quite negative potential/high cathodic current, carbonate attacked then pH of vicinity of embedded steel diminished or the lack of oxygen in vicinity, the reduction of water prevails.



These two processes are connected by an environment that can conduct electricity. In reinforced concrete, that environment is concrete with free ions in pore solution.

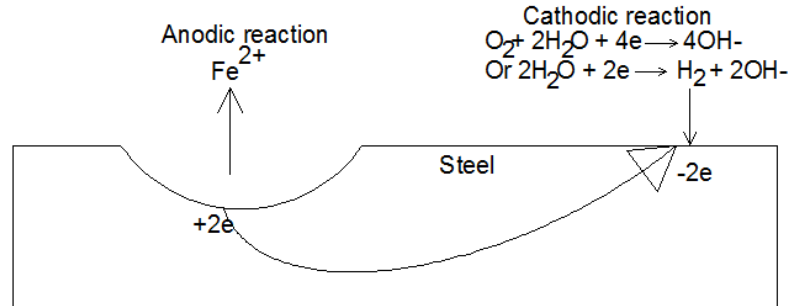


Figure 2.11: Corrosion of steel

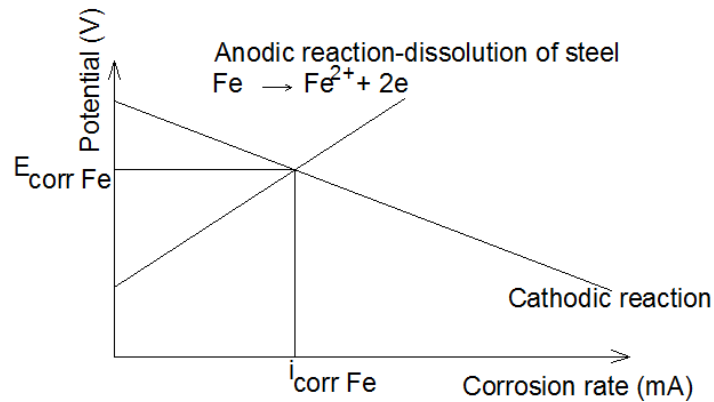


Figure 2.12: Polarization curves of corrosion process

From electrode reactions and polarization curves as shown in Figures 2.11 and 2.12, it seems that, if there is an excess of electrons provided for steel, anodic reaction (the oxidation of steel) will be reduced. Then, the corrosion rate of steel will reduce. That is the principle for cathodic protection or cathodic prevention; the methods can prevent or mitigate the corrosion of steel in particular and of metals in general. That excess of electrons can be supplied by using sacrificial anode or using impressed current.

By using sacrificial anode, electrons spent for cathode reaction are supplied from the other metals such as zinc, aluminum or other comfortable metals which have lower potential than steel and the reduced range of corrosion rate of steel mainly depends upon the potential and properties of sacrificial metal as shown in figure 2.13. The higher corrosion rate of steel results the higher rate of cathode reaction. So, it needs more electrons supplied from sacrificial anode, thus, anode is spent quicker. Therefore, evaluation and choice the suitable anode and its size are very important to provide a corresponded lifetime of structure.

Conversely, by using impressed current, anode is an inert material that has to discharge the impressed current well such as platinum, titanium etc as shown in figure 2.14. Similar with using sacrificial anode, to reduce corrosion rate of anode, cathode rate need to be increased as shown in Figure 2.15. Therefore, computation for impressed current is necessary to obtain the suitable current; so, it can supply enough electrons for cathode reaction, concurrently, conserved energy.

Based on physical state and reactions, corrosion of metal can be divided to many types. Some are usually mentioned in most of cases are uniform corrosion, galvanic corrosion, pitting corrosion, erosion corrosion, crevice corrosion, stress corrosion, intergranular corrosion, hydrogen corrosion, micro-biological corrosion, water line corrosion, soil corrosion, differential aeration corrosion. In marine environment, pitting corrosion plays main role on corrosion process in reinforced concrete.

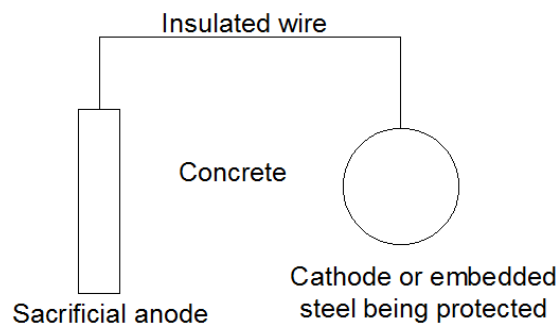


Figure 2.13: Cathode protection by using sacrificial anode diagram

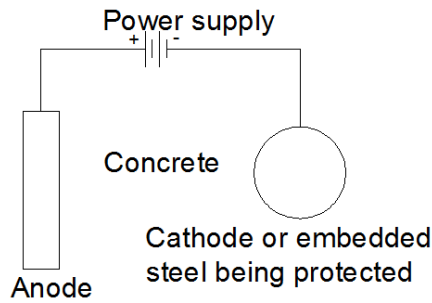


Figure 2.14: Cathodic protection by using impressed current diagram

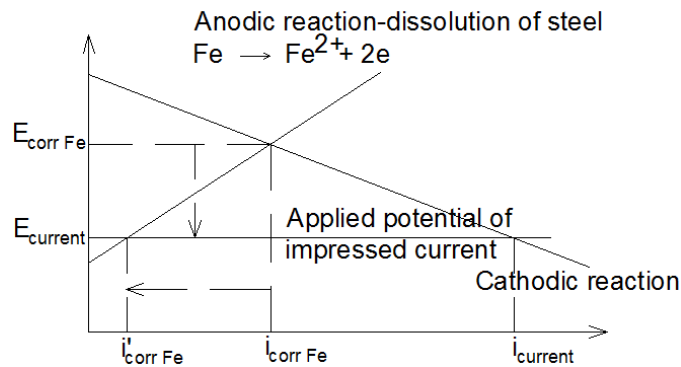


Figure 2.15: Polarization curves of cathodic protection by using impressed current

2.2.2 Factors affecting the corrosion

Corrosion of steel in reinforced concrete can be described in terms of three discrete stages including initiation stage T_i , propagation stage T_p and finally, damage stage T_d as shown in Figure 2.16.

It starts on initiation stage T_i . At this stage, concentration of harmful ions affecting on corrosion are low or the corrosion reactions might occur very slowly and there might not occur physical damage. The duration of that stage T_i may begin from the time structure served depending on the vicinity.

The initiation stage is followed by the propagation stage T_p . In this stage, the corrosion process of embedded steel occurs or be continuing. This stage is accelerated due to the accession of a sufficient amount of aggressive ions such as carbonate, chloride, sulfate, etc. into concrete cover. New expansive products of corrosion process cause a large internal stress at interfacial zone. Although in this stage, this stress is still not enough to break concrete cover the large amount of harmful

aggressive ions diffused in concrete alters the basic pore solution of concrete. It affects strongly on kinetics process of corrosion.

And final stage on deterioration of reinforced structure is damage stage T_d . In this stage, the combination of physical effects and chemical effects occur. The condition of fabric reaches on severity very fast. It may collapse any time and remedial works cannot usually affect. In some cases, structures were demolished to avoid sudden dangerous failure.

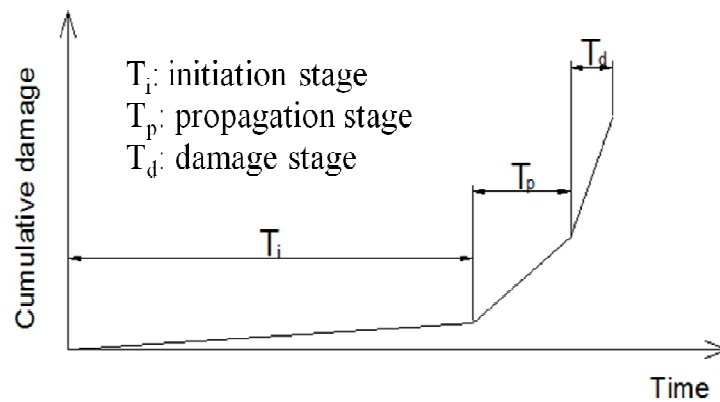


Figure 2.16: Corrosion processes of embedded steel in reinforced concrete

Duration of each stage determines lifetime of fabric and affected by many factors. These factors can be considered as two main groups that are characteristic of steel and property of concrete.

The different types of embedded steel show the different behavior of steel on corrosion process. Moreover, the texture of steel surface also distributes a meaningful role on deterioration process of reinforced concrete structure. Nowadays, coating steel or stainless steel have been studied and applied. They have shown an excellent corrosion resistance in maintaining the capability of structure in chloride environment. However, they have to encounter with two main problems, costing of structure and bonding strength between coating steel bar and concrete.

Pore solution in concrete is the main factor affecting on corrosion kinetics of embedded steel. However, beside concrete properties such as components, permeability, thickness, strength, resistivity, etc. pore solution can change easily under affecting of vicinity such as temperature, present of chloride, carbonation, property of water fluid, etc.

2.2.3 Types of chloride in concrete and their effects on reinforced concrete

In mortar or concrete, chloride can exist under three types (Song, 1998) including absorbed chloride, adsorbed chloride and free chloride. Meanwhile absorbed chloride exists in concrete or mortar by chemical bond due to chemical reactions between some constituents of cement hydration products and chloride as shown in equations (21) and (22) and Figure 2.17, that bond is only broken by the strong acids, such as nitric acid and called as bound chloride; adsorbed chloride exists in concrete or mortar by physical bond such as hydrogen bond, Van Der Waals bond or surface tension, etc. That bonding is easily broken by environmental changes such as temperature, pH, surface area etc. The most important type of chloride in concrete is free chloride, that is the main chloride content can go through concrete cover and contact with steel surface, hence, affected on the corrosion of embedded steel as shown in Figure 2.18.

The corrosion rate of embedded steel has close ties with the $[Cl^-] / [OH^-]$ ratio on the surface of steel. The higher OH^- concentration that ambient environment has; the chloride content needs so it can affect on corrosion of steel is higher. Hence, which can conclude, if the role of chloride dominates, the oxidization of steel is faster, conversely, if the role of hydroxide dominates, the products of oxidization $Fe(OH)_2$ $Fe(OH)_3$ can precipitate and the passive film of steel might re-healed. Some standards such as ASTM or BS suggested the threshold value of $[Cl^-]/[OH^-]$ ratio is 0.4.

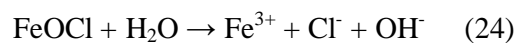


From Ivans diagram for passive iron in aerated water, which seems that, at pH of ambient environment in range of 9.5-13, steel is automatically protected on passive region with quite low corrosion current. And concrete, with alkaline environment on pore solution is a good protective agent (Winston Revie, 2011). However, nowadays it is very easy to realize that even a thick layer of concrete with high density cannot still prevent the corrosion of steel in reinforced concrete through a long time, especially since it worked in chloride condition. Research showed the modification on both Pourbaix diagram and Ivans diagram when reinforced concrete exposed in chloride environment as shown in Figures 2.19 to 2.21 (Gowripalan, 2000).

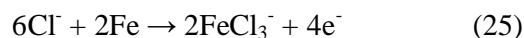
From modified Pourbaix diagram as shown in Figure 2.21, it seems that, with the occurrence of chloride, corrosion zone is expanded significantly compared to original Pourbaix diagram as shown in Figure 2.10. Especially, there is an existence of large pitting corrosion zone, the most important reason responsible for collapse of reinforced structure due to corrosion of steel. Furthermore, modified Evans diagram as shown in Figure 2.20 indicates that, the occurrence of chloride also promotes kinetics of corrosion process. It is clearly that, with the same potential of steel, the corrosion current increases meaningfully when chloride content in ambient environment of steel increases. And when chloride in solution reaches to a threshold value, passive range would disappear, and steel would be totally active.

Mechanisms for the interaction between free chloride, steel and passive layer are still being studied. Nowadays, it is usually explained by three main theories (Luo, 2003), adsorption-induced pitting mechanism, film-breakdown pitting mechanism and ion penetration/migration pitting mechanism, respectively.

On adsorption and adsorption-induced pitting mechanism, this was assumed that, chloride or aggressive anions can adsorbed on the surface of steel and combine with ferrous/ferric of passive layer to form complex compound with higher solubility than original passive layer as shown in equations (23) and (24). Then, passive layer thickness was reduced and finally this layer disappeared.

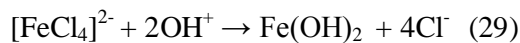
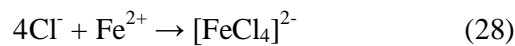
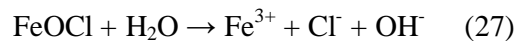


On the other hands, film-breakdown pitting mechanism was assumed that passive film on the surface of steel had already existed defects or cracks, and aggressive anions in general or chloride in particular can access and attack directly the unprotected steel surface as shown in equation (25). This process prevented the re-healed capacity of steel on alkaline environment. Therefore, the localized corrosion was spreaded.



Nowadays, ion penetration/migration pitting mechanism has been accepted more popular than the other mechanisms. In this hypothesis, the authors assumed aggressive anions, such as chloride can transfer through passive layer to metal-oxide

interface. The presence of chloride in the surface of passive oxide layer or in passive oxide layer accelerated the migration of cation vacancies from oxide-electrolyte interface to metal-oxide interface due to the fitting of chloride to anion vacancies O^{2-} . Then, the barrier potential at the surface dropped; meanwhile, the penetration of cation vacancies into the metal phase was prevented; then, they stressed at oxide-metal interface of passive film and broke it down. Moreover, chloride reacted with iron cation to producing temporary complex compound, which had high solubility and transport further away the steel surface. In there, this complex compound dissociated and released chloride. This process described as a range of reactions as shown in equations (26) to (29).



However, some researchers believe that, the mechanism of corrosion of embedded steel in reinforced concrete on chloride environment the association of above three mechanisms.

From the harmful effects of chloride, the question was raised as, what happen if chloride content in concrete reduced, how corrosion of steel would be stopped?

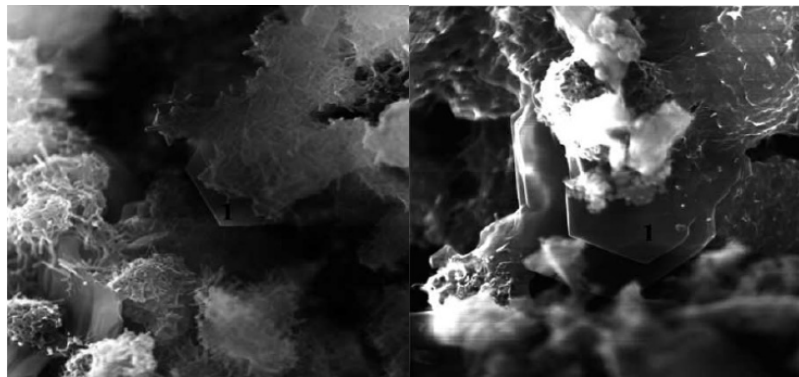


Figure 2.17: Scanning electron microscope (SEM) of Friedel's salt (Luo, 2003)

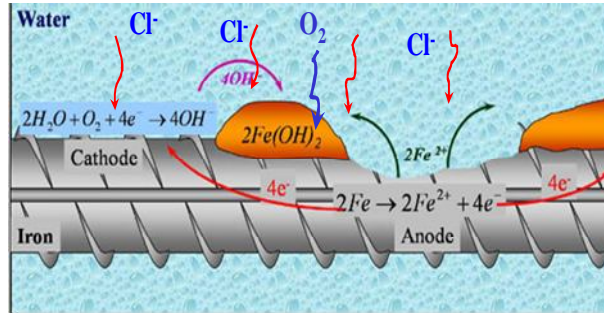


Figure 2.18: Corrosion process in chloride environment

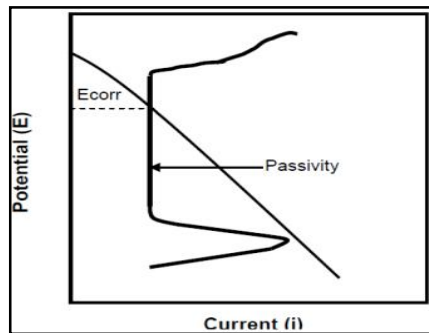


Figure 2.19: Evans diagram

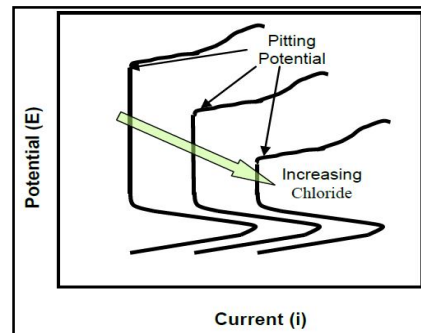


Figure 2.20: Modified Evan diagram

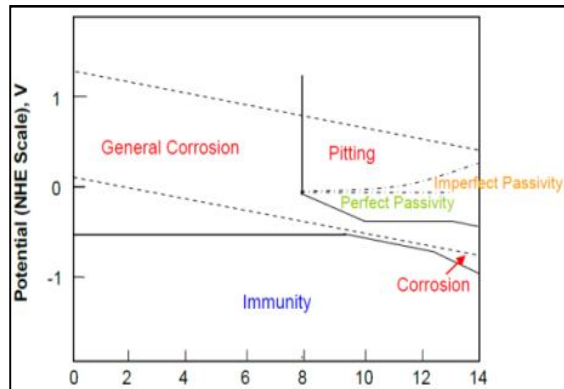


Figure 2.21: Modified Pourbaix diagram

2.3 Electrochemical re-alkalization (ERA) and electrochemical chloride extraction (ECE)

2.3.1 Electrochemical re-alkalization (ERA)

When reinforced concrete fabrics are working in atmospheric condition, they usually confront with carbonated problem, especial in urban areas. In high carbonic concentration environment, it can react with hydroxide ion in pore solution of

concrete and diminish alkalinity of pore solution of concrete. When pH of pore solution is less than 9, it can cause uniform corrosion or generalized corrosion and reduce lifetime of structure. There are many techniques to recover the structure after corrosion due to decreasing alkalinity of pore solution. By many reasons such as cost, time, installation, dust, noise, etc electrochemical re-alkalization is nowadays considered as a good technique to rehabilitate the structure due to carbonation.

In most of studies, they indicated that, four weeks treatment of ERA with sodium solution such as sodium hydroxide, sodium carbonate solution is a appropriate condition of re-alkalization for structure attacked by carbonate.

2.3.2 Electrochemical chloride extraction (ECE)

Nowadays, the role of chloride on the corrosion process in reinforced concrete cannot controvert. So, the question has been put forth that, if chloride content in concrete was reduced by applying electrical current, could corrosion process prevent?

In 1993, some of the first manuals about applying electrochemical chloride extraction on bridge were published due to Strategic Highway Research Program regardless of debating. Simultaneously, this method, at that time, was applying to rehabilitate some contaminated-chloride bridges and substructures in Ohio, New York and Ontario. The useful results on long-term effects of that method on corroding structure did not stop the current argument. Many researches have been occurring to prove for the interest of this method; however, many uncertain results are still remaining. Then its feasibility is still a questionable.

One of first fairly complete research on the effect of electrochemical chloride extraction was the study of Marcotte (Marcotte, 1999). The effect of electrochemical chloride extraction treatment on both embedded-steel and mortar of steel-reinforced mortar with water/cement ratio 0.5 was considered. Chloride sources were supplied by three ways, added sodium chloride into mixing water in admixed chloride case, immersing specimens into 1M sodium chloride solution in ingressed case or both, respectively.

However, the results were not feasible as expected. Although chloride was not detected at interface between mortar and embedded steel, the state of corroded embedded steel showed more harmful by half cell potential of steel measured after

halting extraction process 31 days. Moreover, new cementitious phases were formed with high content of sodium and calcium and less adhesive capability at interface; meanwhile C-S-H was not detected. These were considered as the main reasons for the loss of bonding strength between steel and mortar/concrete after treatment and high concentration of alkali cation there may cause quite high basic environment, a risk for alkali silica reaction. However, extracted process showed that the role of added or ingressed chloride in concrete were the same on ECE.

On the other researches, G. Fajardo and colleagues (Fajardo, 2006) studied the effect of ECE on reinforced concrete chloride-contaminated by immersing in artificial sea water. Besides, they considered the effect of ECE on thickness of concrete. Two sets of thickness cover concrete specimens were casted, 20 mm and 50 mm, respectively with water/cement ratio 0.6. Specimens after curing were immersed with cycles of three days in sea water followed by four days dried at 40⁰ C within 300 days. Extraction process was applied with distilled water as electrolyte and current density 1A/m² in respect of steel surface within 90 days.

Different with the research of Marcotte (Marcotte, 1999), the results in this study showed a feasibility of ECE on mitigating corrosion of steel. Although the increased rate on half cell potential was not enough to re-put embedded steel on passivity zone after extraction, the half cell potential steel increased efficiency in both cases of thickness cover. However, the efficiency on reducing chloride content in concrete was remarkable difference. At specimens with thickness cover 20 mm, chloride content diminished 75% of initial chloride content; meanwhile, chloride content in specimens with thickness cover 50 mm reduced only 34% and the remained chloride content focused on mid-section of concrete thickness.

Studying on microstructure of steel surface and alkali content in concrete after treatment indicated doubtful effect of this method similar as the research of Marcotte (Marcotte, 1999). Accumulation of alkali ions on the concrete layer near steel surface increased the risk for alkali silica aggregate reaction. Furthermore, the higher pH of environment at the surface of steel after ECE treatment made convenient condition for the dissolution of steel at high pH zone. That harmful effect was showed by the darker color of corrosion products at the steel's surface after treatment.

From their results, they deduced that, the extraction treatment had effectively in reducing chloride content in concrete had thin cover layer, however it did not have

more effect in thick concrete cover, even with the concrete had high w/c ratio (0.6). However, they suggested that, ECE method can be applied to rehabilitate the corrosion of steel when we combine this method with other method, such as using inhibitor.

Inversely, S. N Swamy investigated the effectiveness and structural implications of ECE from reinforced concrete beam. Some variables such as w/c ratio, chloride content and reactive aggregates were studied. Sodium chloride was added in mixing water when the beams were casted to provide chloride content. Simultaneously, reactive aggregate was used to evaluate the effect of ECE on the alkali silica reaction by synthesizing from fused silica.

The result showed that, pH of specimens with w/c ratio 0.75 dropped faster than specimens with w/c ratio 0.6. Simultaneously, although the reduction of chloride content was significant on all specimens, the rate of reduction depended upon initiated chloride content, position of the cores; dropped rate of chloride content may reach to 70%-75% at the cover and average 50%-60% at the tensile or compressive zone. Meanwhile, in range of 50-75% of initiated chloride content still remained at the mid-section of specimen after treatment. In the other hands, the higher w/c ratio concrete; the more chloride content which still remained. Specially, chloride profiles were similar for the nonreactive aggregate case or reactive aggregate case, specimens had higher w/c ratio or higher initiated chloride content, EC treatment had better efficient.

When alkali silica reactivity was considered, they realized that, with specimens had 5% fused aggregate, after treatment, crack was not observed by visual examination at specimens had w/c ratio was 0.75, but at specimens had w/c ratio was 0.6, the slight cracks were observed, especial at the non-stirrup compressive zone. With specimens had 15% fused aggregate and w/c ratio was 0.6, the cracks were more clearly after treatment, they extended to a map, especial at the mid-section. The crack map by alkali silica reaction of specimens had w/c ratio was 0.75 showed slighter. Moreover, there was not strong harmful effect on the strength of structure, even the specimens were with or without reactive aggregate. Hence, they inferred that, ECE can apply with the confidence on the loss strength, safety or structural stability and it can be accepted as an efficient and economical rehabilitation method.

However, research results of Xiaogian Gao (Gao, 2011) on pre-corroded reinforced concrete by using ECE was totally different. In their study, they applied

ECE for concrete had quite low w/c ratios (0.45, 0.38 and 0.32), fly ash cement as a binder and pre-corroded steel. Specimens were cylindrical concrete of 100 mm diameter and 150 mm height with central steel rod of 10 mm. 3% chloride content by weight of cement was provided due to sodium chloride mixed with water when casted concrete. Electrolyte was saturated calcium hydroxide. The specimens were fixed titanium mesh and applied ECE with density current was $2A/m^2$ of steel surface. In ECE process, electrolyte was renewed every two days and treatment time was 28 days and treatment period was 7 days, 14 days and 28 days respectively.

Significant increase of resistivity of concrete after treatment was observed; although the increase rate at specimens had fly ash was lower. That was a good signal for ability of rehabilitation of concrete and reinforced concrete after contaminated-chloride.

However, results on steel was not feasible as above result; after treatment, half cell potential of steel reduced meaningful in comparison to SCE, especially at the first 7 days. Moreover, in specimens using fly ash cement, the higher content of fly ash, the decrease rate of corrosion potential was more. Investigation the evolution of density current of steel, unfortunately, after treatment, it increased remarkably. Furthermore, the increase of density corrosion current corresponded with the decrease of half cell potential.

On the other hand, some tests about the accumulation of alkali ions and the transformation of minerals at interface of steel and concrete still showed unfavorable characteristics. Accumulation of Ca^{2+} , Na^+ , K^+ at the surface of steel made convenient condition for corrosion of steel in alkaline environment (proved by white substance on steel surface).

Furthermore, some steel samples had the black-brown rust on their surface, it proved that, that steel samples were corroded very severe. In addition, investigation about the mineral structure at the steel surface showed the risk of loss of adhesion strength due to the formation of sodium-calcium-rich crystals instead of CSH phase in amorphous form or weak crystalline form.

In addition, investigation about the mineral structure at the steel surface showed the risk of loss of adhesion strength due to the formation of sodium-calcium-rich

crystals instead of CSH phase in amorphous form or weak crystalline form. Similarly, with concrete zone near steel bar, it was very easy to observe the large content of plate-like crystals and sodium-calcium-rich crystal.

Besides, C-S-H phases were hardly to observe there. From that result, they inferred that, although ECE can reduce remarkably chloride content in concrete, but it cannot be accepted as a rehabilitation method due to the appreciable decrease of half cell potential as well the significant increase of density corrosion current after treatment. Moreover, results on fly ash concrete, the type concrete has been used popular, showed more disadvantages; when fly ash content was higher, the risk for corrosion of steel after treatment was more severity. In addition, it may reduce the adhesion strength and increased the risk of alkali silica aggregate reaction due to the focus of large concentration of alkali ions at the section near steel surface.

By comparison, many research studied with initial chloride content higher than 2% by mass of cement, such as the research of G Fajardo et al (4.6% initial total chloride by mass of cement) (Fajardo, 2006), Orellan et al (18kg/m³ by mass of concrete, approximate 4.5% initial free chloride content by mass of cement) (Orellan, 2004) or Xiaojian Gao (Xiaojian Gao, 2011) (3% initial total chloride content by mass of cement) also showed the inefficiency of ECE. After treatment, it was easy to observe that remained chloride content in concrete was still quite high in comparison with chloride threshold value (more than three times).

On the contrary, almost research with initial chloride content was lower than 2% by mass of cement indicated the feasibility of this method, such as Elsener (initial chloride around 1%) (Elsener, 2007) or Abdelaziz (1% and 2%) (Abdelaziz, 2009).

Clearly, initial chloride content has affected on corroded situation of steel prior ECE treatment. Since concrete was contaminated high chloride content, embedded steel in reinforced concrete could suffer corrosion on a long time and on more severe condition. Therefore, ECE could be an efficient method only in case the structure is on the beginning of corrosion process. If the corrosion process has happened during a long time, this method may not be a good choice. Investigating the initial chloride content before treatment is a necessary work to decide the practical method to restore the structure.

Impressed current density is also a controversial parameter. A wide range of impressed current density was applied. Some researchers were based on the steel surface to compute impressed current whereas some others based on concrete surface. Usually, in most of previous studies, steel surface/concrete surface was quite small. Then, the current density was computed base on concrete surface supplied an electric field much higher than impressed current density computed with respect to steel surface. Under effect of electric field anions were repulsed far away cathode and forwarded to anode meanwhile cations were attracted towards cathode. Therefore, electrical field played important role on evaluating feasible of ECE.

On the research of Abdelaziz (Abdelaziz, 2009) an impressed current density with $1\text{A}/\text{m}^2$ or $2\text{A}/\text{m}^2$ related to mortar surface (corresponding to $10.95\text{ A}/\text{m}^2$ or $21.9\text{ A}/\text{m}^2$ related to steel surface), respectively were applied. By results of electrochemical parameter measures after treatment, ECE was considered as a feasible method to restore the passivity layer of steel.

Meanwhile, on the researches (Xiaojian Gao, 2011) (Orellan, 2004) (Fajardo, 2006), by using much lower impressed current, in range of $1\text{A}/\text{m}^2$ or $2\text{A}/\text{m}^2$ related to steel surface, corresponding to $0.04\text{-}0.2\text{A}/\text{m}^2$ related to concrete surface, their results showed an inefficiency after treatment. Under effect of so low impressed current, the corresponded electric field cannot form a strong force to repulse chloride out of concrete cover and reduce capable to re-passivate steel surface.

Prolonging time of treatment to release more chloride ion out of concrete was not a good choice. Since ECE was applied too long time, the effectiveness on releasing chloride reduced significant (Fajardo, 2006). Moreover, it brought about the harmful on microstructure of concrete. The average maximum of chloride released could reach 70% of initial chloride content. However, by many research, to lessen the harmful effect on concrete and steel can approach to passive state, chloride should be extracted about 30% to 40% initial chloride content.

Essentially, principle of electrochemical chloride removal is similar with cathodic protection by using impressed current. An impressed current was applied to reinforced concrete with embedded steel as cathode and an external electrode was built up on the concrete surface as anode. However, they also had two basic differences. Firstly, it needs an electrolyte to ensure circuit process. Secondly,

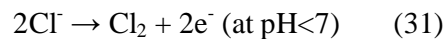
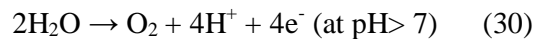
because this method applied on the short time, then, the impressed current is usually higher than cathodic protection.

Some basis differences between ECE, ERA and cathodic protective were given in table 2.1.

Table 2.1 Basic differences between cathodic protection, ECE and ERC

| | Cathodic protection | ECE | ERA |
|--------------------|---|--|--|
| Electrolyte | non | Water Saturated calcium hydroxide solution Sodium or lithium borate solution | Water Sodium carbonate solution Potassium carbonate solution |
| Duration | lifetime | Six to twelve weeks | Four to six weeks |
| Current density | 4 ~ 260 mA/m ² with respect to steel surface | On studying-wide range (Marcotte, 1999) | 1 ~ 2 A/m ² with respect to steel surface |
| Efficiency | Accepted | On arguing | Accepted |
| Cause of corrosion | Aggressive environment | Chloride environment | Carbonation |

Although the electrolyte is only responsible for conducting the current, but due to characteristic of concrete, electrolyte should be an alkaline solution. Under application of impressed current, negative charges, including chloride ions move to the positive electrode. At this electrode, the reduction of water or chloride may occur as shown in equations (30) or (31).



Chloride content is newly formed can re-oxidize and forms an acidic environment as shown as in equation (32).



Therefore, an alkaline electrolyte is necessary to avoid the etching the concrete surface. Due to the solubility of calcium hydroxide at tropical temperature zone is

around 1.55g/l, it associates with pH in range of 12-13. Hence, saturated calcium hydroxide solution is the most popular electrolyte. In addition, some buffer solutions were suggested as sodium borate buffer, lithium borate buffer (pH of these solutions was not below 6) or lithium nitrate (pH=7). In fact, for some structures may be occurred alkali-silica reaction, lithium solutions were usually used due to non-clearly reasons.

The second problem, this is impressed current. Although the higher current of its process is applied, the faster removal of chloride can happen; however, there were many disputes about the response of concrete under conduction current as well as the long-term response of steel after stopping the applied current. And many researchers suggested that impressed current should be in range of 0.5A/m^2 to 5A/m^2 of concrete surface area.

CHAPTER III

METHODOLOGY

3.1 Materials

The first material mentioned here was ordinary Portland cement type 1 in accordance with ASTM C150. Chemical compositions of cement were given as shown in table 3.1. Simultaneously, specific gravity, Blain fineness and strength of cement were also determined as shown in table 3.2.

In accordance with ASTM C114 and ASTM C618, fly ash used in this study was fly ash type F. Chemical compositions and some physical criteria of fly ash (FA) are shown in Table 3.3 and 3.4. The last component of binder was limestone powder (LP) that had chemical compositions, Blain fineness, specific gravity and mineral compositions as shown in tables 3.5 and 3.6.

Superplasticizer type F was used with specification as shown in table 3.7.

Coarse aggregate using in this study was limestone with specific gravity 2.6 g/cm³ and bulk specific density 1.55 g/cm³. The particle size distribution of coarse aggregate is shown in Figure 3.1. Fine aggregate was river sand with fineness modulus 2.62 and particle size distribution given as shown in Figure 3.2.

Due to requirement of applying extraction, some chemical substance need to be prepared such as calcium hydroxide, acid boric, lithium hydroxide and sodium chloride with industrial grade.

Embedded steel using in this study was ordinary deformed bar grade SD40 with diameter 10mm according to TIS 24.

Table 3.1: Chemical compositions of cement (% by weight)

| SiO ₂ | Al ₂ O ₃ | Fe ₂ O ₃ | CaO | MgO | SO ₃ | Na ₂ O | K ₂ O | P ₂ O ₅ | LOI | CaO _{Free} |
|------------------|--------------------------------|--------------------------------|-------|------|-----------------|-------------------|------------------|-------------------------------|------|---------------------|
| 19.87 | 4.87 | 3.55 | 65.03 | 2.52 | 0.73 | 0.02 | 0.45 | 0.07 | 2.26 | 0.20 |

Table 3.2: Physical properties of cement

| Specific gravity (g/cm ³) | Blain fineness (cm ² /g) | Strength (MPa) |
|---------------------------------------|-------------------------------------|----------------|
| 3.11 | 3480 | 50.2 |

Table 3.3: Chemical compositions of fly ash (% by weight)

| SiO ₂ | Al ₂ O ₃ | Fe ₂ O ₃ | CaO | MgO | SO ₃ | Na ₂ O | K ₂ O | P ₂ O ₅ | LOI | CaO _{Free} |
|------------------|--------------------------------|--------------------------------|-------|------|-----------------|-------------------|------------------|-------------------------------|------|---------------------|
| 39.4 | 17.93 | 12.92 | 19.19 | 2.99 | 3.03 | 1.36 | 2.50 | 0.20 | 0.17 | 1.60 |

Table 3.4: Physical properties of fly ash (FA)

| Specific gravity (g/cm ³) | Blain fineness (cm ² /g) | Strength activity index | |
|---------------------------------------|-------------------------------------|-------------------------|---------|
| | | 7 days | 28 days |
| 2.99 | 2836 | 78 | 85 |

Table 3.5: Chemical compositions of limestone powder (LP) (% by weight)

| SiO ₂ | Al ₂ O ₃ | Fe ₂ O ₃ | CaO | MgO | K ₂ O | Na ₂ O | SO ₃ | LOI | Moisture |
|------------------|--------------------------------|--------------------------------|-------|------|------------------|-------------------|-----------------|-------|----------|
| 0.42 | 0.11 | 0.08 | 55.23 | 0.48 | 0.01 | 0.01 | 0.01 | 41.16 | 0.1 |

Table 3.6: Mineral compositions (%), Blain fineness (cm²/g) and specific gravity (g/cm³) of limestone powder

| Calcite | Dolomite | Hematite | Gypsum | Kaolin | Pyrite | Quartz | Blain | SG |
|---------|----------|----------|--------|--------|--------|--------|-------|------|
| 97.0 | 2.0 | 0.7 | - | - | 0.3 | - | 6876 | 2.69 |

Table 3.7: Specifications of superplasticizer

| Items | Specification |
|--|--|
| Visual appearance | Brown viscous liquid |
| Solid content (%) | 40.0±2.0 |
| Density (23 ⁰ C) (g/cm ³) | 1.14±0.02 |
| Chloride content (%) | Non chloride ion |
| pH | 8.5-9.5 |
| Sodium sulfate content (%) | <0.4% |
| Equivalent alkali content (%) | <0.5 |
| Performance | As 0.5%-1.0% of the used cement weight |
| Keeping time | One year at least in closed containers away direct sun |

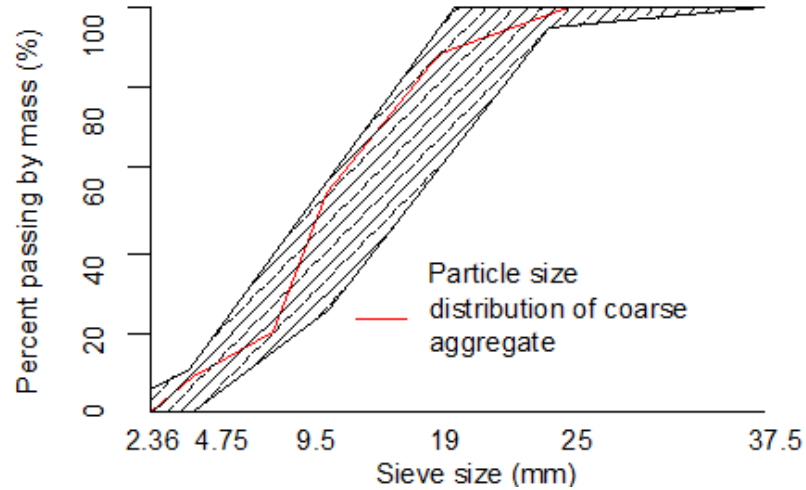


Figure 3.1: Particle size distribution of coarse aggregate (ASTM C136)

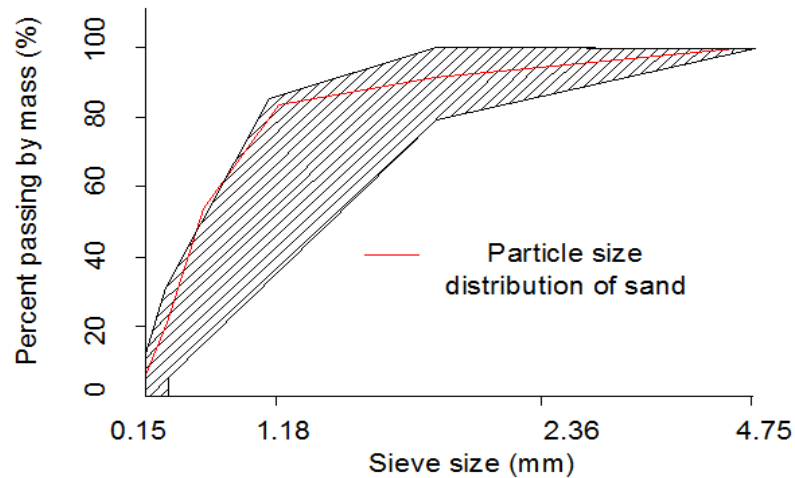


Figure 3.2: Particle size distribution of sand (ASTM C136)

3.2 Specimen preparation

As above mentioned, the application of ECE on concrete with low water/binder ratio or blended cement has been rarely investigated. Thus, its effectiveness on types of concrete is still unknown. Therefore, concrete with low water/binder ratio and admixture concrete should be researched to contribute some basic data for following research.

As well known, the most popular chloride environment is sea water, so, as ACI 381 and ACI 211, the maximum water/binder ratio is 0.40; the minimum compressive strength and concrete thickness cover are 5000ksi (34.5MPa) and 7cm, respectively. Therefore, in this study, concrete with below criteria would be designed:

- Water/binder ratio was 0.40.
- Compressive strength was higher than 35MPa.
- Concrete thickness covers were 7 cm and 4.5 cm, respectively.
- Fly ash content in fly ash concrete was 0% and 30% by mass of binder, respectively.
- In limestone fly ash concrete, limestone content and fly ash content were 5% and 25% by mass of binder, respectively.

Mix preparation of concrete was shown in table 3.8.

Chloride source was provided from sodium chloride. According DPT 1332-50, reinforced concrete with ordinary carbon steel, chloride threshold content is 0.4% by mass of binder, this content associate with 0.66% sodium chloride content. Thus, 2% sodium chloride by mass of cement was mixed with water when concrete mixed.

Concrete specimens were cylindrical specimens 150x300 mm and 100x200 mm with ordinary carbon steel rod at the centre of specimen as shown in Figures 3.3 and 3.4. Then, specimens were cured in water three months before testing. However, as mentioned, in this study, influence of ECE on steel would be investigated, so, the part steel have not covered by concrete (it would be cathode in electric circuit) should be protected by anti-paint to ensure the corrosion process of steel in this research affected only by contaminating chloride of concrete. After curing, specimens were measured resistivity of concrete and then, wrapped by stainless steel mesh to provide external anode for electric circuit as shown in Figures 3.5 and 3.6.

Table 3.8: Mix proportion of concrete

| Type | Content (kg/m ³) | | | | | | |
|------|------------------------------|--------|-----|----|------|------|-----|
| | Water | Cement | FA | LP | Sand | CA | S.P |
| PC | 190 | 475 | 0 | 0 | 659 | 1056 | 0.9 |
| FC | 190 | 333 | 142 | 0 | 659 | 1056 | 0.9 |
| LC | 190 | 333 | 119 | 24 | 659 | 1056 | 0.9 |

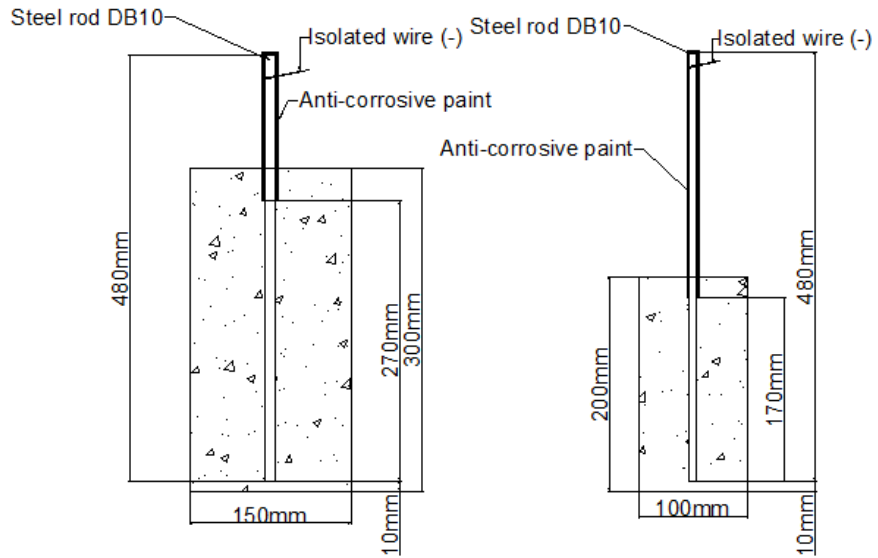


Figure 3.3: Cross-section and preparing specimens for experimental testing



Figure 3.4: Specimens for experimental testing

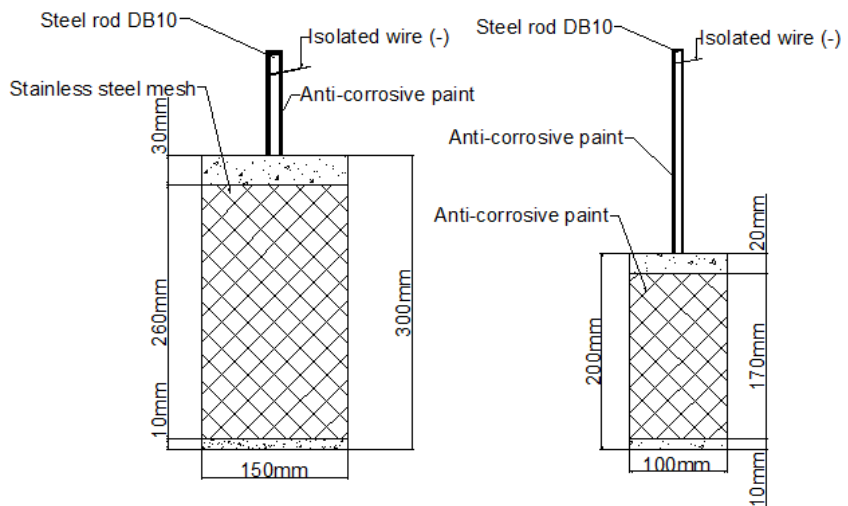


Figure 3.5: Installation for testing specimen



Figure 3.6: Installation for experimental testing specimen

3.3 Testing

As mentioned in literature review, electrolyte should be an alkalinity or basic buffer. Moreover, it should not be the solution of sodium or potassium because some research observed that after treatment, these ions may result from high alkaline environment due to chemical equilibrium. Thus, with solubility at the normal condition (28°C) is 0.155 g/ml; saturated calcium hydroxide (SC) respects to pH around 12.6; its solution is suitable to use as an electrolyte in this method.

Moreover, sodium borate buffer solution or lithium borate buffer solution was suggested by Strategic highway research program. However, nowadays, sodium compounds are avoided for concrete because it may make the alkali silica reaction risk, then lithium borate buffer would be applied to avoid the accumulation of sodium ions at the steel surface after treatment. In this, lithium borate buffer LiH_2BO_3 0.5M (LBB) was used.

Applied electric current was $0.5\text{A}/\text{m}^2$ (respect to surface area of concrete). By using equation (33) to convert concrete resistivity (measured by resipod concrete resistivity meter) as shown in table 4.2 to concrete resistance, voltage of supply power can be computed and applied to system.

$$R = \frac{\rho}{2\pi L} \ln\left(\frac{D}{d}\right) \quad (33)$$

R: the resistance of concrete (Ω)

ρ : the resistivity of concrete ($\Omega \cdot \text{cm}$)

L: the length of specimen (cm)

D: diameter of concrete specimen (cm)

d: diameter of steel (cm)

Table 3.9: Electrical parameters of specimens

| | D (cm) | Concrete surface (cm^2) | Current density (A/m^2) | Current (A) | ρ ($\text{k}\Omega \cdot \text{cm}$) | R (Ω) | Voltage (V) |
|-----|-----------|---------------------------------------|---|----------------|---|-------------------|----------------|
| PC | 10 | 534 | 0.5 | 0.027 | 12.7 | 258 | 7 |
| | 15 | 1225 | 0.5 | 0.061 | 11.3 | 180 | 11 |
| FC | 10 | 534 | 0.5 | 0.027 | 53.4 | 1259 | 31 |
| | 15 | 1225 | 0.5 | 0.061 | 49.4 | 819 | 50 |
| LFC | 10 | 534 | 0.5 | 0.027 | 37.9 | 815 | 22 |
| | 15 | 1225 | 0.5 | 0.061 | 36.6 | 606 | 37 |

Electrical parameters for each specimen were shown in table 3.9. The installation of fly ash concrete, limestone fly ash concrete and plain concrete with different applying electrical parameter was shown in figure 3.7 to 3.9.

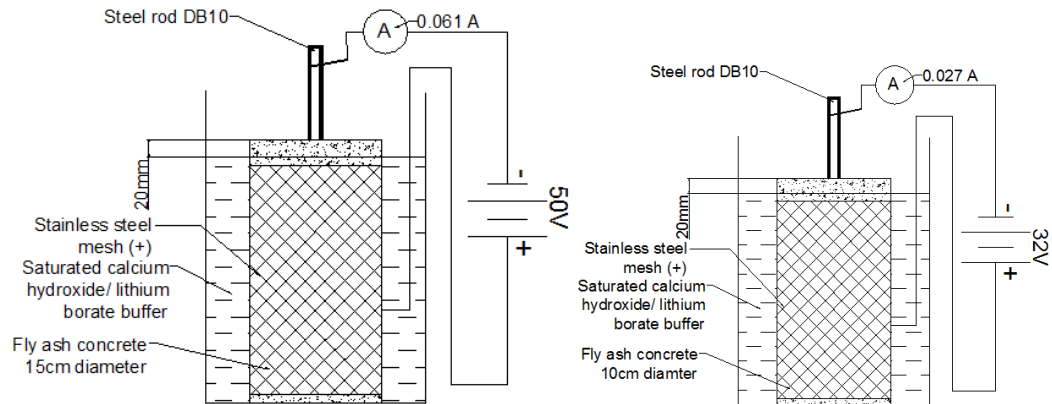


Figure 3.7: Installation of fly ash concrete in 15cm diameter and 10cm diameter

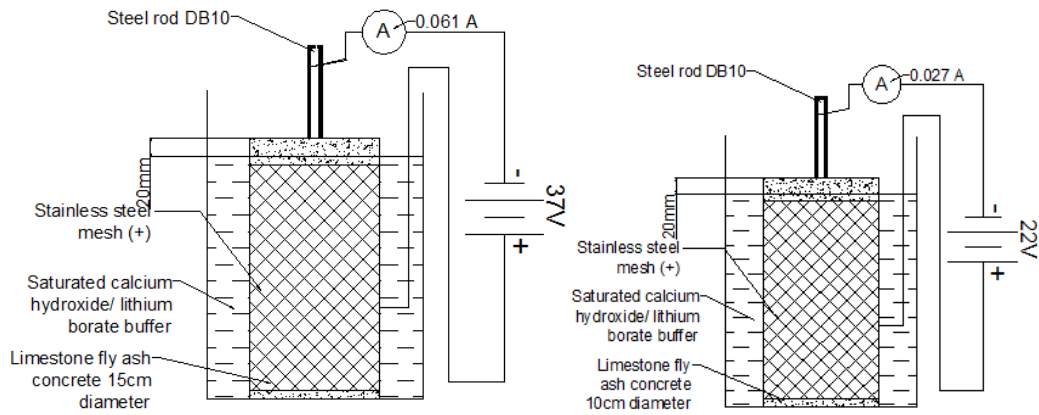


Figure 3.8: Installation of limestone fly ash concrete in 15cm diameter and 10cm diameter

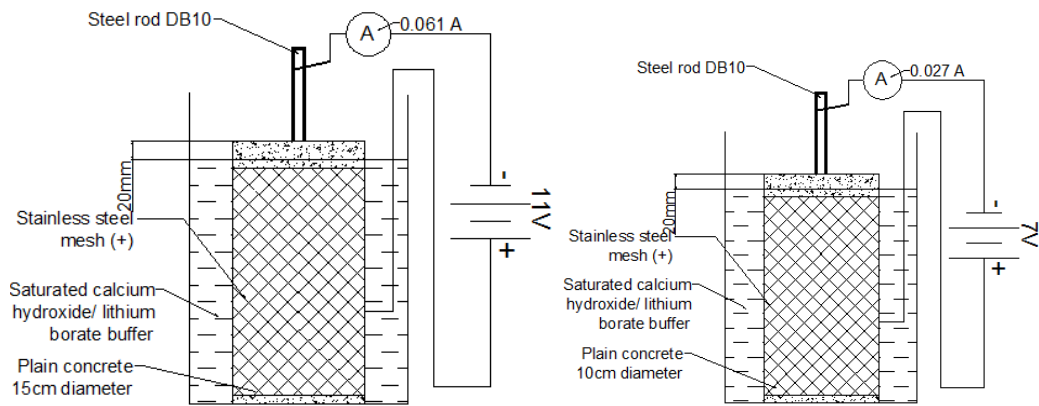


Figure 3.9: Installation of plain concrete in 15cm diameter and 10cm diameter

3.4 Measurement

Main purpose of this technique is to rehabilitate or mitigate the corrosion of steel due to chloride-contaminated in concrete. Therefore, characteristics of reinforced concrete would be compared before and after treatment. Moreover, long-term effects should be considered after treatment to estimate the feasibility of this method for extending lifetime of contaminated-chloride structure.

3.4.1 Effects of electrochemical chloride extraction on concrete

Chloride is one of the main reasons responsible for corrosion of embedded steel in reinforced concrete exposed marine environment. Then the distribution of chloride in concrete and the rate of reduction of chloride in concrete after ECE treatment have to determine. However, it is not an only criterion need to investigate.

Table 3.10: Timetable of extraction process

| Timetable during extraction process | Work |
|-------------------------------------|---|
| First week | -Turned on the system. -Analyzed chloride concentration in electrolyte at the end time. |
| Second week | -Turned off the system. -Replaced electrolyte. |
| Third week to sixth week | -Turned on the system. -Analyzed chloride content at the end of each week. |
| Seventh week | Turned off and replaced electrolyte |
| Eighth week to ninth week | Turned on the system and analyzed chloride concentration in electrolyte at the end of each week |
| Tenth week | Turned off and replaced electrolyte |
| Eleventh week to twelfth week | Turned on the system and analyzed chloride concentration in electrolyte at the end of each week |

As mentioned, in this study, the extraction process would be halted since 30-40% of initial total chloride content (acid soluble chloride content) was extracted. Extraction process was applied as shown in Table 3.10. Then, released chloride in electrolyte had to determine to control the process. Specimens was put on the same container and introduced with the same volume of electrolyte V.

After each week of extracting, about 150ml of electrolyte was collected to analyze chloride content was extracted from concrete by titrating the solution with silver nitrate 0.1N. Based on initial total chloride content was determined before extracting, released chloride content was measured by equation (34).

$$\% Cl_{released}^{-} = \frac{C_{AgNO_3} * V_{AgNO_3} * V_{Electrolyte} * 35.5}{V * \frac{V_{concrete} * \% Cl_{total}^{-} * 475}{100}} \quad (34)$$

Where: $\%Cl^-_{\text{released}}$: extracted chloride content (% by percentage of initial total chloride content).

C_{AgNO_3} : concentration of silver nitrate (N) = 0.1N

V_{AgNO_3} : volume of silver nitrate for titrating chloride in electrolyte (ml)

$V_{\text{electrolyte}}$: Volume of electrolyte in each particular container (V)

V: volume of electrolyte used for titrating (ml) = 25ml

V_{concrete} : volume of concrete in each container (m^3)

$\%Cl^-_{\text{total}}$: initial total chloride content in concrete before extraction (% by weight of cement)

Under the effect of electric field, anions migrate to anode and cations migrate to cathode. These processes affect on the microstructure of concrete, such as porosity, distribution of porosity and minerals in concrete, especial C-S-H phase, may decompose/transform and affect on the bonding strength between concrete and steel. Hence, these factors affect to long-term work of structure. To get a comprehensive view of effectiveness of ECE on concrete of reinforced concrete, some below criteria need to consider and compare.

Firstly, there are the distributions of bound chloride Cl^- content before and after treatment. Bound chloride content here was determined according to ASTM C1152M.

The distribution of sodium ion Na^+ , potassium ion K^+ , calcium ion Ca^+ and lithium ion Li^+ were also considered. These criteria can be determined by using ion chromatography method on extracting solution prepared from concrete. Concrete powder at each depth was obtained by drilling concrete specimens at different depth. An exact amount of concrete powder about 3gram was weighed into 250 ml beaker. The sample was dispersed by about 100ml distilled water and broke lumps with glass rod. The beaker was covered by aluminum foil and boiled within five minutes, cool it and then, filtering the sample through fine-texture filter paper by vacuum filter with funnel and filtration flask. The washing was discarded and funnel was rinsed with distilled water. The filtrate was normalized to 500ml by volumetric flask. This solution was measured sodium, potassium, calcium and lithium ion by ion chromatography C_i (mg/l). By equation (35), content of each ion in concrete was measured.

$$\%i = \frac{C_i * V_{extracted} * 100 * D_{concrete}}{1000 * m_{concrete} * W_{binder}} \quad (35)$$

Where: i: percentage of ion i by weight of cement (%)

C_i : concentration of ion i determined by ion chromatography (mg/l)

$V_{extracted}$: volume of extracted solution from concrete (l)

$m_{concrete}$: weight of concrete sample (g)

$D_{concrete}$: gravity of concrete (kg/m³)

W_{binder} : weight of binder in cubic meter of concrete (kg)

Secondly, mineral constituents of concrete at interface should be analyzed. And X-ray diffraction is the most powerful method to analyze both quality and quantity of mineral. Drilled sample of concrete was pulverized up to whole sample pass the sieve with size 150 μ m. That powder was investigated mineral constituent in concrete.

Moreover, as well known, almost phase components of concrete are instable. Therefore, the transformation of phase components in concrete due to ECE treatment is inevitable. So, the transformation of phase components at interface is also one of criteria need to survey. For concrete and mortar microstructure, combination of scanning electron microscopy (SEM) and energy dispersive X-ray spectroscopy (EDS) is a popular method to investigate morphology of mineral.

3.4.2 Effect of ECE on steel rod

Corrosion of steel would determine by half cell potential in accordance to ASTM C 876 to evaluate corrosion risk of embedded steel.

CHAPTER 4

RESULTS AND DISCUSSION

4.1 Resistivity of concrete

Under perspective suggested that macrocell corrosion is the main corrosion occurred in reinforced concrete with distinction between corroding area (anode) and un-corroding area (cathode) on reinforcing bar due to chloride-inducing, corrosion rate flows between cathode and anode can be calculated by applying equation (36).

$$I_C = \frac{U_{R,c} - U_{R,a}}{\frac{r_a}{A_a} + \frac{r_c}{A_c} + \frac{\rho_{con}}{k}} = \frac{\Delta U}{R_a + R_c + R_{con}} \quad (36)$$

Where: I_c : corrosion rate (μA)

$U_{R,c}$: rest potential at cathode area in steel surface (mV)

$U_{R,a}$: rest potential at anode area in steel surface (mV)

ΔU : voltage in macrocell element (mV)

r_c : specific cathodic polarization resistance ($\Omega \cdot \text{cm}^2$)

R_c : cathodic resistance (Ω)

r_a : specific anodic polarization resistance ($\Omega \cdot \text{cm}^2$)

R_a : anodic resistance (Ω)

P_{con} : resistivity of concrete ($\Omega \cdot \text{cm}$)

A_a : anodic steel surface area (cm^2)

A_c : cathodic steel surface area (cm^2)

k : cell constant geometry (cm)

R_{con} : concrete resistance (Ω)

Usually, resistance of anode and cathode much lower than resistance of concrete, then equation (36) can be approximately as equation (37).

$$I_C = \frac{\Delta U}{R_{con}} \sim \frac{1}{R_{con}} \sim \frac{1}{\rho_{con}} = \sigma_{con} \quad (37)$$

Where: σ_{con} : conductivity of concrete (S/m)

Hence, in many guideline and studies, resistivity of concrete or conductivity of concrete is one of criteria to monitor corrosion of embedded steel in reinforced concrete as shown in table 4.1.

Table 4.1: Resistivity and conductivity of concrete versus embedded steel condition

| Resistivity (k Ω . cm) | Conductivity (S/m) | Probable corrosion rate |
|---------------------------------|------------------------------|-------------------------|
| <5 | $>2 \times 10^{-2}$ | Very high |
| 5-10 | $2 \times 10^{-2} - 10^{-2}$ | High |
| 10-20 | $10^{-2} - 5 \times 10^{-3}$ | Low to moderate |
| >20 | $<5 \times 10^{-3}$ | Low |

Table 4.2: Resistivity of concrete before and after extracted

| Concrete | Electrolyte | D (cm) | Resistivity (k Ω .cm) | | Increased rate (% by resistivity before extraction) |
|----------|-------------|-----------|------------------------------|---------------------|---|
| | | | Before extraction | After extraction | |
| PC | SC | 10 | 12.7 | 16.7 | 31.5 |
| | | 15 | 11.3 | 15.3 | 35.3 |
| | LBB | 10 | 12.7 | 15.9 | 25.2 |
| | | 15 | 11.3 | 14.5 | 28.3 |
| FC | SC | 10 | 53.4 | 107.6 | 101.5 |
| | | 15 | 49.4 | 110.9 | 124.5 |
| | LBB | 10 | 53.4 | 86.2 | 61.4 |
| | | 15 | 49.4 | 73.5 | 48.8 |
| LFC | SC | 10 | 37.9 | 89.8 | 136.9 |
| | | 15 | 36.6 | 85.4 | 133.3 |
| | LBB | 10 | 37.9 | 65.1 | 71.8 |
| | | 15 | 36.6 | 59.0 | 61.2 |

In this study, with almost the same initial content of acid soluble chloride (approximate 1.5% chloride by mass of cement) by adding sodium chloride in mixing water during casting concrete, however, resistivity of concrete using ordinary Portland cement, concrete using fly ash cement and limestone fly ash cement before extracted are remarkable different. Meanwhile resistivity of plain concrete showed a probable

high corrosion rate of steel; resistivity of fly ash concrete and limestone fly ash concrete showed such higher than plain concrete and a probable low corrosion rate of steel as shown in tables 4.1 and 4.2 and figure 4.1 and 4.2.

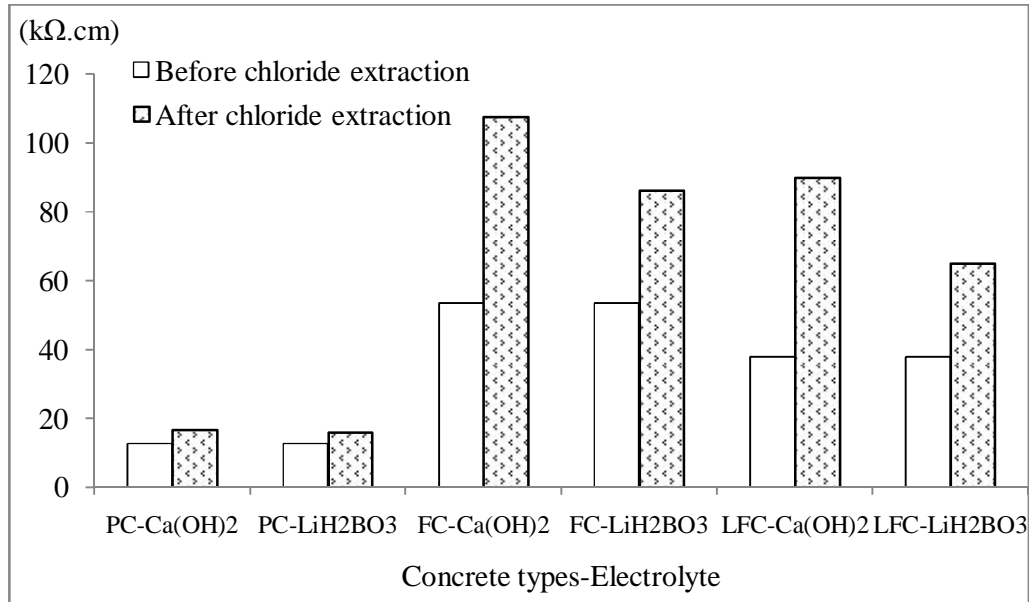


Figure 4.1: Enhancement of resistivity of concrete with 10cm diameter

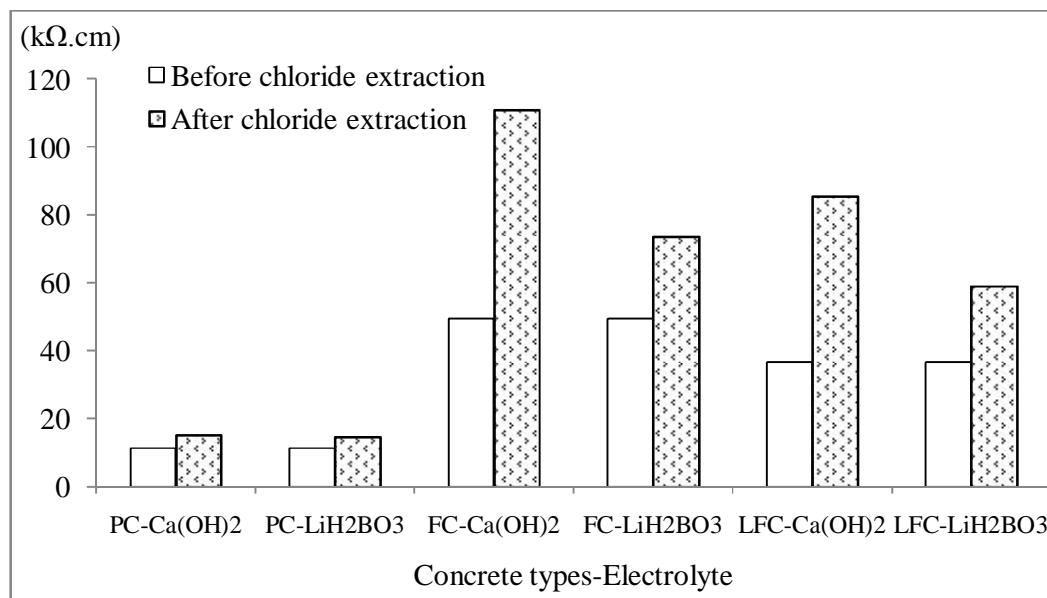


Figure 4.2: Enhancement of resistivity of concrete with 15cm diameter

After finishing extraction process, resistivity increased in all cases. However, the rate of increase in resistivity in three types of concrete was quite different. In plain concrete, resistivity after extraction increased just about 30%. Resistivity of fly ash concrete and limestone fly ash concrete after extraction increased more significant, and increased rate influenced by electrolyte, about 48% to 71% in case lithium borate buffer and about 100% to 133% in case saturated calcium hydroxide.

Using only resistivity of concrete to evaluate corrosion condition of embedded steel might not give a trustable result in this study. Based on half cell potential of steel rod versus saturated copper sulfate electrode before extraction as shown in tables 4.38 and 4.39, although there was much lower on resistivity, half cell potential of embedded steel in plain concrete figured out in intermediate corrosion risk, meanwhile steel rod in fly ash concrete and limestone fly ash concrete showed high corrosion rate. Then, in this study, resistivity of concrete can be just referred as an indirect criterion to evaluate free ion content in pore solution of concrete as well as capability of fly ash and limestone in discontinuing channels in concrete structure.

The increase of resistivity could be attributed to the reduction of ions with high mobility in pore solution of concrete. Moreover, the consistency on increasing of resistivity in all cases of concrete pointed out the initial applied condition in this study may probably be a suitable initial applied condition to eliminate apart harmful effects of ECE on structure of concrete such as cracking of concrete or destruction of concrete structure during extraction.

4.2 Chloride removal

4.2.1 Release of chloride into electrolyte

Although release of chloride ion from concrete to electrolyte does not play direct role on evaluating properties of concrete and steel after extracted, it is also an important criterion to monitor extraction process. They can play as a referential criterion to choose an appropriate applying condition in extraction process such as impressed current density, initial chloride content, etc. the conditions affected strongly on the feasibility of ECE.

Applying ECE with long time can cause many harmful effects on properties of concrete such as the accumulation of alkaline ions at interface, the release of hydrogen (as shown in Figure 4.3), the embrittlement of steel due to hydrogen, etc.

then, measuring chloride extracted in electrolyte during extracting is an indirectly method to determine remained chloride content in concrete and anticipate probably time for halting extraction process. In this study, as mentioned, about 30-40% initial total chloride would be extracted.

Released chloride content is computed by percentage of average initial acid-soluble chloride content in concrete before extracting as mention in chapter 3. Accumulated chloride content extracted here is the totality of released chloride content.

Combining timetable of operating process as shown in table 3.10 and released chloride content every week as shown in table 4.5 permitted to propose that, a consecutive operating condition was not an efficient mode for applying ECE.



Figure 4.3: Release of hydrogen during extracting

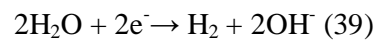
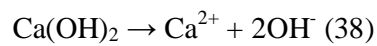
After one first week for checking and correcting the system, consecutive operating mode was applied on uninterrupted four weeks as shown in timetable 4.3.

At the first week of these four weeks process, chloride ion in concrete extracted into electrolyte with approximate 5.0% of total initial acid-soluble chloride content, however released chloride content diminished quickly at the weeks later, about 30% at the second week and 50% at the third week with respect to the first week. At the fourth week of consecutive four weeks process, released chloride amount into electrolyte was much lower than the first week, just around 20% of released chloride at the first week.

However, after halted process for replacing electrolyte and immersing specimens in electrolyte on only one week, the velocity of releasing chloride process

into electrolyte during powering augmented much more than extracted chloride amount at the week before halting as shown in table 4.5 and figures 4.3a to 4.8a.

With initial acid soluble chloride content in all cases was approximate 1.5% by weight of cement, meanwhile by analyzing from XRD, minimum calcium hydroxide content was in fly ash concrete and approximate 2% by mass of concrete as shown in figure. From equivalent equation as shown in equation (38), there was equal 22% hydroxide ion by mass of cement was always ready there to be extracted. Moreover, by cathodic reaction, during extracting, concrete was always supplied by a new amount of hydroxide OH⁻ ion as shown in equation (39).



There may be many reasons for the quick diminution of extracted chloride efficiency during extraction process with consecutive mode. At alternative mode, breaking time was perhaps the time for chloride ion from cavities and small pores transported to larger channels as well as the time for chloride desorbed out the surface of minerals to form a new equilibrium condition. Moreover, it may be the time for bound chloride in concrete shifted to free chloride. That induced a higher concentration of free chloride in pore solution than before breaking. And on the turning-on time later, extracted chloride content was higher.

It seemed that using saturated calcium hydroxide as electrolyte had slightly more efficient than lithium borate buffer on repulsing chloride ion. It was observed by both released chloride content and accumulated chloride content in all three types of concrete studied here with different concrete thickness as shown in figure 4.4 to 4.8 and tables 4.5 and 4.6.

Electrical ionic mobility of calcium is lower than electrical ionic mobility of lithium as shown in table 14 could be one of the reasons. Although mobility of ions in pore solution of concrete quite different with water and very difficult to determine exactly due to tortuous channels, complicated compositions, etc. of concrete. However, mobility of ions in concrete was assumed three orders of magnitude lower than in water.

To circuit the current, both positive ions (including calcium ions) and negative ions (including chloride) contribute to the flow of ions. When positive ions contributed a smaller amount in flow of current, negative ions needed to supply a larger corresponding amount to maintain the current. Here, calcium ion with lower mobility than lithium ion, then, it perhaps contributed a less role in flow of ions in pore solution to circuit the electrical current than lithium; so, pore solution needed more contribution of the other ions to maintain the current, including chloride ion. Therefore, chloride ion could be transferred to anodic charge quicker.

Contrasting to most of deduction attributed that blended concrete may have less efficient than plain concrete, in this study, at the first time of extraction process velocity of extracting chloride in plain concrete was quite clearly lower than in fly ash concrete and limestone fly ash concrete as shown in figures 4.10a to figure 4.13a. However, that phenomenon just happened within four first weeks. Afterwards, chloride of plain concrete tended to release quicker than fly ash concrete and limestone fly ash concrete. Then, at the later of process, accumulated released chloride in all cases of concrete was insignificant difference as shown in figure 4.10b to 4.13b.

This phenomenon may concern with two main problems. Firstly, according to resistivity of concrete, to install a same current density for all concrete types, much different voltage was supplied as shown in figures 3.7, 3.8 and 3.9. The much higher voltage applying for fly ash concrete and limestone fly ash concrete may generate more heat emission in fly ash concrete and limestone fly ash concrete than plain concrete (it was proved by the quicker vaporization of water in electrolyte during extracting), a great advantageous condition for transporting of ions in pore solution including chloride. Simultaneously, probably higher temperature due to much higher voltage, physical binding chloride was easier to desorb.

Second was the reduction of Van De Waals force of concrete using fly ash. C-S-H in blended concrete in general or fly ash concrete in particular formed with lower CaO/SiO₂ ratio (approximate 1.5) and these was considered as a defect product of tobermorite crystal with surface area, the main factor affected to Van Der Waals attractive force, remarkably lower. Therefore, free chloride in fly ash concrete and limestone fly ash concrete may be slightly higher than plain concrete at the same total chloride content.

Table 4.4: Mobility of some ions dissolved

| Ion | Ionic mobility x 10^{-4} ($\text{cm}^2 \cdot \text{V}^{-1} \cdot \text{s}^{-1}$) |
|------------------|--|
| Cl^- | 7.91 |
| OH^- | 20.64 |
| Na^+ | 5.19 |
| Ca^{2+} | 2.17 |
| Li^+ | 4.01 |
| K^+ | 7.62 |

Table 4.5: Released chloride content after every week

| Concrete | Electrolyte | Diameter (cm) | Released chloride content (% by initial acid-soluble chloride) | | | | | | | | |
|----------|-------------|---------------|--|----------------------|----------------------|----------------------|----------------------|----------------------|----------------------|-----------------------|-----------------------|
| | | | 1 st week | 3 rd week | 4 th week | 5 th week | 6 th week | 8 th week | 9 th week | 11 th week | 12 th week |
| PC | SC | 10 | 4.51 | 4.97 | 3.47 | 2.52 | 1.34 | 3.27 | 2.14 | 2.78 | 1.64 |
| | | 15 | 4.50 | 4.79 | 3.70 | 2.66 | 1.74 | 3.43 | 2.19 | 2.82 | 1.82 |
| | LBB | 10 | 4.35 | 5.15 | 3.34 | 2.22 | 1.10 | 3.24 | 1.82 | 2.42 | 1.56 |
| | | 15 | 4.40 | 5.05 | 3.66 | 2.75 | 1.70 | 3.23 | 2.04 | 2.84 | 1.63 |
| FC | SC | 10 | 5.60 | 5.00 | 3.30 | 2.58 | 1.11 | 2.92 | 1.33 | 2.28 | 1.64 |
| | | 15 | 5.54 | 5.50 | 4.11 | 2.63 | 1.28 | 2.99 | 2.05 | 2.72 | 1.62 |
| | LBB | 10 | 5.23 | 4.87 | 3.27 | 2.05 | 1.06 | 2.88 | 1.61 | 2.45 | 1.61 |
| | | 15 | 5.31 | 4.79 | 3.57 | 2.59 | 1.32 | 3.14 | 1.96 | 2.58 | 1.51 |
| LFC | SC | 10 | 5.48 | 4.58 | 2.90 | 2.09 | 1.07 | 3.11 | 1.68 | 2.65 | 1.60 |
| | | 15 | 6.01 | 5.45 | 4.04 | 2.33 | 1.54 | 3.00 | 1.66 | 2.47 | 1.61 |
| | LBB | 10 | 5.36 | 4.42 | 2.84 | 2.04 | 1.17 | 2.90 | 1.40 | 2.78 | 1.22 |
| | | 15 | 5.88 | 4.81 | 3.70 | 2.76 | 1.64 | 3.25 | 1.78 | 2.63 | 1.54 |

*Initial acid soluble chloride was about 1.5% by weight of binder

Table 4.6: Accumulated released chloride content

| Concrete | Electrolyte | Diameter (cm) | Accumulated chloride content (% by initial acid-soluble chloride) | | | | | | | | |
|----------|-------------|---------------|---|----------------------|----------------------|----------------------|----------------------|----------------------|----------------------|-----------------------|-----------------------|
| | | | 1 st week | 3 rd week | 4 th week | 5 th week | 6 th week | 8 th week | 9 th week | 11 th week | 12 th week |
| PC | SC | 10 | 4.51 | 9.48 | 12.95 | 15.47 | 16.81 | 20.08 | 22.22 | 24.99 | 26.63 |
| | | 15 | 4.50 | 9.29 | 12.98 | 15.64 | 17.38 | 20.82 | 23.01 | 27.65 | 29.47 |
| | LBB | 10 | 4.35 | 9.50 | 12.85 | 15.07 | 16.17 | 19.41 | 21.23 | 25.21 | 26.77 |
| | | 15 | 4.40 | 9.45 | 13.10 | 15.86 | 17.55 | 20.78 | 22.82 | 27.30 | 28.93 |
| FC | SC | 10 | 5.60 | 10.60 | 13.90 | 16.48 | 17.59 | 20.51 | 21.84 | 25.76 | 27.40 |
| | | 15 | 5.54 | 11.04 | 15.15 | 17.78 | 19.07 | 22.05 | 24.11 | 28.44 | 30.06 |
| | LBB | 10 | 5.23 | 10.10 | 13.38 | 15.42 | 16.49 | 19.37 | 20.98 | 25.05 | 26.66 |
| | | 15 | 5.31 | 10.10 | 13.67 | 16.26 | 17.59 | 20.73 | 22.69 | 26.78 | 28.29 |
| LFC | SC | 10 | 5.48 | 10.06 | 12.96 | 15.05 | 16.12 | 19.23 | 20.92 | 25.16 | 26.76 |
| | | 15 | 6.01 | 11.46 | 15.50 | 17.82 | 19.36 | 22.36 | 24.02 | 28.10 | 29.71 |
| | LBB | 10 | 5.36 | 9.78 | 12.62 | 14.67 | 15.84 | 18.73 | 20.14 | 24.13 | 25.35 |
| | | 15 | 5.88 | 10.69 | 14.38 | 17.14 | 18.79 | 22.04 | 23.82 | 28.00 | 29.54 |

*Initial acid soluble chloride was about 1.5% by weight of binder

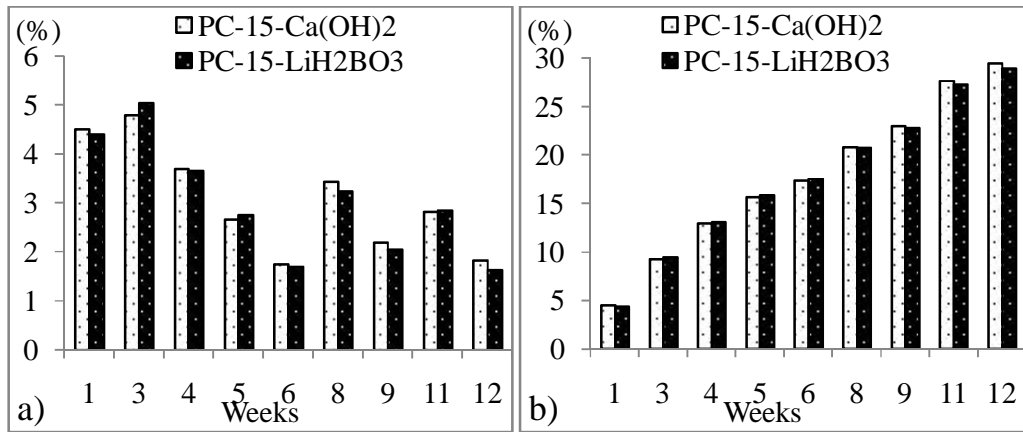


Figure 4.4: a) Released chloride content and b) Accumulated released chloride content in electrolyte of plain concrete with concrete thickness 70 mm

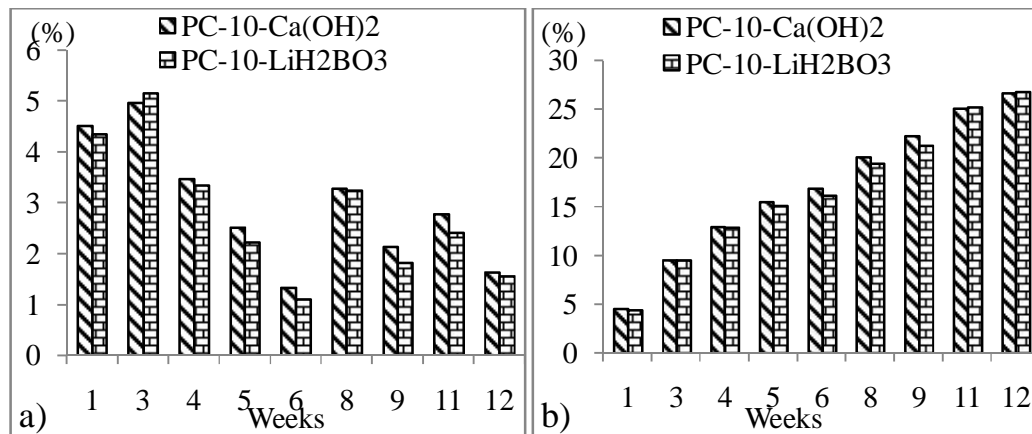


Figure 4.5: a) Released chloride content and b) Accumulated released chloride content in electrolyte of plain concrete with concrete thickness 45 mm

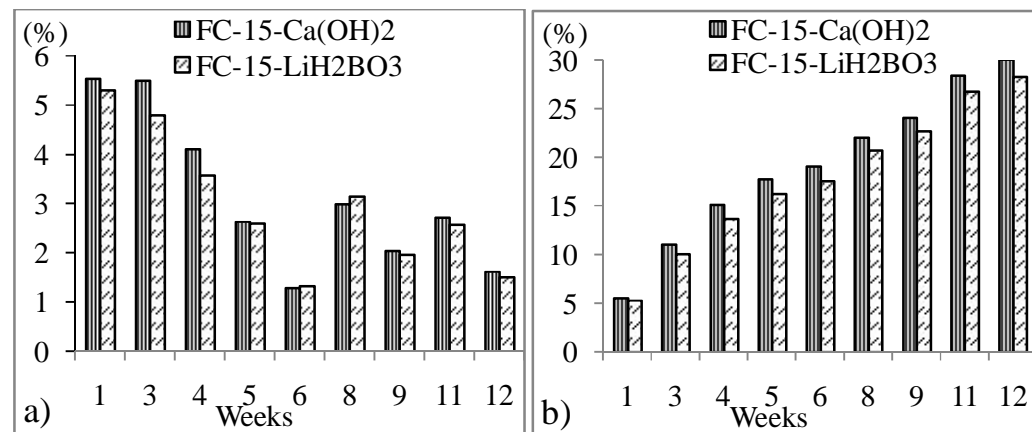


Figure 4.6: a) Released chloride content and b) Accumulated released chloride content in electrolyte of fly ash concrete with concrete thickness 70 mm

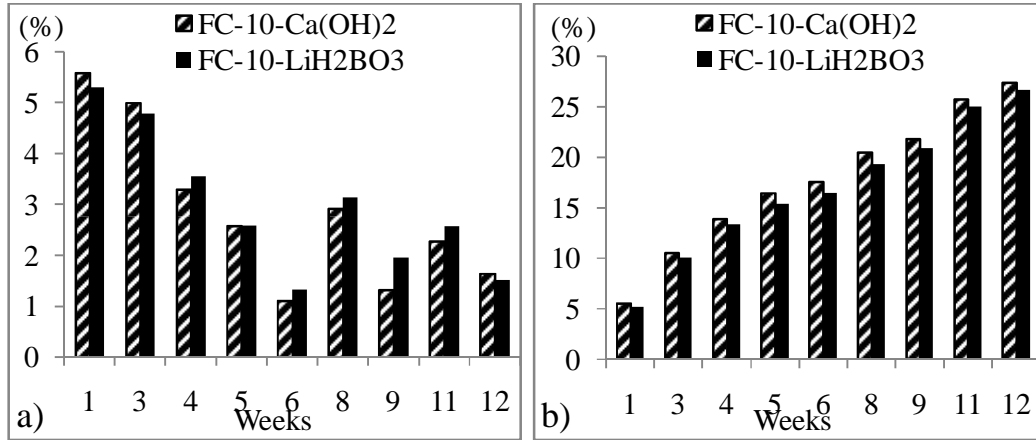


Figure 4.7: a) Released chloride content and b) Accumulated released chloride content in electrolyte of fly ash concrete with concrete thickness 45 mm

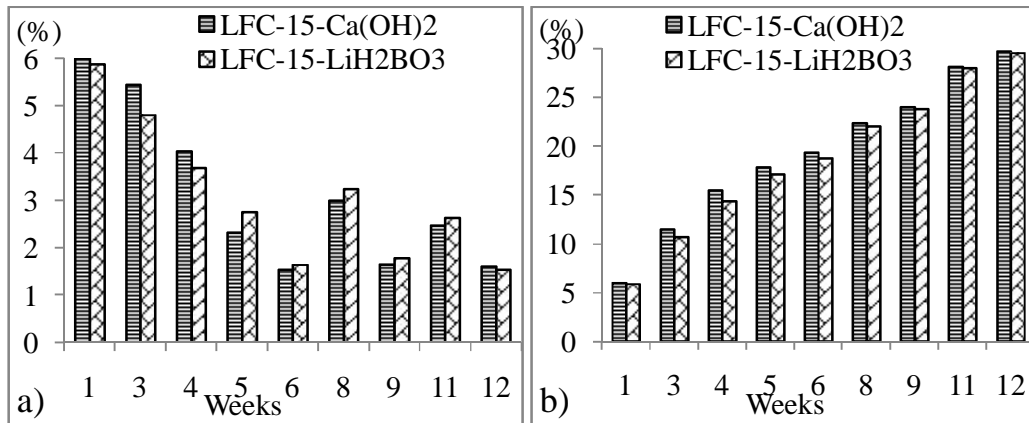


Figure 4.8: a) Released chloride content and b) Accumulated released chloride content in electrolyte of limestone fly ash concrete with concrete thickness 70 mm

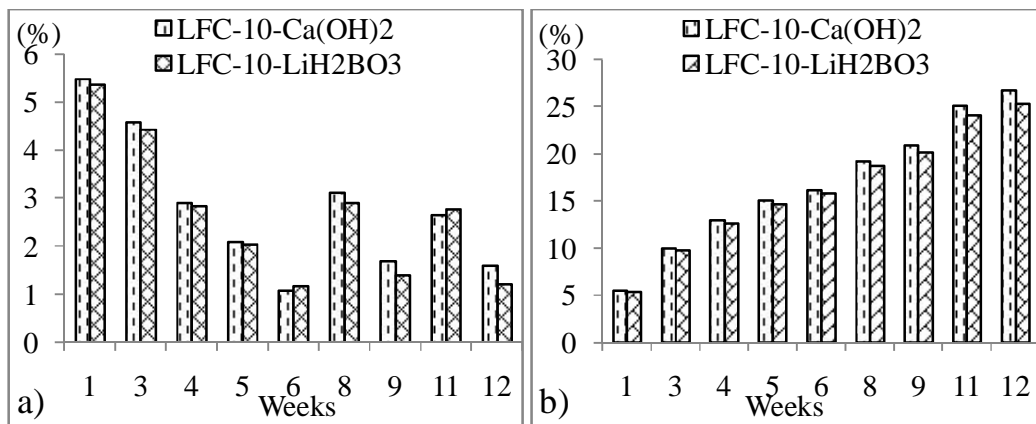


Figure 4.9: a) Released chloride content and b) Accumulated released chloride content in electrolyte of limestone fly ash concrete with concrete thickness 45 mm

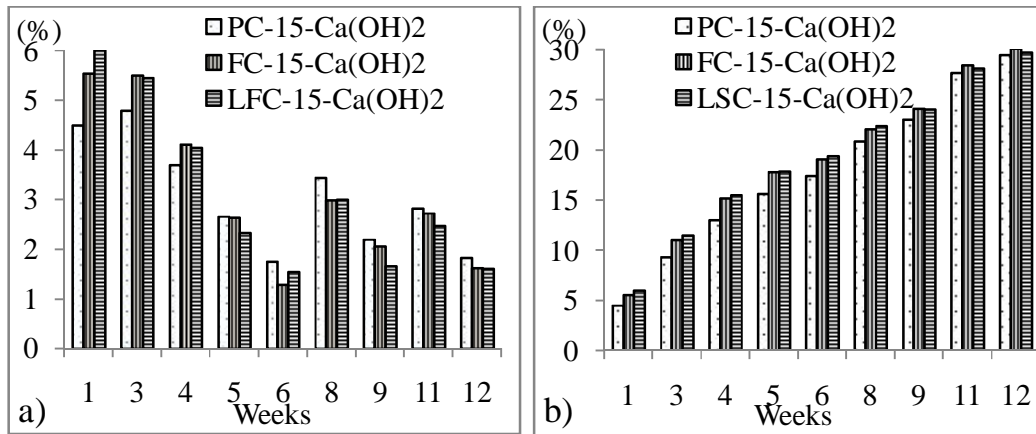


Figure 4.10: a) Released chloride and b) Accumulated released chloride of different concrete types with saturated calcium hydroxide as electrolyte on specimen diameter 15cm

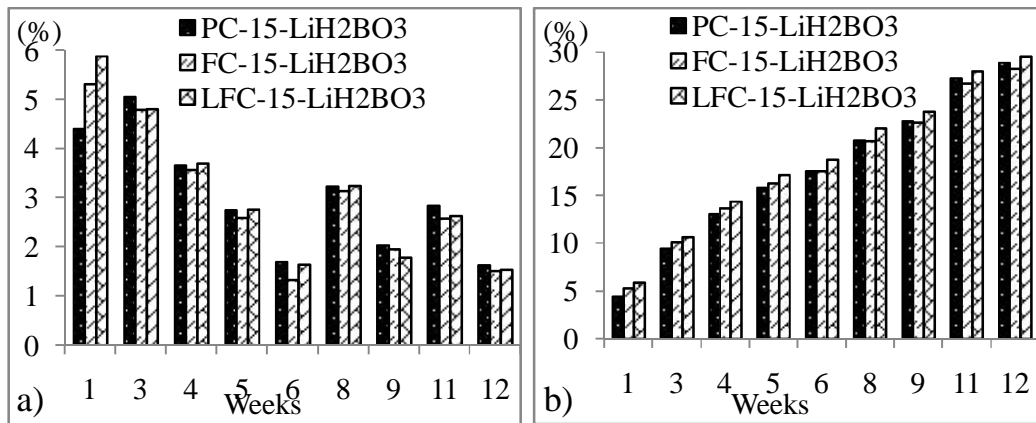


Figure 4.11: a) Released chloride and b) Accumulated released chloride of different concrete types with lithium borate buffer as electrolyte on specimen 15cm

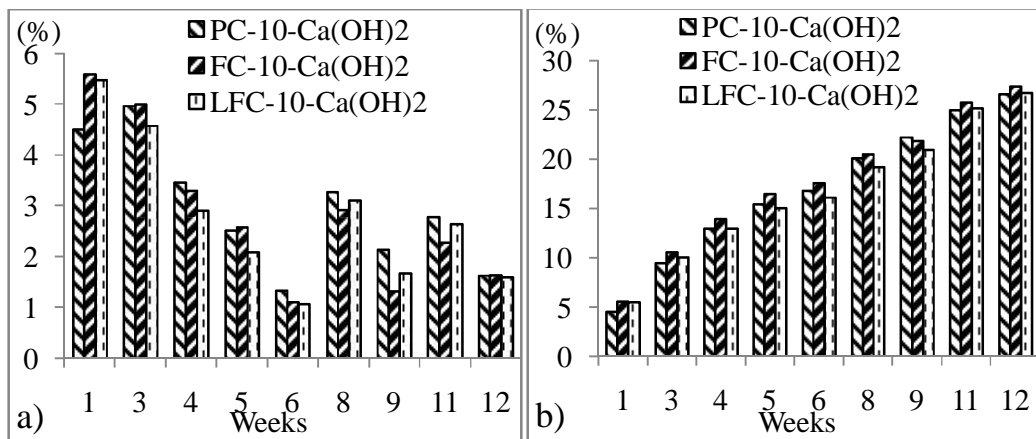


Figure 4.12: a) Released chloride and b) accumulated chloride of different concrete types with saturated calcium hydroxide as electrolyte on specimen diameter 10cm

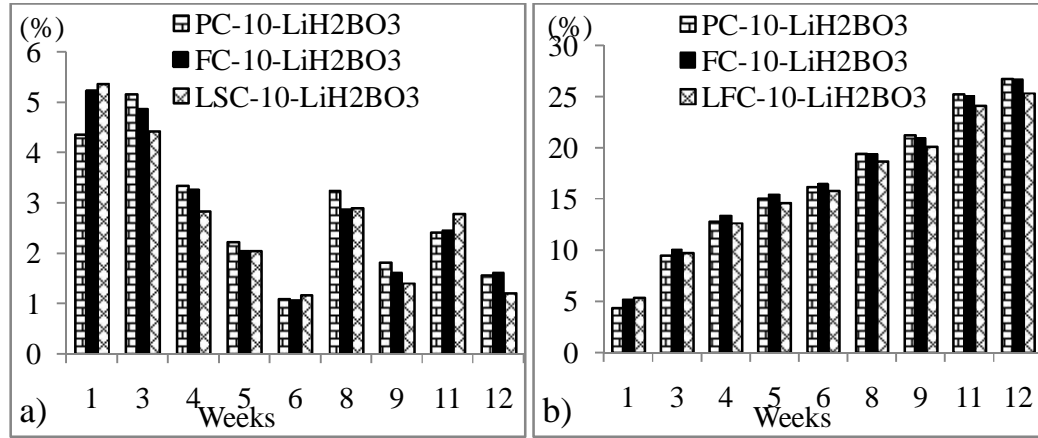


Figure 4.13: a) Released chloride and b) Accumulated released chloride of different concrete types with lithium borate buffer as electrolyte on specimen 10cm

Simultaneously, combining the effects of the reduction of hydroxide ion in pore solution of fly ash concrete and limestone fly ash concrete due to consuming Portlandite of fly ash and the contribution of each ion on electrical current in solution as shown in equation (40), it seemed with the same chloride content, the lower content of the other ions including hydroxide, sulfate, etc. chloride content has higher ratio in total free ion content, then, it may played a higher contribution in transferring charge in electrical current.

$$\frac{I_{Cl^-}}{I_{Current}} = \frac{C_{Cl^-} U_{Cl^-} |Z_{Cl^-}|}{\sum C_i U_i |Z_i|} \quad (40)$$

Where: I_{Cl^-} : amount of current carried by chloride ion

$I_{Current}$: electrical impressed current

C_{Cl^-} : concentration of chloride ion in pore solution

U_{Cl^-} : mobility of chloride in pore solution

Z_{Cl^-} : charge of chloride ion = 1

C_i : concentration of ion i in pore solution

U_i : mobility of ion i in pore solution

Z_i : charge of ion i

In addition, capability of fly ash on reducing porosity and pore size distribution of fly ash in fly ash concrete and blend of limestone powder and fly ash in limestone fly ash concrete in concrete with low water/binder ratio may be also an affecting factor. In fact, the role of fly ash and limestone powder in diminishing porosity and pore size distribution of concrete cannot be neglect; it was proved in this study by much higher concrete resistivity.

However, it should be notice that, the lower water/binder ratio, the less efficient in reducing porosity and pore size distribution in comparison to plain concrete with the same water/binder ratio. That fact was proven by the reduction of the less different in chloride diffusion coefficient in fly ash concrete and plain concrete when water/binder reduced, especially for concrete with water/binder ratio lower than 0.45.

By using equation (41) to compute the affected coefficient of fly ash replacement to chloride diffusion coefficient, there were 0.75 and 0.79 for fly ash concrete and limestone fly ash concrete, respectively.

$$\alpha_{fa} = \left\{ \left[3.5 \times \frac{(f/b)^{3.5}}{1-(w/b)} \right] - \left[1.5 \times \frac{(f/b)}{(1-(w/b))^{0.1}} \right] + 1 \right\} \times t_r^{\left(\frac{-(f/b)}{(e^{3 \times (f/b)})} \right)} \quad (41)$$

Where α_{fa} : affecting coefficient of fly ash

f/b: fly ash/binder ratio

w/b: water/binder ratio

In this study, with symmetric cross section specimen and the same electrical field, thickness cover may not affect strongly. There was insignificant difference in released chloride content and accumulated chloride content detected.

4.2.2 Remained chloride in concrete

After extraction, chloride content in concrete diminished certainly. However, diminution rate was affected strongly on the depth of concrete; the nearer cathode, the stronger reducing rate of chloride ion as shown in tables 4.7 to 4.12 and Figures 4.14 to 4.15.

At the surface of concrete, chloride content reduced slightly, just around 5% to 16% initial acid-soluble chloride content at specimen 15cm diameter and may reach to

25% at specimen 10cm diameter. However, chloride content at interfacial zone decreased meaningfully, it may reach to 70% of initial acid soluble chloride. That reducing rate induced chloride content at interfacial zone of steel and concrete approached to threshold value after extraction.

Corresponding to released chloride to electrolyte as shown above in tables 4.5, 4.6 and figures 4.4 to 4.9, in most of cases here, saturated calcium hydroxide showed slightly more efficient than lithium borate buffer as shown in tables 4.7 to 4.12 and figures 4.14 to 4.16.

Based on figures 4.17 and 4.18, although average total remained chloride in plain concrete, fly ash concrete and limestone fly ash concrete was insignificant different, remained chloride content at interfacial zone in plain concrete was quite lower than fly ash concrete and limestone fly ash concrete. Specially, in the case of plain concrete using saturated calcium hydroxide as electrolyte, remained chloride at interfacial zone was even lower than threshold value.

Comparing fly ash concrete to limestone fly ash concrete, fly ash concrete showed more affected by ECE than limestone fly ash concrete; remain chloride content in fly ash concrete was a bit lower than in limestone fly ash concrete. It was perhaps due to the influence of porosity and pore size distribution of concrete. However, remained chloride in fly ash concrete and limestone fly ash concrete were still higher than threshold value. Capability of fly ash as well as blended of limestone powder and fly ash on reducing porosity and pore size distribution in fly ash concrete and limestone fly ash concrete could be one of reasons.

From results of released chloride in electrolyte and remained chloride in concrete, it seemed like specimen with 10cm diameter had lower efficient than specimen with 15cm diameter, especially at the interfacial zone. Certainly, that conclusion is totally unreasonable.

Here, impressed current was applied with respect to surface area of concrete. Specimen with 10 cm diameter had smaller concrete surface than 15 cm diameter specimen, then, electrical current in cathode of 10cm diameter specimen lower than in 15cm diameter specimen. Therefore, it induced an approximate electrical field at the zone nearby concrete surface, but caused lower electrical field at the zone nearby embedded steel (interfacial zone), the zone affected mainly by negative pole, than specimen with 15cm diameter. The lower electrical field induced lower electrical force attacked on ions in pore solution in general and chloride ion in particular. Then,

chloride in this zone repulsed towards the external zone with slower rate than 15cm diameter specimens. Afterwards, remained chloride in concrete at this zone of 10cm diameter specimen was higher.

However, considering the zone nearby concrete surface and middle zone, the zones affected mainly by external positive pole, remained chloride in 10cm diameter specimen was appropriate to 15cm diameter specimen. It seemed not only the applying impressed current with respect to embedded steel surface area or concrete surface area but the density of embedded steel in structure also played very important role on releasing chloride and efficiency of ECE.

Generally, average remained chloride content in concrete in all cases was still much higher than the threshold value of chloride in concrete specified. However, corrosion state of steel after extracted showed the less risk state than before treatment as shown in Table 4.39. Then, re-distribution and re-diffusion of chloride after ECE should be studied on long-term research.

Table 4.7: Remained chloride in plain concrete with diameter 15cm

| | | Remained chloride content (% by weight of binder) | | | | |
|-----|-----|---|--------------|--------------|--------------|--------------|
| | | 0-1.5 (cm) | 1.5-3.0 (cm) | 3.0-4.5 (cm) | 4.5-6.0 (cm) | 6.0-7.0 (cm) |
| B.E | | 1.541 | 1.460 | 1.419 | 1.433 | 1.483 |
| A.E | SC | 1.288 | 0.995 | 0.975 | 0.522 | 0.389 |
| | LBB | 1.459 | 1.067 | 0.758 | 0.679 | 0.448 |

B.E: before extraction

A.E: after extraction

Table 4.8: Remained chloride in plain concrete with diameter 10cm

| | | Remained chloride content (% by weight of binder) | | | |
|-----|-----|---|--------------|--------------|--------------|
| | | 0-1.5 (cm) | 1.5-2.5 (cm) | 2.5-3.5 (cm) | 3.5-4.5 (cm) |
| B.E | | 1.507 | 1.460 | 1.430 | 1.443 |
| A.E | SC | 1.115 | 0.888 | 0.651 | 0.433 |
| | LBB | 1.142 | 0.714 | 0.731 | 0.462 |

Table 4.9: Remained chloride in fly ash concrete with diameter 15cm

| | | Remained chloride content (% by weight of binder) | | | | |
|-----|-----|---|--------------|--------------|--------------|--------------|
| | | 0-1.5 (cm) | 1.5-3.0 (cm) | 3.0-4.5 (cm) | 4.5-6.0 (cm) | 6.0-7.0 (cm) |
| B.E | | 1.541 | 1.460 | 1.419 | 1.433 | 1.483 |
| A.E | SC | 1.314 | 0.995 | 0.833 | 0.564 | 0.418 |
| | LBB | 1.382 | 0.963 | 0.880 | 0.674 | 0.483 |

Table 4.10: Remained chloride in fly ash concrete with diameter 10cm

| | | Remained chloride content (% by weight of binder) | | | |
|-----|-----|---|--------------|--------------|--------------|
| | | 0-1.5 (cm) | 1.5-2.5 (cm) | 2.5-3.5 (cm) | 3.5-4.5 (cm) |
| B.E | | 1.507 | 1.460 | 1.430 | 1.443 |
| A.E | SC | 1.157 | 0.820 | 0.794 | 0.594 |
| | LBB | 1.297 | 0.958 | 0.812 | 0.593 |

Table 4.11: Remained chloride in limestone fly ash concrete with diameter 15cm

| | | Remained chloride content (% by weight of binder) | | | | |
|-----|-----|---|--------------|--------------|--------------|--------------|
| | | 0-1.5 (cm) | 1.5-3.0 (cm) | 3.0-4.5 (cm) | 4.5-6.0 (cm) | 6.0-7.0 (cm) |
| B.E | | 1.541 | 1.460 | 1.419 | 1.433 | 1.483 |
| A.E | SC | 1.302 | 1.033 | 0.834 | 0.577 | 0.427 |
| | LBB | 1.394 | 1.135 | 1.104 | 0.506 | 0.522 |

Table 4.12: Remained chloride in limestone fly ash concrete with diameter 10cm

| | | Remained chloride content (% by weight of binder) | | | |
|-----|-----|---|--------------|--------------|--------------|
| | | 0-1.5 (cm) | 1.5-2.5 (cm) | 2.5-3.5 (cm) | 3.5-4.5 (cm) |
| B.E | | 1.507 | 1.460 | 1.430 | 1.443 |
| A.E | SC | 1.150 | 1.018 | 0.895 | 0.578 |
| | LBB | 1.295 | 1.076 | 0.915 | 0.611 |

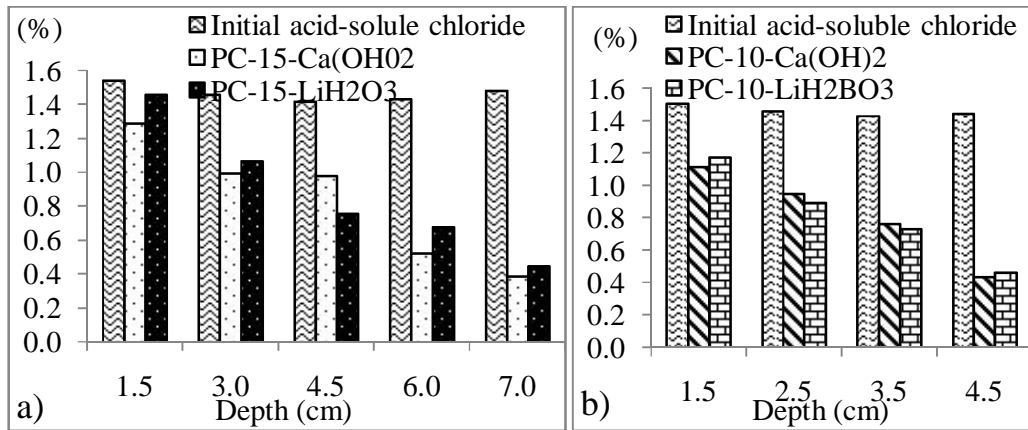


Figure 4.14: Remained chloride content of plain concrete in different electrolyte with diameter a) 15cm and b) 10cm

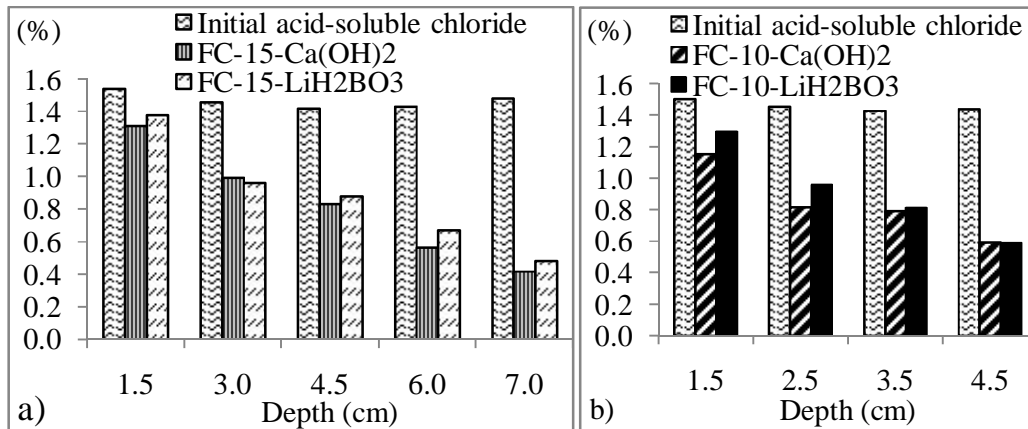


Figure 4.15: Remained chloride content of fly ash concrete in different electrolyte with diameter a) 15cm and b) 10cm

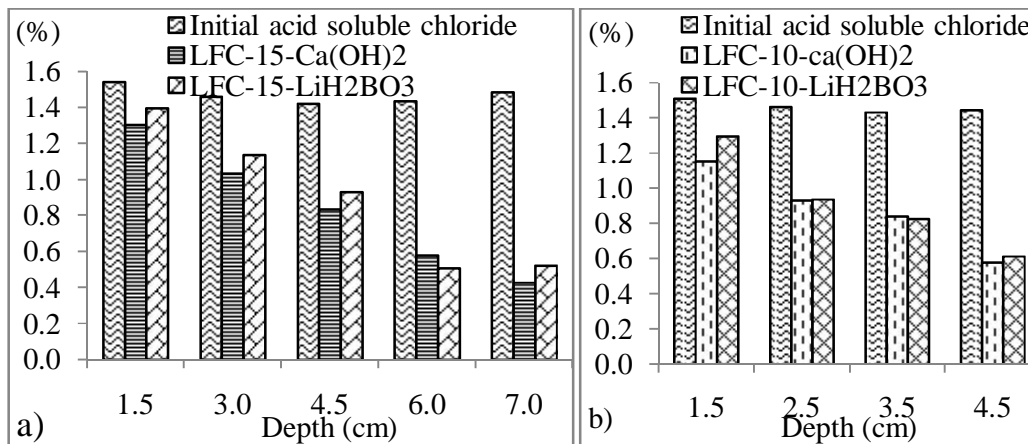


Figure 4.16: Remained chloride content of limestone fly ash concrete in different electrolyte with diameter a) 15cm and b) 10cm

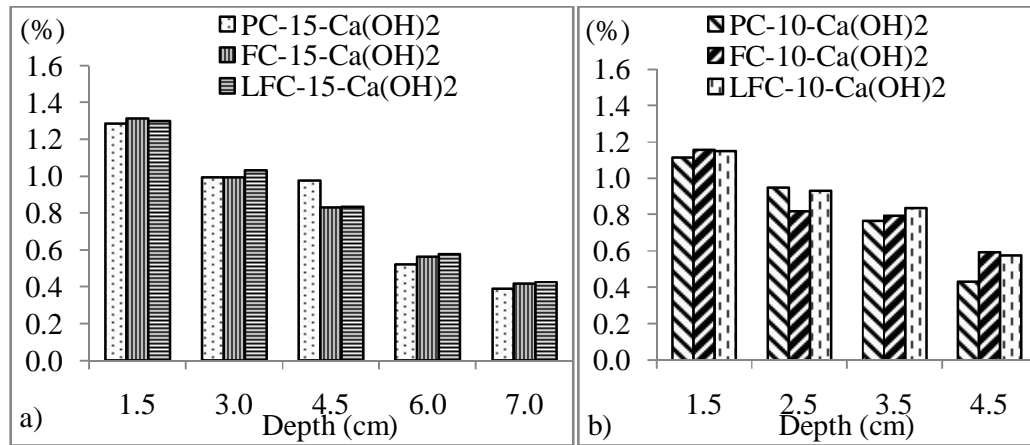


Figure 4.17: Remained chloride content of plain concrete, fly ash concrete and limestone fly ash concrete with diameter a) 15cm and b) 10cm in saturated calcium hydroxide

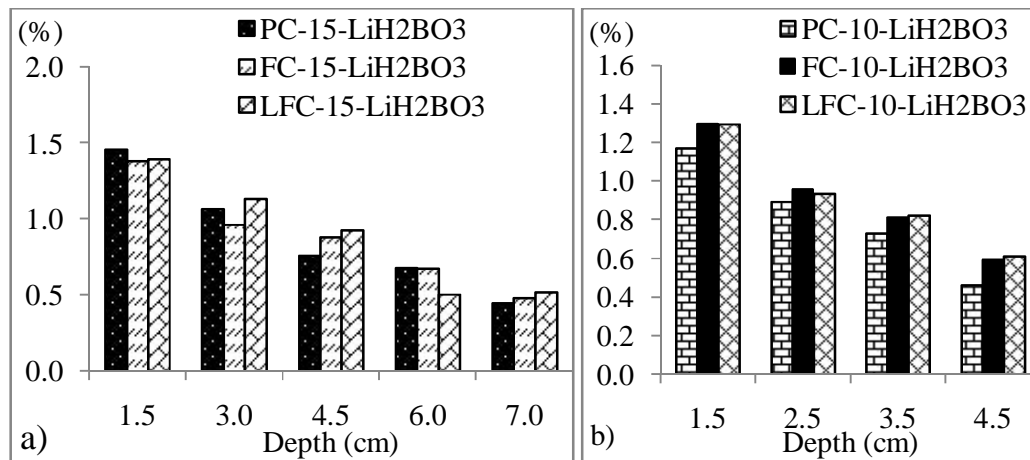


Figure 4.18: Remained chloride content of plain concrete, fly ash concrete and limestone fly ash concrete with diameter a) 15cm and b) 10cm in lithium borate buffer 0.5M

4.3 Distribution of water solubility of sodium ion, potassium ion, lithium ion and calcium ion

Due to affecting of force induced by electrical field, positive ions from electrolyte and pore solution would attract toward cathode. The presence of high concentration of alkali ion generates high hydroxide ion to satisfy ion equivalence.

Occurrence of high hydroxide ion concentration in pore solution of concrete is a favorable condition for passivity of embedded steel maintained in range of pH 9-13.4. However, high content of alkali ions is not only a risky condition for alkali silica reactivity if source of aggregate might contaminate by certain reactive silica but also caused a reducing relative content of adhesive minerals due to accumulating of Portlandite or sodium hydroxide crystal, then, diminish strength of concrete and bonding strength of steel and concrete.

Moreover, hydrated products of binder as C-S-H, C-A-H, etc may absorb sodium and potassium and might exchange with calcium ion in structure of C-S-H, which were unstable products and their volume can contract and expand under fluctuating humidity of external working environment of structure. The gel with higher content of equivalent alkalis Na_2O_e or lower $\text{CaO}/\text{Na}_2\text{O}_e$ can cause more volumetric change under fluctuating humidity condition.

Contrasting to the other alkalis, lithium ion in many compounds has been proved as an element can prevent expansion due to alkali silica reaction or swelling of calcium silicate hydrate contaminated alkalis ion. Lithium ion might substitute sodium or potassium ion in alkali silica reaction products or in alkali-contaminated calcium silicate hydrates to form more stable products than the silicate product of the other alkalis. Therefore, using lithium as electrolyte is one of method to lessen the supply of a new amount of calcium to concrete from electrolyte and diminish the concentration of alkalis in ion current in pore solution during extraction. Hence, the accumulation of Portlandite, sodium hydroxide and risk of alkali silica reaction can be reduced.

From the distribution of sodium and potassium after treatment as shown in figures 4.19 to 4.22, it indicated quite clear that the transportation of sodium and potassium in concrete during ECE affected by both type of concrete and type of electrolyte as well.

In plain concrete, the movement of alkaline ions in case of saturated calcium hydroxide to cathode was higher than in case of lithium borate buffer as electrolyte as shown in figures 4.19 and 4.22. On the contrary, in fly ash concrete and limestone fly ash concrete, with a bit higher content of alkaline ions than in plain concrete, the movement of alkaline ions in case of lithium borate buffer as electrolyte was higher as shown in Figures 4.20, 4.21, 4.23 and 4.24.

Table 4.13: Distribution of sodium ion in plain concrete with diameter 15cm

| | | Content (% by weight of binder) | | | | |
|-----|-----|---------------------------------|--------------|--------------|--------------|--------------|
| | | 0-1.5 (cm) | 1.5-3.0 (cm) | 3.0-4.5 (cm) | 4.5-6.0 (cm) | 6.0-7.0 (cm) |
| A.E | B.E | 1.1238 | 1.1258 | 1.1248 | 1.1274 | 1.1259 |
| | SC | 0.3844 | 0.6586 | 1.0013 | 1.5851 | 5.1467 |
| | LBB | 0.5580 | 0.7057 | 0.8838 | 1.2903 | 4.3920 |

Table 4.14: Distribution of sodium ion in plain concrete with diameter 10cm

| | | Content (% by weight of binder) | | | |
|-----|-----|---------------------------------|--------------|--------------|--------------|
| | | 0-1.5 (cm) | 1.5-2.5 (cm) | 2.5-3.5 (cm) | 3.5-4.5 (cm) |
| A.E | B.E | 1.1238 | 1.1258 | 1.1248 | 1.1274 |
| | SC | 0.2414 | 0.4600 | 1.1664 | 4.9391 |
| | LBB | 0.2952 | 0.6802 | 0.8953 | 3.8211 |

Table 4.15: Distribution of sodium ion in fly ash concrete with diameter 15cm

| | | Content (% by weight of binder) | | | | |
|-----|-----|---------------------------------|--------------|--------------|--------------|--------------|
| | | 0-1.5 (cm) | 1.5-3.0 (cm) | 3.0-4.5 (cm) | 4.5-6.0 (cm) | 6.0-7.0 (cm) |
| A.E | B.E | 1.1997 | 1.2085 | 1.2220 | 1.2224 | 1.2238 |
| | SC | 0.4543 | 0.8846 | 1.2085 | 2.1430 | 5.3855 |
| | LBB | 0.3021 | 0.8427 | 1.0206 | 2.0919 | 5.7295 |

Table 4.16: Distribution of sodium ion in fly ash concrete with diameter 10cm

| | | Content (% by weight of binder) | | | |
|-----|-----|---------------------------------|--------------|--------------|--------------|
| | | 0-1.5 (cm) | 1.5-2.5 (cm) | 2.5-3.5 (cm) | 3.5-4.5 (cm) |
| A.E | B.E | 1.2001 | 1.2089 | 1.2221 | 1.2224 |
| | SC | 0.3683 | 0.3937 | 1.5058 | 4.9752 |
| | LBB | 0.2735 | 0.6885 | 1.3080 | 5.0460 |

Table 4.17: Distribution of sodium ion in limestone fly ash concrete with diameter 15cm

| | | Content (% by weight of binder) | | | | |
|-----|-----|---------------------------------|--------------|--------------|--------------|--------------|
| | | 0-1.5 (cm) | 1.5-3.0 (cm) | 3.0-4.5 (cm) | 4.5-6.0 (cm) | 6.0-7.0 (cm) |
| B.E | | 1.1921 | 1.2077 | 1.2197 | 1.2217 | 1.2226 |
| A.E | SC | 0.3374 | 0.7998 | 1.1371 | 1.8103 | 5.8372 |
| | LBB | 0.3107 | 0.7183 | 1.1305 | 1.7683 | 5.9435 |

Table 4.18: Distribution of sodium ion in limestone fly ash concrete with diameter 10cm

| | | Content (% by weight of binder) | | | |
|-----|-----|---------------------------------|--------------|--------------|--------------|
| | | 0-1.5 (cm) | 1.5-2.5 (cm) | 2.5-3.5 (cm) | 3.5-4.5 (cm) |
| B.E | | 1.1931 | 1.2075 | 1.2196 | 1.2207 |
| A.E | SC | 0.4453 | 0.6952 | 1.7445 | 4.1393 |
| | LBB | 0.4434 | 0.6353 | 1.6614 | 5.4874 |

Table 4.19: Distribution of potassium ion in plain concrete with diameter 15cm

| | | Content (% by weight of binder) | | | | |
|-----|-----|---------------------------------|--------------|--------------|--------------|--------------|
| | | 0-1.5 (cm) | 1.5-3.0 (cm) | 3.0-4.5 (cm) | 4.5-6.0 (cm) | 6.0-7.0 (cm) |
| B.E | | 0.4024 | 0.4018 | 0.4025 | 0.4025 | 0.4027 |
| A.E | SC | 0.0000 | 0.2289 | 0.2878 | 0.6366 | 3.9835 |
| | LBB | 0.0000 | 0.2671 | 0.2993 | 0.7474 | 3.2445 |

Table 4.20: Distribution of potassium ion in plain concrete with diameter 10cm

| | | Content (% by weight of binder) | | | |
|-----|-----|---------------------------------|--------------|--------------|--------------|
| | | 0-1.5 (cm) | 1.5-2.5 (cm) | 2.5-3.5 (cm) | 3.5-4.5 (cm) |
| B.E | | 0.4025 | 0.4022 | 0.4024 | 0.4025 |
| A.E | SC | 0.000 | 0.2190 | 0.6870 | 3.6551 |
| | LBB | 0.0000 | 0.2352 | 0.7965 | 2.4159 |

Table 4.21: Distribution of potassium ion in fly ash concrete with diameter 15cm

| | | Content (% by weight of binder) | | | | |
|-----|-----|---------------------------------|--------------|--------------|--------------|--------------|
| | | 0-1.5 (cm) | 1.5-3.0 (cm) | 3.0-4.5 (cm) | 4.5-6.0 (cm) | 6.0-7.0 (cm) |
| A.E | B.E | 0.9734 | 0.9756 | 0.9757 | 0.9750 | 0.9777 |
| | SC | 0.2606 | 0.5852 | 0.8387 | 1.6526 | 4.5311 |
| | LBB | 0.2480 | 0.5012 | 0.6945 | 1.4859 | 4.9092 |

Table 4.22: Distribution of potassium ion in fly ash concrete with diameter 10cm

| | | Content (% by weight of binder) | | | |
|-----|-----|---------------------------------|--------------|--------------|--------------|
| | | 0-1.5 (cm) | 1.5-2.5 (cm) | 2.5-3.5 (cm) | 3.5-4.5 (cm) |
| A.E | B.E | 0.9755 | 0.9758 | 0.9754 | 0.9775 |
| | SC | 0.0000 | 0.3932 | 1.2400 | 4.2753 |
| | LBB | 0.2073 | 0.3581 | 0.4694 | 4.3866 |

Table 4.23: Distribution of potassium ion in limestone fly ash concrete with diameter 15cm

| | | Content (% by weight of binder) | | | | |
|-----|-----|---------------------------------|--------------|--------------|--------------|--------------|
| | | 0-1.5 (cm) | 1.5-3.0 (cm) | 3.0-4.5 (cm) | 4.5-6.0 (cm) | 6.0-7.0 (cm) |
| A.E | B.E | 0.8884 | 0.8937 | 0.8892 | 0.8911 | 0.8896 |
| | SC | 0.2330 | 0.4177 | 0.8742 | 1.4479 | 4.7381 |
| | LBB | 0.000 | 0.3192 | 0.8169 | 1.3991 | 5.5051 |

Table 4.24: Distribution of potassium ion in limestone fly ash concrete with diameter 10cm

| | | Content (% by weight of binder) | | | |
|-----|-----|---------------------------------|--------------|--------------|--------------|
| | | 0-1.5 (cm) | 1.5-2.5 (cm) | 2.5-3.5 (cm) | 3.5-4.5 (cm) |
| A.E | B.E | 0.8927 | 0.8895 | 0.8921 | 0.8899 |
| | SC | 0.2947 | 0.4502 | 1.4387 | 3.8692 |
| | LBB | 0.1448 | 0.4366 | 1.6450 | 3.9354 |

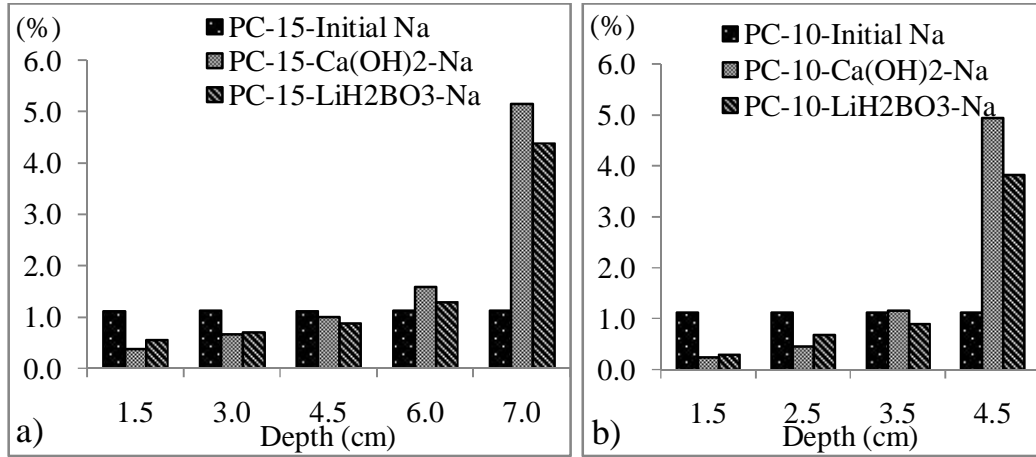


Figure 4.19: Distribution sodium ion in plain concrete with diameter a) 15cm b) 10cm

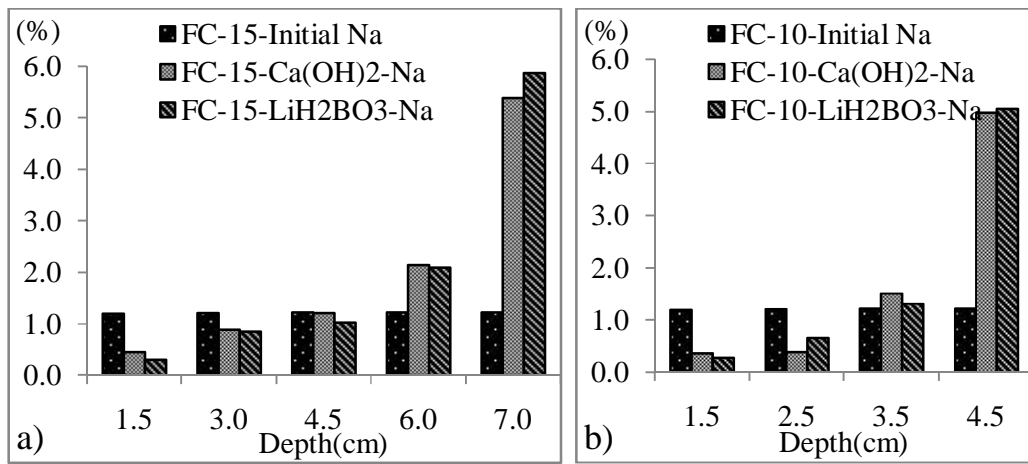


Figure 4.20: Distribution sodium ion in fly ash concrete with diameter a) 15cm b) 10cm

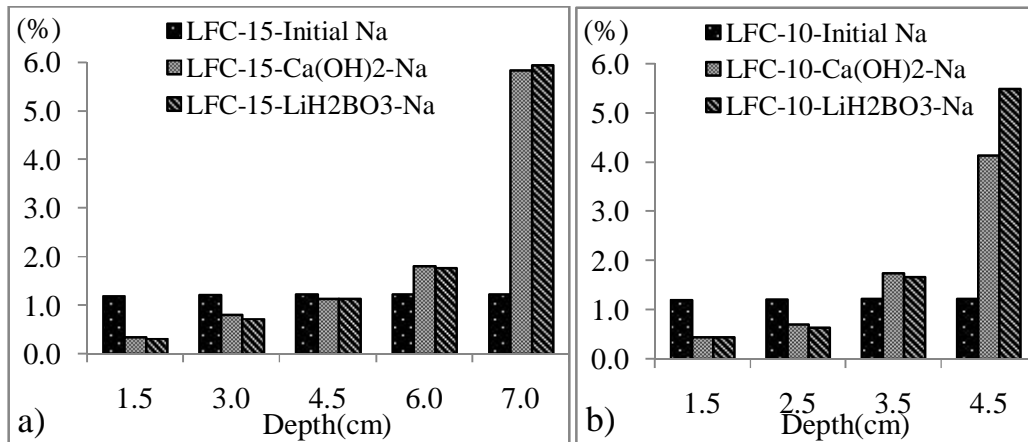


Figure 4.21: Distribution sodium ion in limestone fly ash concrete with diameter a) 15cm b) 10cm

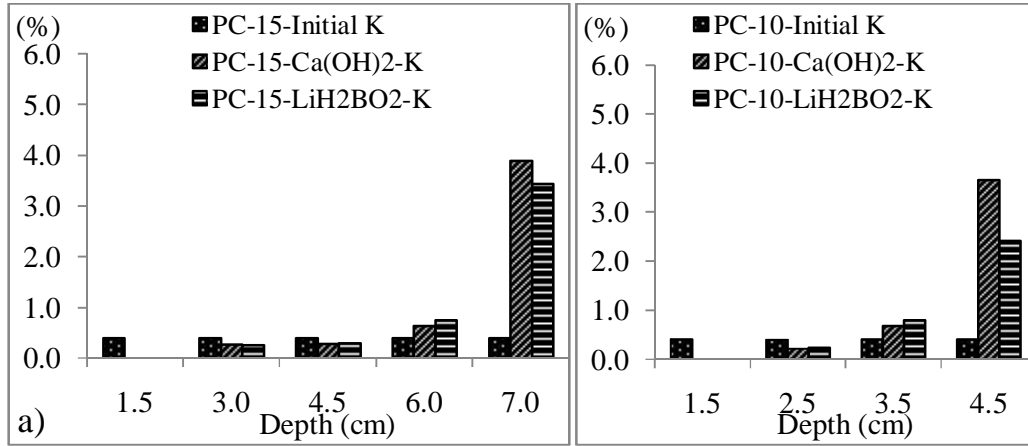


Figure 4.22: Distribution potassium ion in plain concrete with diameter a) 15cm b) 10cm

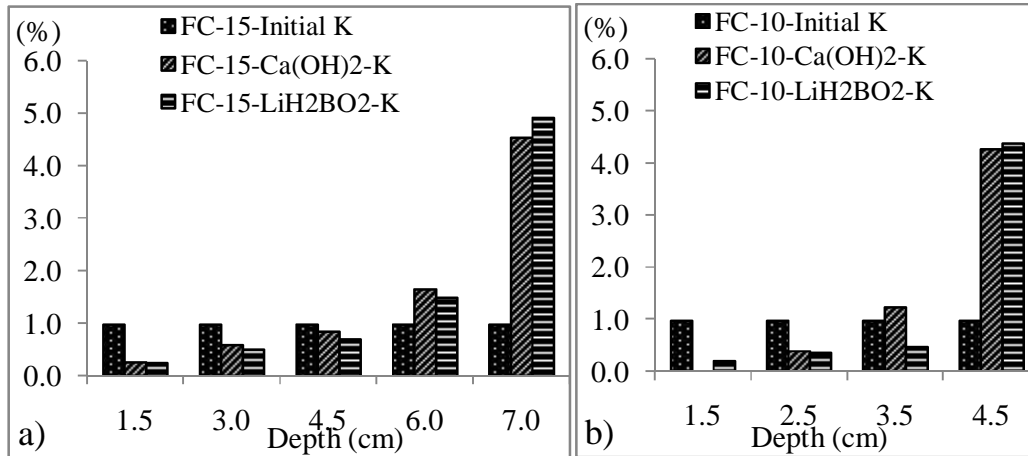


Figure 4.23: Distribution potassium ion in fly ash concrete with diameter a) 15cm b) 10cm

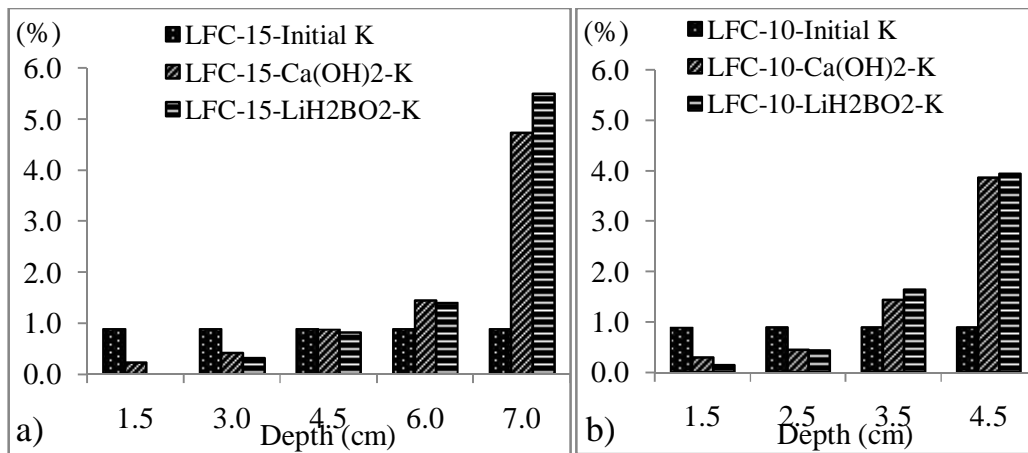


Figure 4.24: Distribution potassium ion in limestone fly ash concrete with diameter a) 15cm b) 10cm

From the results of water soluble calcium ion in concrete at different electrolyte as shown in Figures 4.25 to 4.27, it indicated clearly that at all depth of all type of concrete, water-soluble calcium content after treatment was quite higher than before treatment. That phenomenon was not only occurred in case of saturated calcium hydroxide used as electrolyte, where a new amount of calcium ion could be supplied by electrolyte but also occurred in case lithium borate buffer used as electrolyte, where were no new amount of calcium supplied from external vicinity.

This phenomenon permitted to propose that, during ECE treatment, there was the decomposition or transformation of hydrated cement products such as calcium silicate hydrate, calcium aluminate hydrate, etc. in concrete. That decomposition/transformation liberated an amount of bound calcium or physical binding calcium to free calcium ions can be dissolved in water. Then, prolongation ECE process was not a good technique. It may be the more harmful for strength of concrete, bond strength t, porosity and pore size distribution in concrete even though chloride ion in concrete can be extracted more. The rate of decomposition/transformation during extraction need more study to choose appropriate extracting time, suitable extracted chloride. Then, the harmful effects of ECE to strength of concrete can be lessened.

Here, it was very difficult to affirm the effect of different type of electrolyte to decomposition/ transformation rate of same type of concrete in case of saturated calcium hydroxide as electrolyte, even though from the results, it seemed like at the same type of concrete, saturated calcium hydroxide showed more affected; however, as mentioned above, result of water soluble calcium ion in case of saturated calcium hydroxide used as electrolyte could be the combination of available free calcium ion in concrete, a new amount due to decomposition/transformation and a new amount of calcium ion transfer from electrolyte.

Moreover, at different types of concrete, due to the influence of porosity and pore size distribution; so, it affected to transportation of calcium ion from electrolyte into concrete; therefore, it was also very difficult to evaluate the rate of decomposition/transformation of different type of concrete in case saturated calcium hydroxide although from figure 4.28, the decomposition/transformation of plain concrete predominated than fly ash concrete and limestone fly ash concrete.

However, in case of lithium borate buffer as shown in figure 4.29, where there was no effect from external calcium content, it pointed out clearly that the

decomposition/transformation of adhesive hydrated cement product in plain concrete was much more than in fly ash concrete or limestone fly ash concrete. This phenomenon may concern to the difference in morphology of hydrated cement products of ordinary cement, fly ash cement and limestone fly ash cement. As well-known, adhesive hydrated cement products of ordinary Portland cement usually had higher content of calcium oxide CaO than in fly ash cement and limestone fly ash cement; meanwhile the higher content of calcium oxide CaO in adhesive hydrated products, the more vulnerable of hydrated products since the environmental condition changed.

It was observed here that the difference in the re-distribution of alkaline ions and calcium ion after treatment. Meanwhile after extraction, main amount of alkaline ions was attracted to the zone nearby cathode; calcium ion content at surface zone or middle zone was slightly higher than the zone nearby cathode. In case of saturated calcium hydroxide as electrolyte, at the same type of concrete, calcium ion content decreased gradually from the surface of concrete to cathode as shown in figure 4.28; whereas in case of lithium borate buffer, water soluble calcium content was slightly higher at the middle thickness as shown in figure 4.29. The diffusion of calcium ion from saturated calcium hydroxide into concrete should be reason for that difference.

From the diffusion of lithium from electrolyte to concrete as shown in figure 4.30, it figured out that, the ingress of ion from electrolyte into concrete was quite small in comparison to available ion in concrete. It permitted to infer that, available ions in concrete were the main part responsible for transferring charge in electrical current from anode to cathode, especially sodium ion, potassium ion, hydroxyl and chloride.

Table 4.25: Distribution of calcium ion in plain concrete with diameter 15cm

| | | Content (% by weight of binder) | | | | |
|-----|-----|---------------------------------|--------------|--------------|--------------|--------------|
| | | 0-1.5 (cm) | 1.5-3.0 (cm) | 3.0-4.5 (cm) | 4.5-6.0 (cm) | 6.0-7.0 (cm) |
| B.E | | 4.4928 | 4.4990 | 4.5005 | 4.5020 | 4.4804 |
| A.E | SC | 9.2846 | 9.0495 | 9.7338 | 9.1317 | 7.0199 |
| | LBB | 8.1196 | 9.0684 | 8.2365 | 9.1457 | 7.3392 |

Table 4.26: Distribution of calcium ion in plain concrete with diameter 10cm

| | | Content (% by weight of binder) | | | |
|-----|-----|---------------------------------|--------------|--------------|--------------|
| | | 0-1.5 (cm) | 1.5-2.5 (cm) | 2.5-3.5 (cm) | 3.5-4.5 (cm) |
| A.E | B.E | 4.4938 | 4.4992 | 4.5015 | 4.5023 |
| | SC | 8.5667 | 8.2204 | 8.5229 | 6.7804 |
| | LBB | 6.1660 | 7.2764 | 5.5503 | 4.6236 |

Table 4.27: Distribution of calcium ion in fly ash concrete with diameter 15cm

| | | Content (% by weight of binder) | | | | |
|-----|-----|---------------------------------|--------------|--------------|--------------|--------------|
| | | 0-1.5 (cm) | 1.5-3.0 (cm) | 3.0-4.5 (cm) | 4.5-6.0 (cm) | 6.0-7.0 (cm) |
| A.E | B.E | 2.7973 | 2.8535 | 2.8873 | 2.8402 | 2.8548 |
| | SC | 5.6912 | 6.2891 | 6.2020 | 5.5088 | 4.4414 |
| | LBB | 4.8721 | 5.3569 | 5.6271 | 5.2884 | 3.6497 |

Table 4.28: Distribution of calcium ion in fly ash concrete with diameter 10cm

| | | Content (% by weight of binder) | | | |
|-----|-----|---------------------------------|--------------|--------------|--------------|
| | | 0-1.5 (cm) | 1.5-2.5 (cm) | 2.5-3.5 (cm) | 3.5-4.5 (cm) |
| A.E | B.E | 2.7973 | 2.8535 | 2.8873 | 2.8402 |
| | SC | 5.3361 | 4.8679 | 4.7022 | 4.2380 |
| | LBB | 3.8759 | 4.3782 | 4.3782 | 3.0390 |

Table 4.29: Distribution of calcium ion in limestone fly ash concrete with diameter 15cm

| | | Content (% by weight of binder) | | | | |
|-----|-----|---------------------------------|--------------|--------------|--------------|--------------|
| | | 0-1.5 (cm) | 1.5-3.0 (cm) | 3.0-4.5 (cm) | 4.5-6.0 (cm) | 6.0-7.0 (cm) |
| A.E | B.E | 2.9978 | 2.9935 | 3.0054 | 2.9957 | 3.0067 |
| | SC | 8.0069 | 7.8391 | 7.7424 | 4.7574 | 4.4027 |
| | LBB | 4.6601 | 4.6601 | 6.5703 | 6.5845 | 3.71 |

Table 4.30: Distribution of calcium ion in fly ash concrete with diameter 10cm

| | | Content (% by weight of binder) | | | |
|-----|-----|---------------------------------|--------------|--------------|--------------|
| | | 0-1.5 (cm) | 1.5-2.5 (cm) | 2.5-3.5 (cm) | 3.5-4.5 (cm) |
| A.E | B.E | 2.9981 | 2.9939 | 3.0034 | 2.9987 |
| | SC | 7.0893 | 6.6999 | 6.3024 | 4.7828 |
| | LBB | 4.4816 | 5.2002 | 5.0440 | 4.4111 |

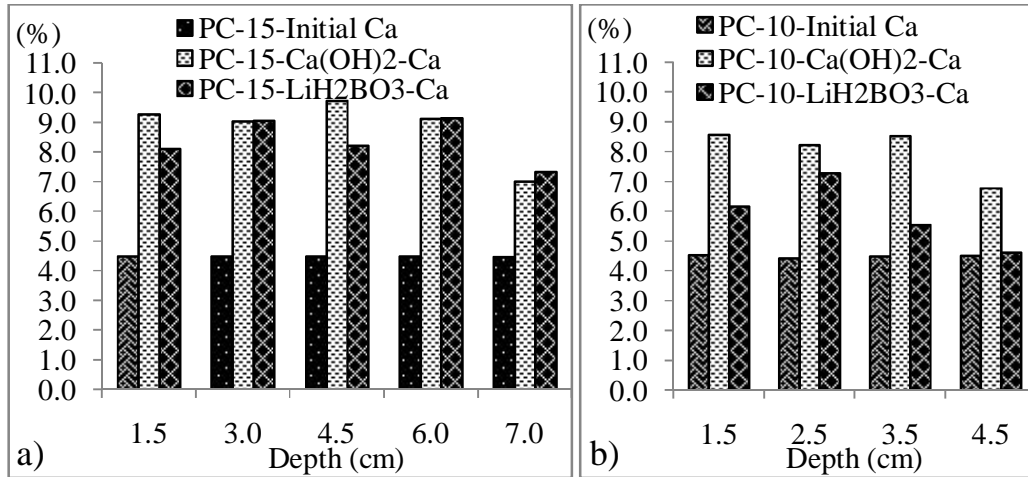


Figure 4.25: Distribution calcium ion in plain concrete with diameter a) 15cm b) 10cm

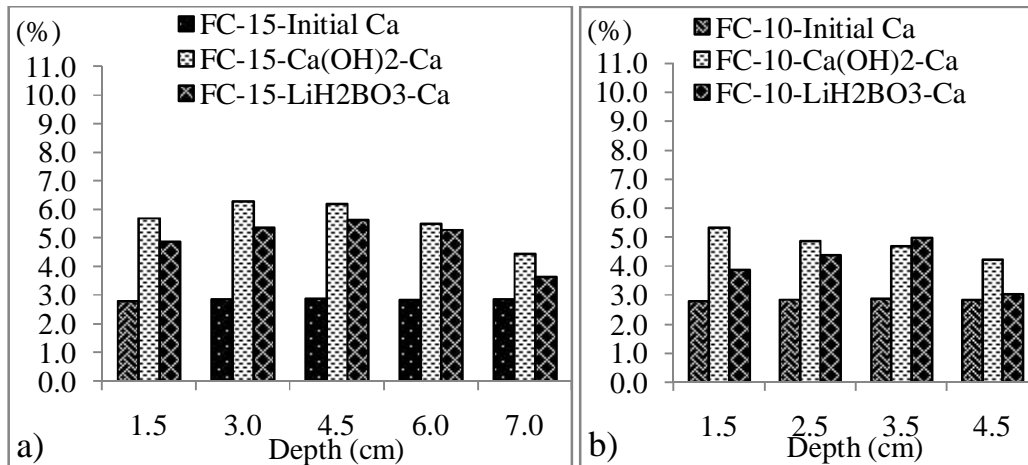


Figure 4.26: Distribution calcium ion in fly ash concrete with diameter a) 15cm b) 10cm

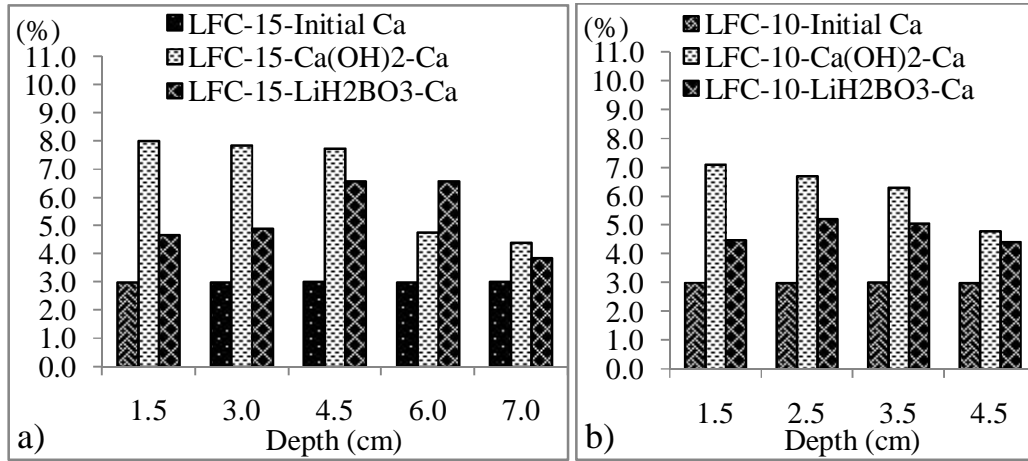


Figure 4.27: Distribution calcium ion in limestone fly ash concrete with diameter a) 15cm b) 10cm

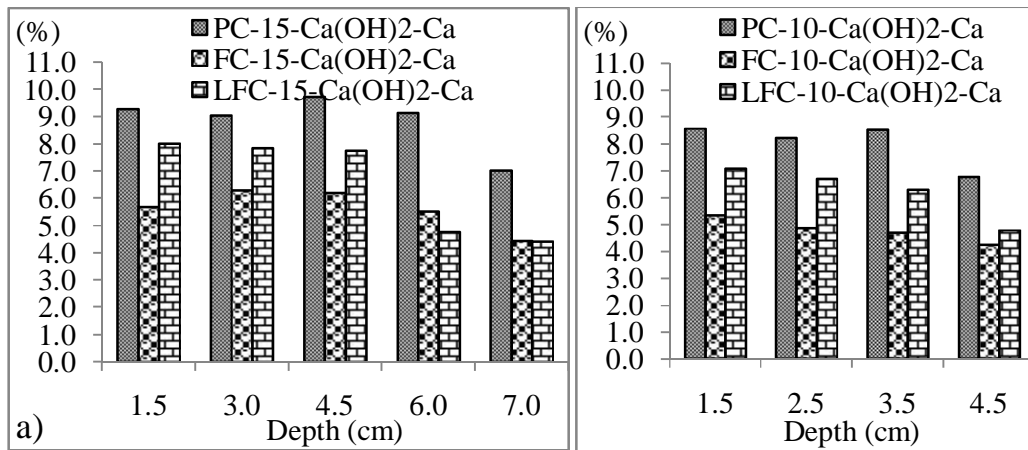


Figure 4.28: Distribution calcium ion in limestone fly ash concrete with diameter a) 15cm b) 10cm

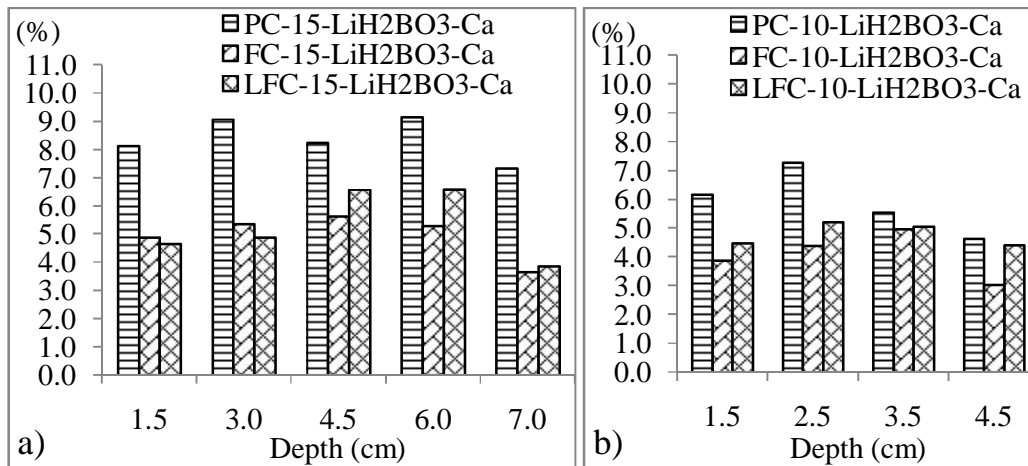


Figure 4.29: Distribution calcium ion in limestone fly ash concrete with diameter a) 15cm b) 10cm

Table 4.31: Distribution of lithium ion in concrete with diameter 15cm in case lithium borate buffer as electrolyte

| Concrete | Content (% by weight of binder) | | | | |
|----------|---------------------------------|--------------|--------------|--------------|--------------|
| | 0-1.5 (cm) | 1.5-3.0 (cm) | 3.0-4.5 (cm) | 4.5-6.0 (cm) | 6.0-7.0 (cm) |
| PC | 0.3316 | 0.1314 | 0.0790 | 0.0404 | 0.0417 |
| FC | 0.3467 | 0.1278 | 0.1001 | 0.0824 | 0.0372 |
| LFC | 0.2664 | 0.1529 | 0.1001 | 0.0831 | 0.0425 |

Table 4.32: Distribution of lithium ion in concrete with diameter 10cm in case lithium borate buffer as electrolyte

| Concrete | Content (% by weight of binder) | | | |
|----------|---------------------------------|--------------|--------------|--------------|
| | 0-1.5 (cm) | 1.5-3.0 (cm) | 3.0-4.5 (cm) | 4.5-6.0 (cm) |
| PC | 0.2878 | 0.1172 | 0.0746 | 0.0356 |
| FC | 0.2891 | 0.0876 | 0.0567 | 0.0382 |
| LFC | 0.2689 | 0.1033 | 0.0888 | 0.0353 |

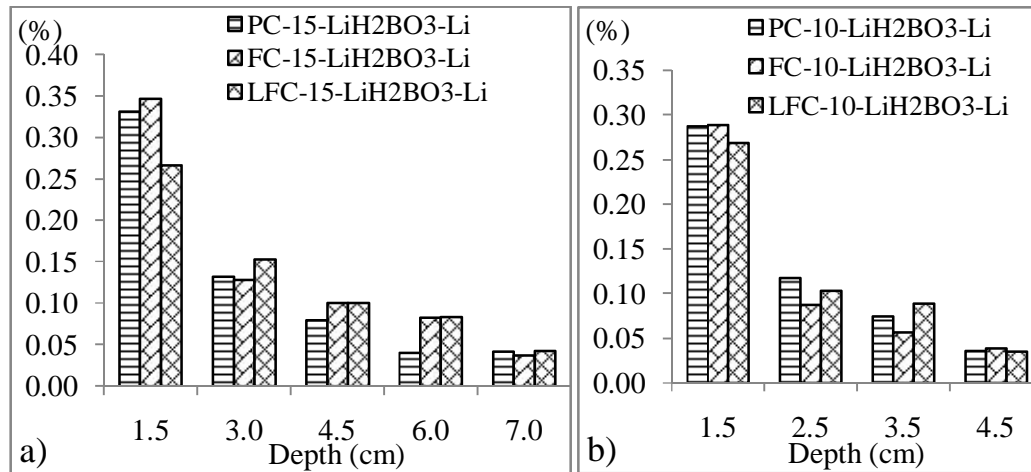


Figure 4.30: Distribution of lithium ion in concrete with diameter a) 15cm b) 10cm

4.4 Microstructure of concrete at interfacial zone between steel and concrete

Calcium hydroxide and C-S-H played important role on both durability and strength capability of concrete. Here, these were the main minerals considered by combining results from x-ray diffraction (XRD) of concrete powder gathering at depth 1 cm from steel surface and scanning electron microscope (SEM) on concrete at

steel/concrete interface as shown in Figure 4.31. High content of calcium hydroxide crystal (Portlandite) at interface and their accumulation to big layer at that zone have been attributed to the reduction of bond strength.

After treatment, Portlandite content increased in all cases of concrete. However, the clearly different result was observed here in comparison to the other previous studies on ECE that was the detection of C-S-H at interfacial zone by SEM after extracting; meanwhile most of the previous studies showed the disappearance of C-S-H and the occurrence of big plate-like crystal with high content of calcium and aluminum. That was a great advantageous signal for feasibility of ECE with chosen parameters in this study.



Figure 4.31: Specimen for SEM test

Firstly, from SEM result, ettringite was not observed at interfacial zone in all cases. The disappearance of ettringite at interface can be predicted easily. Under affecting of electrical field induced by cathode (embedded steel), negative ions in pore solution such as Cl^- , SO_4^{2-} , OH^- were repulsed away. The diminution of free sulfate ion in pore solution broke the equilibrium condition between free sulfate and bound sulfate. To re-establish a new equilibrium condition, ettringite and monosulfate were dissolved to supply an appropriate concentration of free sulfate.

The suggestion assumed the dissolution of ettringite and monosulfate were supported by XRD results of concrete powder as shown in table 4.33 to 4.35. Meanwhile ettringite content reduced remarkably in all three types of concrete; monosulfate content showed different tendency. In plain concrete, both ettringite content and monosulfate content reduced remarkably. It indicated that sulfate ion in pore solution of plain concrete was strongly repulsed away cathode and the zone nearby cathode, both low sulfate mineral, monosulfate, and high sulfate mineral,

ettringite also decomposed. Otherwise, in fly ash concrete and limestone fly ash concrete, meanwhile ettringite content diminished, monosulfate tended to increase. It indicated that in fly ash concrete and limestone fly ash concrete, after ECE treatment, although sulfate ion reduced, but remained sulfate content was still enough to produce monosulfate. In other words, due to the lack of sulfate ion, a part of ettringite transformed to the other mineral with lower sulfate ion in structure, monosulfate. Finally, in fly ash concrete and limestone fly ash concrete, ettringite content reduced and monosulfate content increased.

The augmentation of Portlandite after treatment was inevitable. It was observed in all cases. However, the rate of increase was affected by electrolyte and type of concrete. By XRD results as shown in table 4.33 to 4.35 and figure 4.32 to 4.49, in fly ash concrete and limestone fly ash concrete, Portlandite content augmented around 35% to 45% percent respect to Portlandite content before extracting; in plain concrete, Portlandite content increased more sharply, it may reach to 60%. These results were obvious correspondence to the results of calcium ion after extraction where calcium ion was dissolved mainly from Portlandite.

As mentioned, higher calcium content after extraction were perhaps contributed by two factors, slightly transportation of calcium from outside depth of concrete (mainly at middle thickness of concrete) and decomposition/transformation of the other minerals in concrete to release calcium. The decomposition of ettringite contributed an amount of free calcium, then, form Portlandite; however, the transformation of trisulfate (ettringite) to monosulfate did not release bound calcium to free calcium as much as the decomposition of ettringite, therefore, it was not effect so much on water soluble calcium. Corresponding to that phenomenon, in plain concrete, ettringite and monosulfate were mostly decomposed and released a large amount of calcium to form quite higher Portlandite content than before extraction. Meanwhile, in fly ash concrete and limestone fly ash concrete, most amount of trisulfate transferred to monosulfate; released calcium was increased insignificant. Therefore, Portlandite content measured by XRD as well as water soluble calcium ion at 1cm depth from interface of fly ash concrete and limestone fly ash concrete much less than in plain concrete.

Table 4.33: The result XRD of plain concrete

| Component | Content (% by weight of concrete) | | | | | |
|-------------|-----------------------------------|-------|-------|---------------|-------|-------|
| | 15cm diameter | | | 10cm diameter | | |
| | BE | AE | | BE | AE | |
| | | SC | LBB | | SC | LBB |
| Ettringite | 2.297 | 0.017 | 0.248 | 2.232 | 0.381 | 0.130 |
| Monosulfate | 1.720 | 0.328 | 0.109 | 1.698 | 0.246 | 0.127 |
| Portlandite | 5.062 | 8.616 | 7.942 | 5.002 | 8.456 | 7.105 |

Table 4.34: The result XRD of fly ash concrete

| Component | Content (% by weight of concrete) | | | | | |
|-------------|-----------------------------------|-------|-------|---------------|-------|-------|
| | 15 cm diameter | | | 10cm diameter | | |
| | BE | AE | | BE | AE | |
| | | SC | LBB | | SC | LLB |
| Ettringite | 1.256 | 0.558 | 0.579 | 1.145 | 0.705 | 0.309 |
| Monosulfate | 0.129 | 0.801 | 0.484 | 0.179 | 0.604 | 0.332 |
| Portlandite | 2.142 | 4.068 | 4.324 | 1.535 | 4.360 | 3.387 |

Table 4.35: The result XRD of limestone fly ash concrete

| Component | Content (% by weight of concrete) | | | | | |
|-------------|-----------------------------------|-------|-------|---------------|-------|-------|
| | 15cm diameter | | | 10cm diameter | | |
| | BE | AE | | BE | AE | |
| | | SC | LBB | | SC | LBB |
| Ettringite | 2.578 | 0.592 | 0.002 | 2.068 | 0.933 | 0.500 |
| Monosulfate | 0.666 | 1.032 | 0.418 | 0.975 | 0.170 | 0.672 |
| Portlandite | 2.973 | 4.620 | 4.269 | 2.464 | 3.780 | 4.128 |

The decomposition/transformation of ettringite and monosulfate were not the only source for increasing of calcium ion as well as Portlandite content after

extraction. Calcium silicate hydrate and morphology of calcium silicate hydrate also contributed an important role.

As well known, the higher CaO/SiO₂ ratio in C-S-H hydrated cement products, the less stable of this product since condition changed; here this was the change of pore solution during extracting. In case of plain concrete, C-S-H was form with higher ratio of CaO/SiO₂ (approximate 1.7 to 2) than in fly ash concrete and limestone fly ash concrete (approximate 1.5). So, due to the alteration of pore solution, the influence of electrical field as well as the re-establish of a new appropriate equilibrium corresponded to new condition, C-S-H with high CaO/SiO₂ tended to transform to minerals that was more stable on morphology, C-S-H with lower CaO/SiO₂ ratio.

By SEM and EDS result as shown in figures 4.32 to 4.49, it can be observed that, C-S-H mineral after extraction in all cases had lower C/S ratio than before extraction. Whereas, the lower rate of C/S ratio slightly affected by type of concrete. In plain concrete, C/S ratio in C-S-H after extracting reduced remarkably than in fly ash concrete and limestone fly ash concrete. Moreover, in most of cases, C-S-H detected after treatment contaminated by a large amount of sodium, especial in plain concrete.

C-S-H from hydrated cement products of ordinary Portland cement (usually type I) has higher porosity than in C-S-H from hydrated cement products of fly ash cement (usually type II or type III). So, sodium ion could ingress easier into its structure and substitute a part of calcium ion than in fly ash cement or limestone fly ash cement; then, hydrated cement products of plain concrete could liberate a higher amount of calcium ion than fly ash concrete and limestone fly ash concrete.

The higher rate of transformation/decomposition of hydrated cement product during extracting and the substituting a part of calcium ion by sodium ion in their structure could be possible to explain the quite higher content of water soluble calcium ion in plain concrete than in fly ash concrete and limestone fly ash concrete as shown in figures 4.29 and 4.30.

Sodium-rich crystal was detected easily at interfacial zone by SEM and EDX, especially at fly ash concrete and limestone fly ash concrete as shown in figures 4.33, 4.39, 4.42, 4.48 and 4.49, it was even easier to detect than Portlandite. The accumulation of sodium-rich crystal at interface was corresponding to the distribution

of sodium ion to interface, where sodium ion content at interfacial zone of fly ash concrete and limestone fly ash concrete was higher than in case of plain concrete.

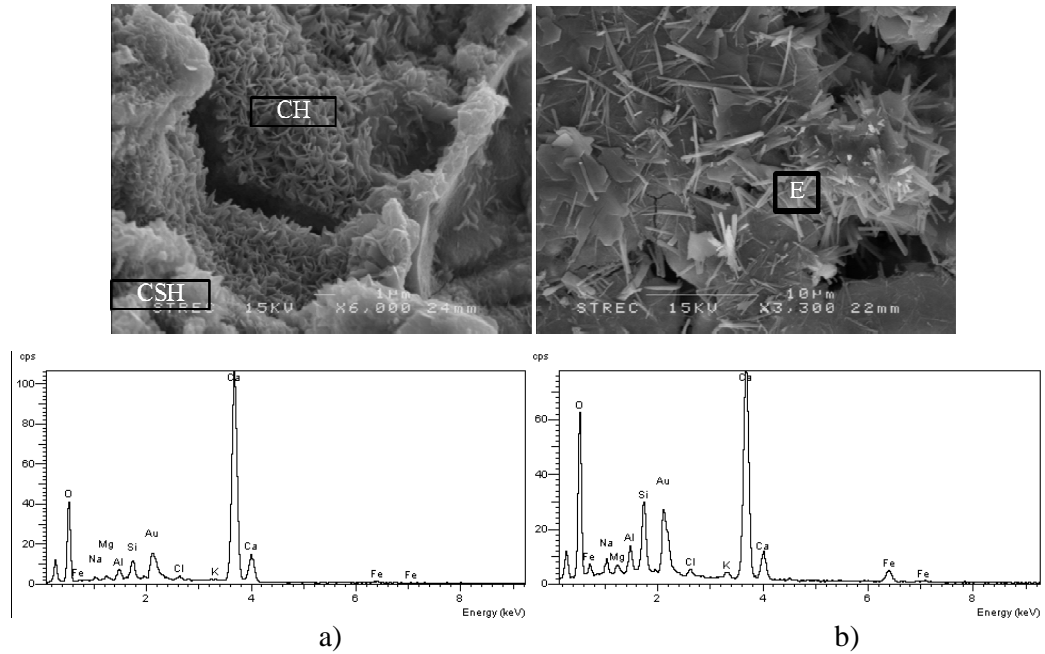


Figure 4.32: Scanning electron microscopy (SEM) of Portlandite (CH), C-S-H (CSH) and ettringite (E) and energy dispersive spectroscopy (EDS) at interfacial zone of plain concrete with diameter 10cm before extraction a) CH b) CSH

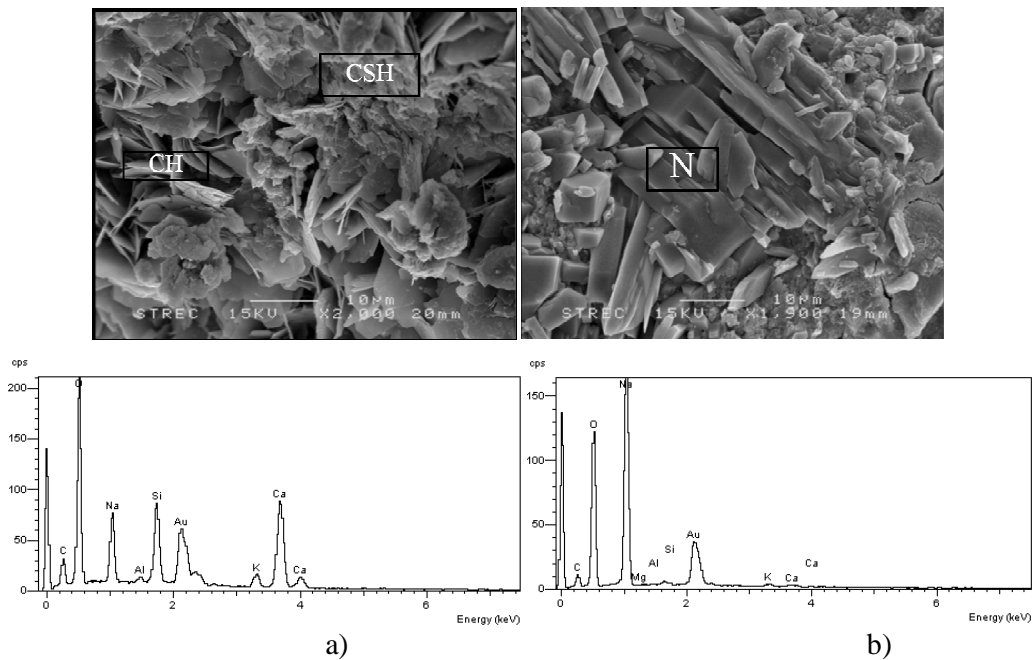


Figure 4.33: SEM and EDS after extraction with d=10cm of plain concrete in saturated calcium hydroxide a) CSH b) Sodium-rich crystal (N)

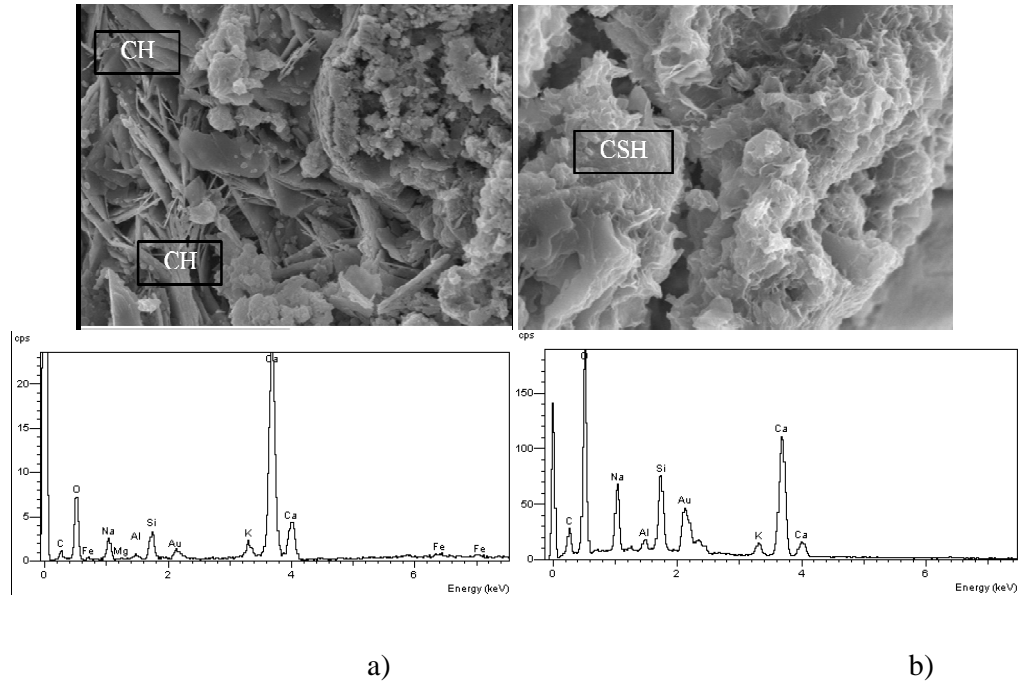


Figure 4.34: SEM and EDS after extraction with $d=10\text{cm}$ of plain concrete in lithium borate buffer a) CH b) CSH

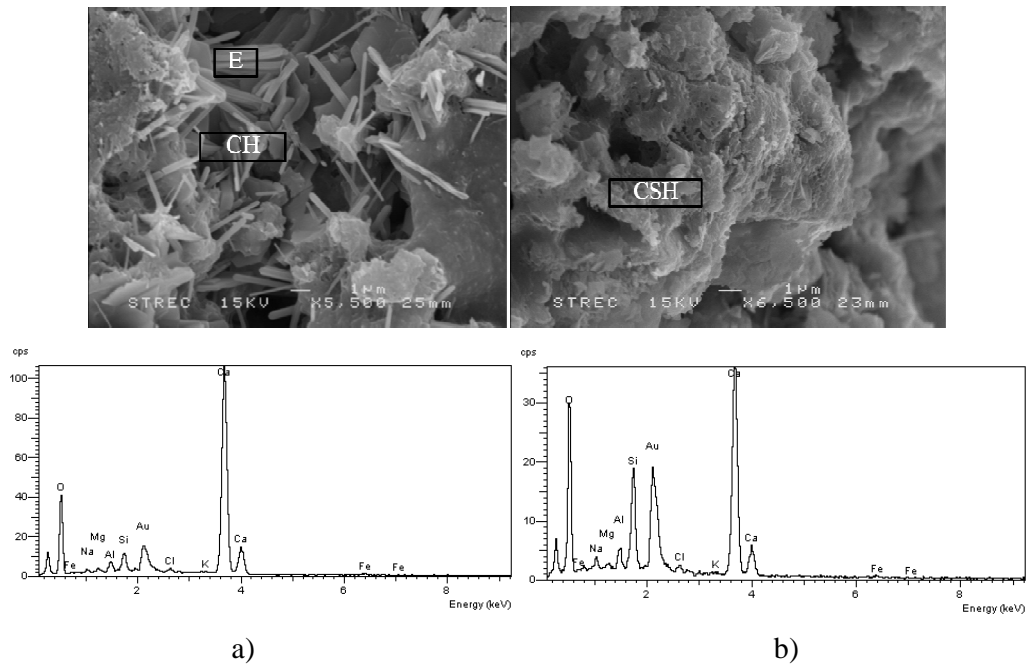


Figure 4.35: SEM and energy EDS at interfacial zone of plain concrete with diameter 15cm before extraction a) CH b) CSH

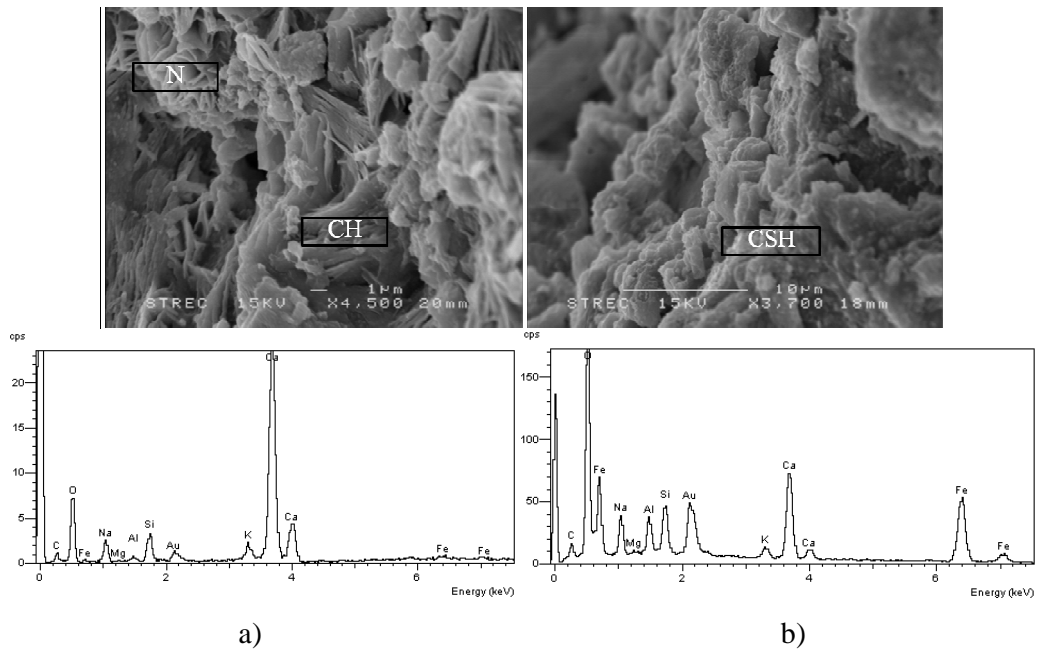


Figure 4.36: SEM and EDS after extraction with $d=15\text{cm}$ of plain concrete in saturated calcium hydroxide a) CH b) CSH

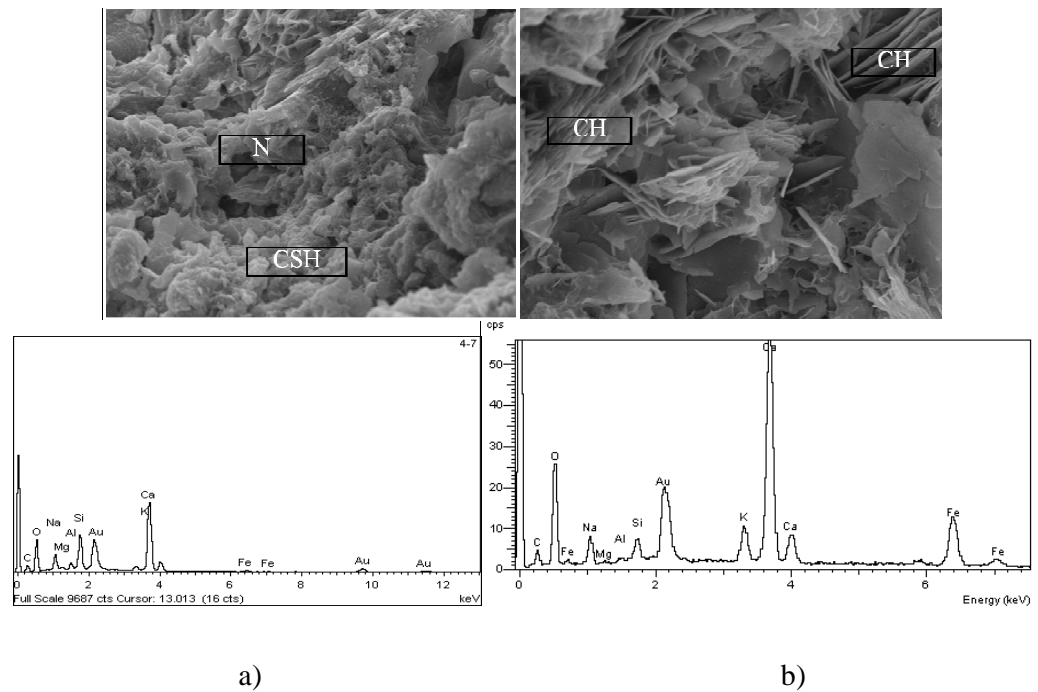


Figure 4.37: SEM and EDS after extraction with $d=15\text{cm}$ of plain concrete in lithium borate buffer a) CSH b) CH

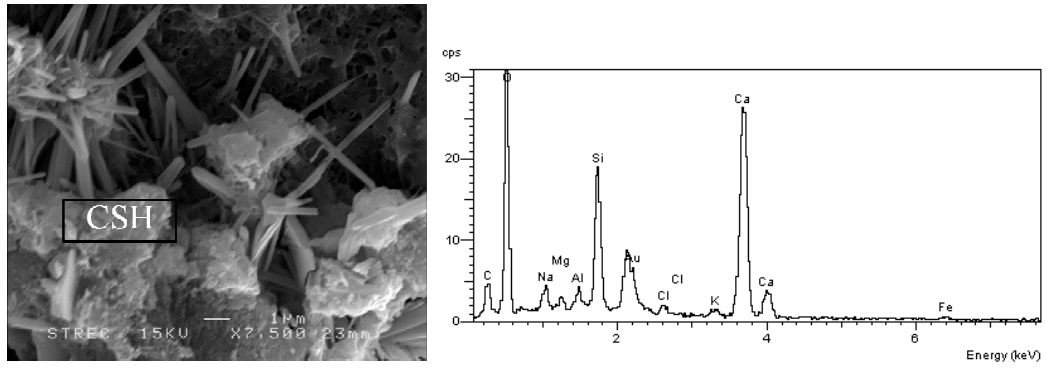
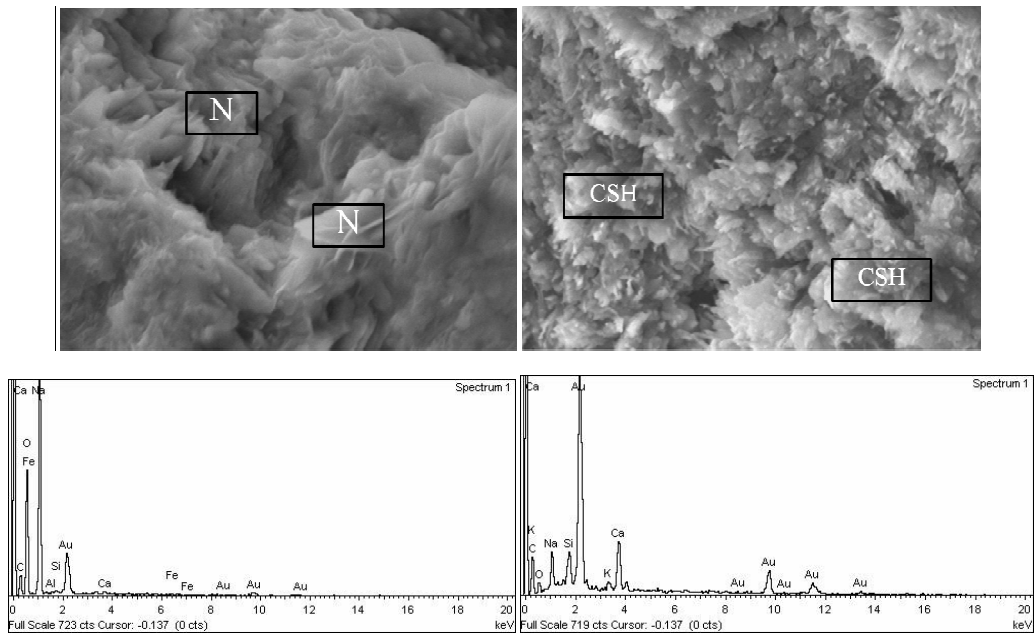


Figure 4.38: SEM and EDS (CSH) at interfacial zone of fly ash concrete with diameter 10cm before extraction



a)

b)

Figure 4.39: SEM and EDS at interfacial zone of fly ash concrete in saturated calcium hydroxide with diameter 10cm after extraction a) N b) CSH

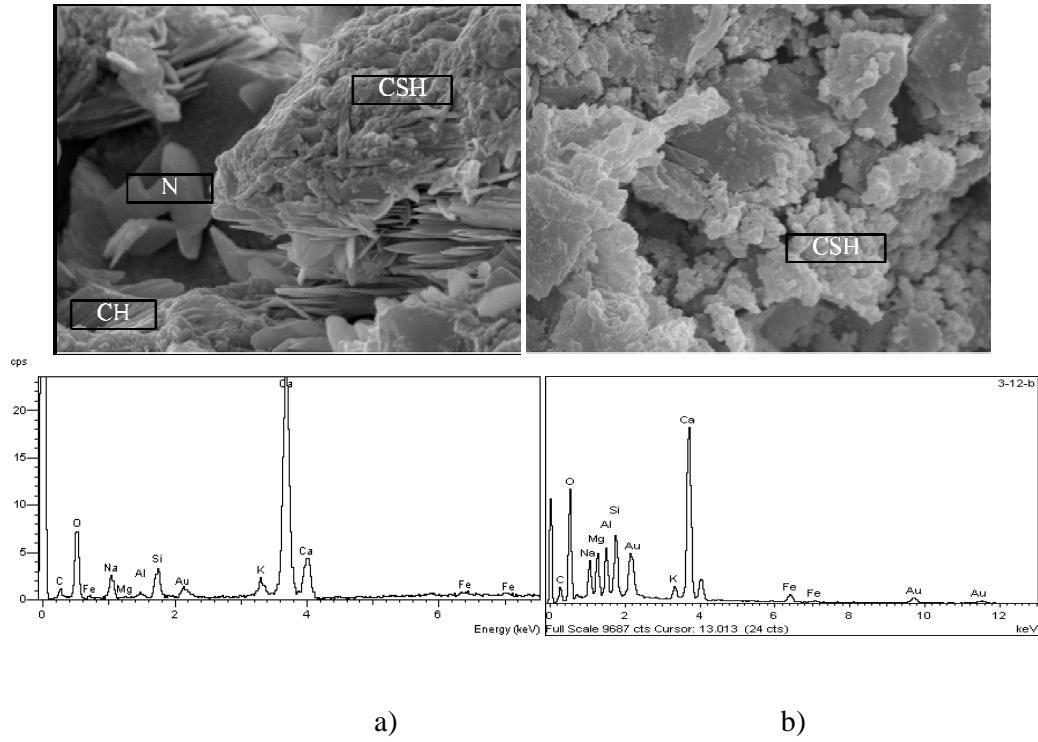


Figure 4.40: SEM and EDS at interfacial zone of fly ash concrete in lithium borate buffer with diameter 10cm after extraction a) CH b) CSH

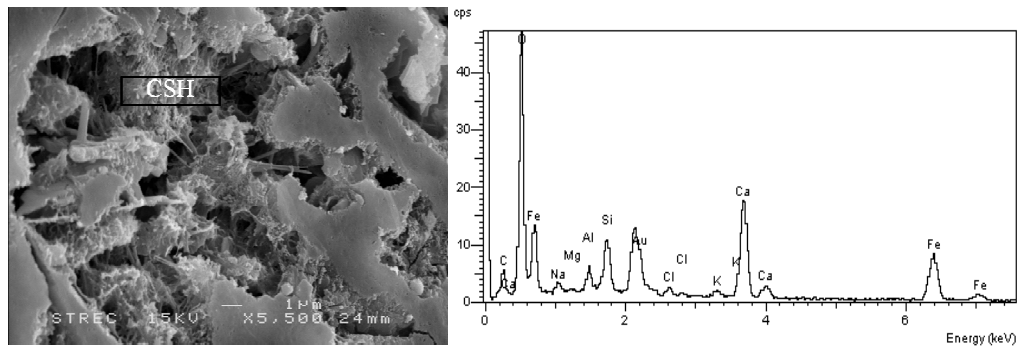


Figure 4.41: SEM and EDS (CSH) at interfacial zone of fly ash concrete with diameter 15cm before extraction

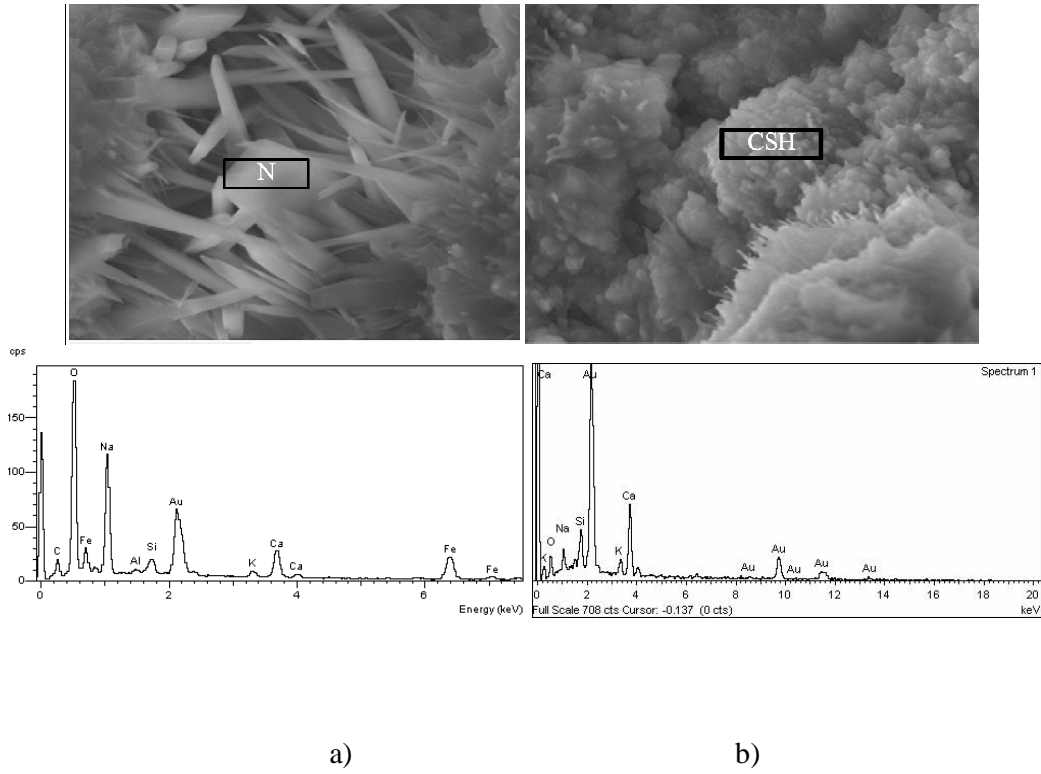


Figure 4.42: SEM and EDS at interfacial zone of fly ash concrete in saturated calcium hydroxide with diameter 15cm after extraction a) N b) CSH

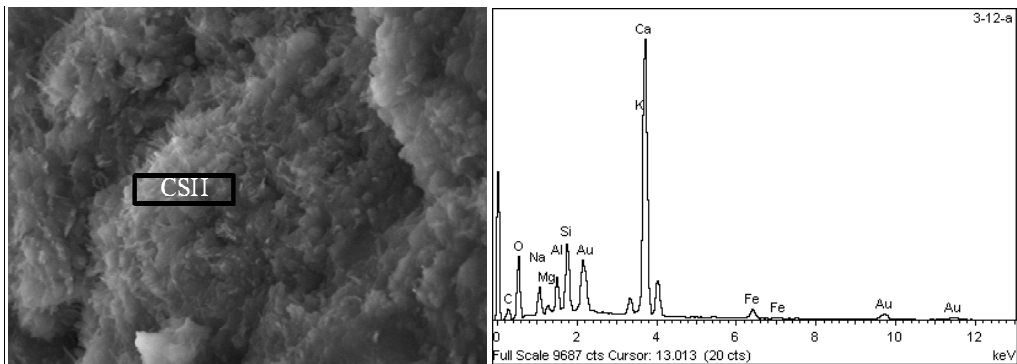


Figure 4.43: SEM and EDS (CSH) at interfacial zone of fly ash concrete in lithium borate buffer with diameter 15cm after extraction

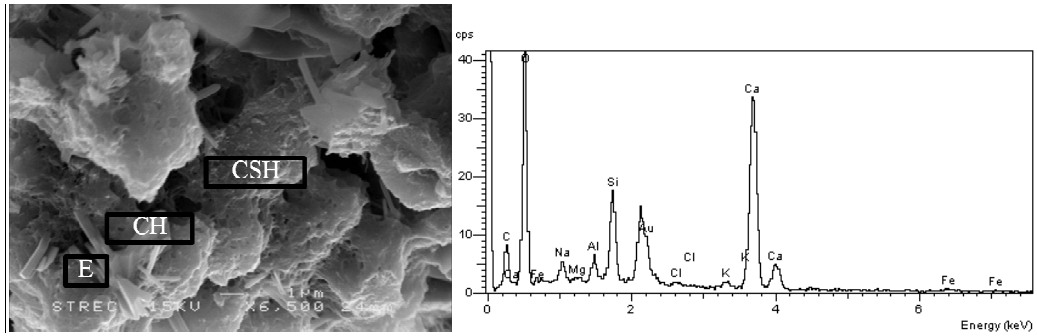


Figure 4.44: SEM and EDS (CSH) at interfacial zone of limestone fly ash concrete with diameter 10cm before extraction

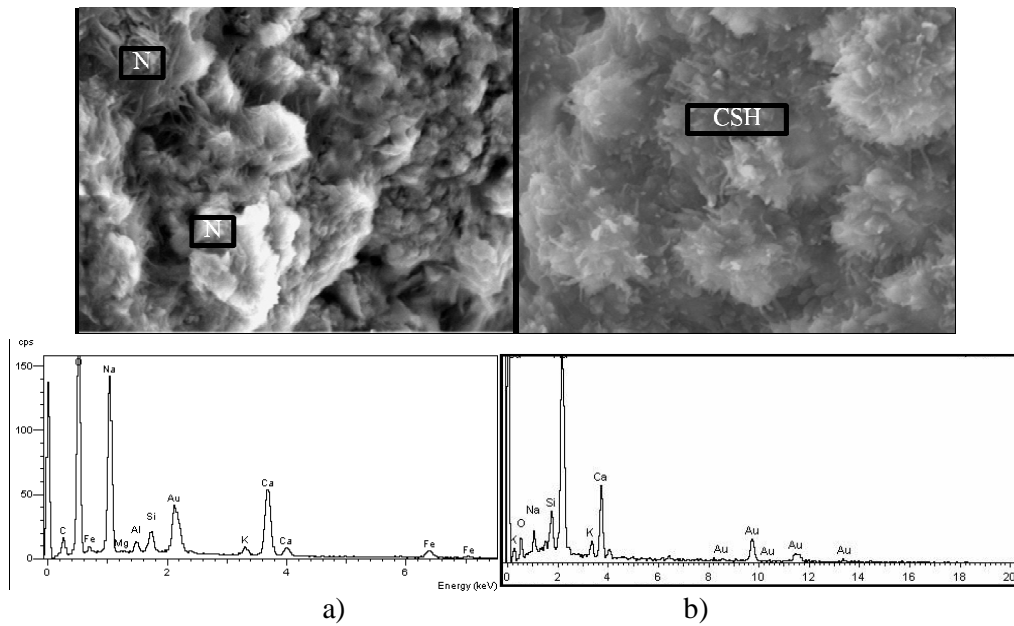


Figure 4.45: SEM and EDS at interfacial zone of limestone fly ash concrete with diameter 10cm after extraction with saturated calcium hydroxide a) N b) CSH

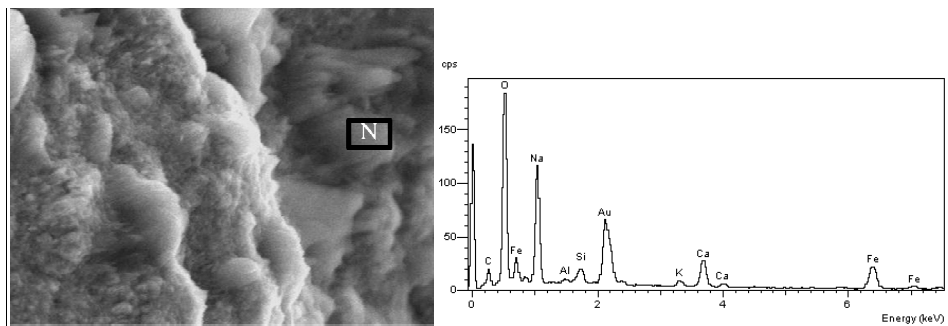


Figure 4.46: SEM and EDS (N) at interfacial zone of limestone fly ash concrete with diameter 10cm after extraction with lithium borate buffer

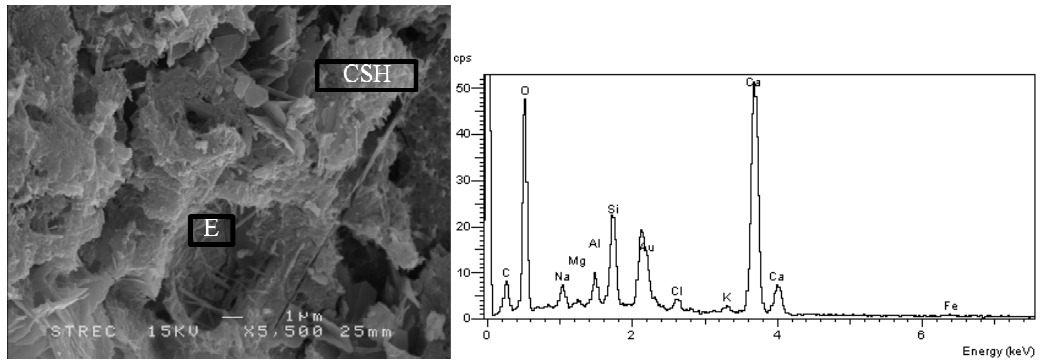


Figure 4.47: SEM and EDS (CSH) at interfacial zone of limestone fly ash concrete with diameter 15cm before extraction

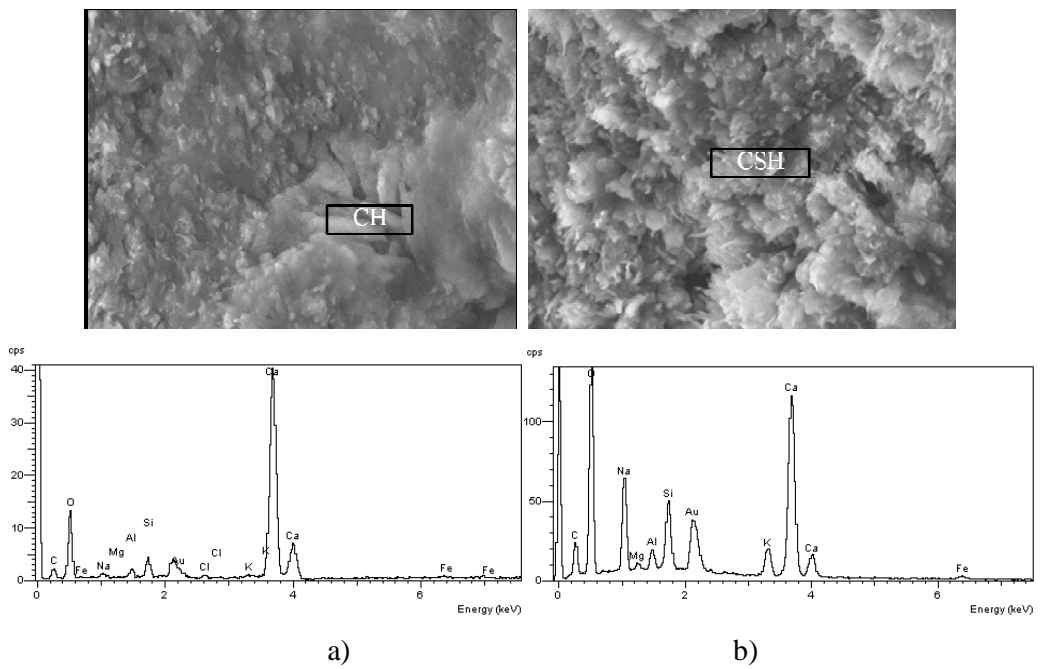


Figure 4.48: SEM and EDS at interfacial zone of limestone fly ash concrete with diameter 15cm after extraction with calcium hydroxide a) CH b) CSH

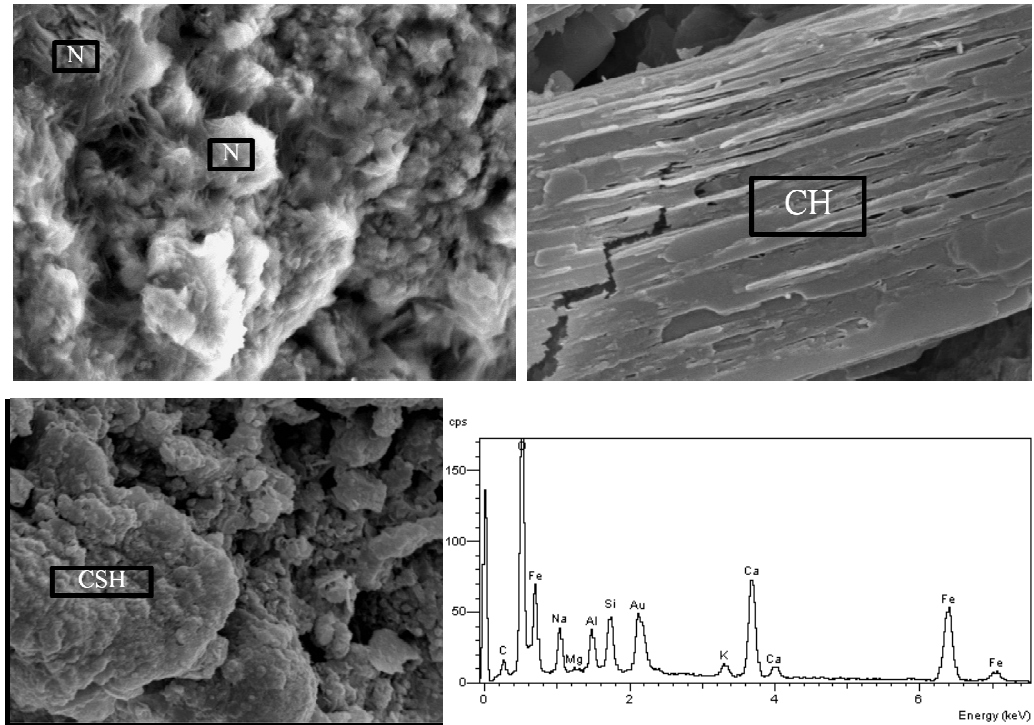


Figure 4.49: SEM and EDS (CSH) at interfacial zone of limestone fly ash concrete with diameter 15cm after extraction with lithium borate buffer

As mentioned above, available ions in pore solution of concrete played the main role in transferring the charge in concrete. By combining the results of the distribution of positive ions in concrete and inference from XRD, SEM and EDX, the flow of ions in pore solution of concrete to circulate the current included positive ions and negative ions., however, at the first time of treatment, it could include high content of ions with higher ionic mobility such as hydroxide, sulfate, chloride, potassium and sodium. Flow of positive ions from the zone outside transported from anode to cathode, since free content of these ions reduced, unstable minerals in concrete could decompose/transform to supply free ion for ionic flow. Calcium ion was a large source to supply free ion. Therefore, the transformation/decomposition of hydrated cement products was happened to release positive ion to pore solution.

In addition, the accumulation of calcium at cathode due to the transfer of calcium ion from outside concrete layer depended on treatment time; the longer time treatment, calcium ion, even with quite low ionic mobility, can transport to the zone nearby cathode. At the zone nearby surface of concrete, due to the lack of positive

ions in pore solution, calcium ion may release more from hydrated cement product than the zone nearby cathode, where accumulated much positive ions.

From these, it indicated that, extracted chloride was about 30% of initial chloride was probably a appropriate amount to lessen the accumulation of calcium ion at interface and the decomposition/transformation of hydrated cement products, therefore, the softening of concrete structure due to ECE can be reduce.

4.5 Half cell potential of embedded steel

With almost the same initial acid soluble chloride content, according to ASTM C876, the state of steel rod before extraction in plain concrete was on intermediate corrosion risk, meanwhile in fly ash concrete and limestone fly ash concrete, they were on high corrosion rate. This may concern to the influence of $[Cl^-]/[OH^-]$ ratio to corrosion of reinforcing steel.

Table 4.36: Half cell potential of steel versus corrosion risk

| Potential (mV) | | Corrosion rate |
|----------------|--------------|-----------------------------|
| Versus SCE | Versus CSE | |
| >-128 | >-200 | Low (10% corrosion risk) |
| -128 to -278 | -350 to -200 | Intermediate corrosion risk |
| <-278 | <-350 | High (90% corrosion risk) |
| <-426 | <-500 | Severe corrosion |

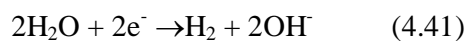
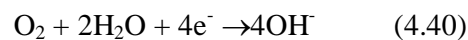
The effect of ECE on reinforcing steel was measured regularly every week after stopping the treatment up to five weeks. One week after halting, half cell potential of embedded steel was measured. And in all cases of concrete and electrolytes, it figured out a great severe corrosion rate of embedded steel. However, at the week later, difference was recognized. During the testing process, most of cases, the un-corroded paint covered on steel surface was prepared before casting concrete was still working. However, there were some specimens that cover was broken. Meanwhile half cell potential of specimens with working un-corroded paint cover increased substantially at the weeks later, half cell potential of specimens that un-corroded paint cover broken was still as low as the week before. And the great severe corrosion rate on destroying un-corroded paint cover was maintained all the time measured half cell potential of

reinforcing steel. Here, half cell potential of specimens with working un-corroded paint cover would be discussed.

From result of specimens with working un-corroded paint cover as shown in table 4.39 and figures 4.50 to 4.52, one week after stopping ECE, half cell potential of reinforcing steel in all cases of concrete and electrolytes were such negative versus copper sulfate electrode. However, it increased significantly at two weeks later. And up to the fourth week, half cell potential of embedded steel approached to static and they were on low corrosion risk state.

These results indicated that ECE can be accepted as a technique method to mitigate or delay corrosion of reinforcing steel in reinforced concrete with initial condition of steel before extraction was on intermediate corrosion risk or beginning on high corrosion risk; whether concrete here was plain concrete, fly ash concrete or limestone fly ash concrete with water/binder ratio 0.4. Moreover, it also indicated that, the evaluation the effect of ECE on corrosion state of reinforcing steel by using parameter measured immediately or just short time after stopping ECE was unreliable.

There were many previous researchers measured half cell potential of reinforcing steel immediately or just a short time after halting ECE treatment. And received data indicated that after treatment, state of embedded steel was more harmful, or in some research, they investigated half cell potential within one month after halting ECE, it increased but increased rate was not enough to put embedded steel on passivity zone. Since then, two suppositions were assumed to explain the diminution of half cell potential measured after extraction. On hand, some authors assumed that phenomenon due to the depletion of oxygen or the hydrolysis of water at cathode during extracting as shown in equations 4.40 and 4.41. On the other hand, some authors explained that phenomenon by using Pourbaix diagram of iron. They inferred that, after extraction, high basic condition at interfacial zone was a favorite environment for forming HFeO_2^- and FeO_2^{2-} .



During extraction process, cathodic sites and anodic sites in reinforcing steel rod totally altered to cathodic site; simultaneously, passive layer on steel surface can also alter to iron. Then, the surface of embedded steel immediately or short time after

stopping treatment could be very susceptible. By Nernst equation, half cell potential of copper/copper sulfate electrode and iron/ferrous can be computed by equations (4.42) and (4.43).

$$E_{Cu^{2+}/Cu} = E_{Cu^{2+}/Cu}^0 + \frac{0.059}{2} \log[Cu^{2+}] = 0.34 + \frac{0.059}{2} \log[Cu^{2+}](V) \quad (4.42)$$

$$E_{Fe^{2+}/Fe} = E_{Fe^{2+}/Fe}^0 + \frac{0.059}{2} \log[Fe^{2+}] = -0.45 + \frac{0.059}{2} \log[Fe^{2+}](V) \quad (4.43)$$

$$E_{Measure} = E_{Fe^{2+}/Fe} - E_{Cu^{2+}/Cu} \quad (4.44)$$

With reference electrode was copper-copper sulfate and assuming that concentration of ferrous was insignificant, half cell potential of reinforcing steel measured as shown in table 4.39 was totally reasonable. The re-diffusion of oxygen and alkaline surrounding environment was great advantage for re-forming of passive layer. That was perhaps the reason for increasing of half cell potential of reinforcing steel at four weeks later. It was perhaps the reason for maintaining of severe corrosion state of reinforcing steel in case un-corroded paint cover was destroyed where susceptible iron surface was not protected by un-corroded paint cover or basic environment was easy to corrode.

However, assumption of forming high soluble products of ferrous such as $HFeO_2^-$ or FeO_2^{2-} should be on doubting, at least in this study. Although it was clear that after ECE treatment, calcium hydroxide content at interfacial increased significantly; the solubility of it is limited, at normal temperature condition around 25°C to 30°C, just around 1.52 g/l. This amount of calcium hydroxide can just induce a basic environment with pH approximately 12.3; meanwhile to corrode iron on alkaline condition, pH of environment must be higher than 13.6. Then, this assumption needs more study to prove it. Half cell potential results of this research showed above assumption did not happen. Nevertheless, from the results of positive ion above, the accumulation of alkaline ions could have very high solubility (proven by the result of water soluble alkaline ions) and can induce high basic environment. Therefore, measuring pH on pore solution extracted directly from concrete is a necessary study to gain an appropriate mechanism can be explained for quite low half cell potential of embedded steel at short time after ECE treatment.

In this study, by table 4.39, it indicated most of cases, at the same type of concrete and electrolyte, half cell potential of embedded steel in 10cm diameter specimens at one week after halting ECE were slightly higher than in 15cm diameter specimens. However, the rate of lower was not so far. They were both on great severe corrosion condition.

It was not clear enough to have any conclusion the effect of type of concrete or type of electrolyte on augment of half cell potential to reach on low corrosion state as shown in Figure 4.53 to 4.54. The approximate basic environment in pore solution may be the reason.

Table 4.37: Half cell potential of steel rod versus saturated copper sulfate electrode

| | | Half cell potential of steel(Versus CSE, mV) | | | | | | |
|----------|-------------|--|------|--------|---------|---------|---------|---------|
| Concrete | Electrolyte | D (cm) | AE | | | | | |
| | | | BE | 1 week | 2 weeks | 3 weeks | 4 weeks | 5 weeks |
| PC | SC | 10 | -220 | -780 | -423 | -180 | -40 | -41 |
| | | 15 | -320 | -950 | -534 | -239 | -49 | -48 |
| | LBB | 10 | -220 | -894 | -338 | -174 | -96 | -90 |
| | | 15 | -320 | -953 | -594 | -242 | -138 | -112 |
| FC | SC | 10 | -341 | -982 | -621 | -299 | -88 | -82 |
| | | 15 | -350 | -1004 | -644 | -257 | -64 | -68 |
| | LBB | 10 | -341 | -893 | -564 | -274 | -112 | -110 |
| | | 15 | -350 | -967 | -582 | -326 | -101 | -99 |
| LFC | SC | 10 | -358 | -949 | -521 | -192 | -92 | -94 |
| | | 15 | -375 | -1001 | -528 | -257 | -65 | -62 |
| | LBB | 10 | -358 | -893 | -464 | -274 | -115 | -110 |
| | | 15 | -375 | -877 | -582 | -317 | -102 | -100 |

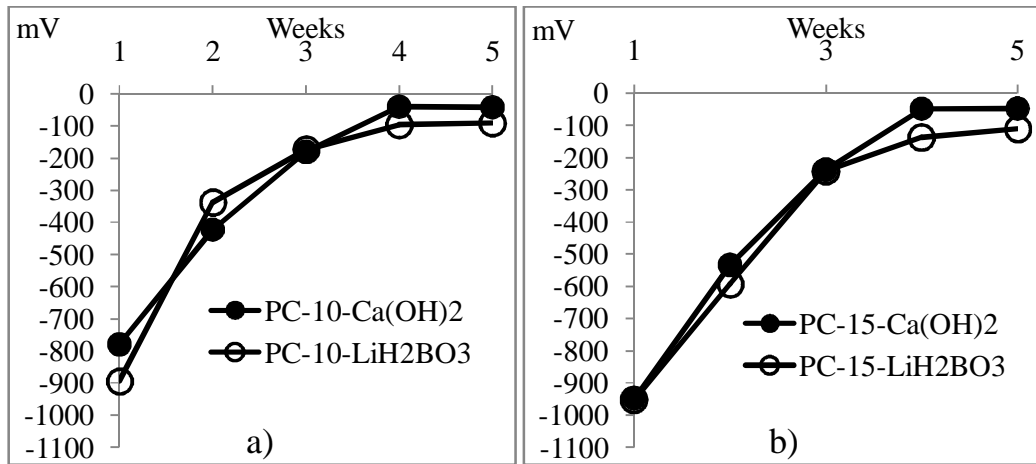


Figure 4.50: Half cell potential of reinforcing steel after stopped ECE treatment on plain concrete with diameter a) 10cm b) 15cm

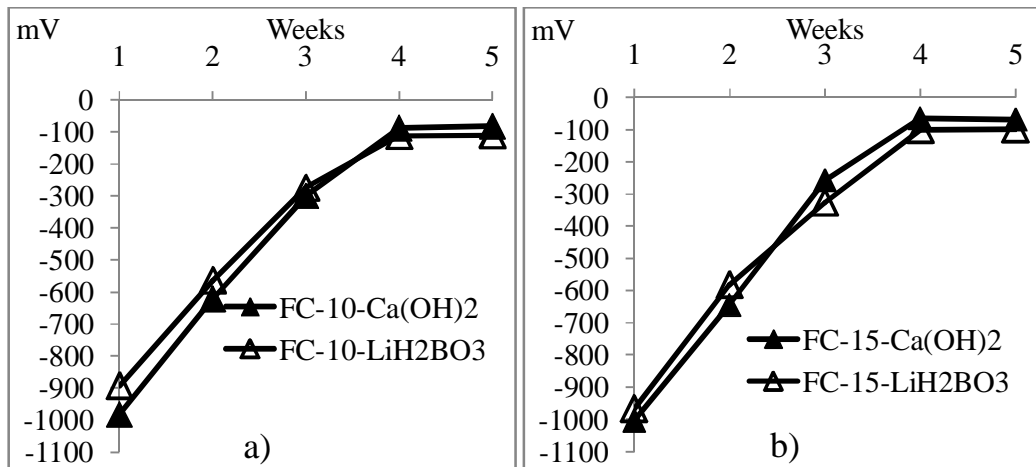


Figure 4.51: Half cell potential of reinforcing steel after stopped ECE treatment on fly ash concrete with diameter a) 10cm b) 15cm

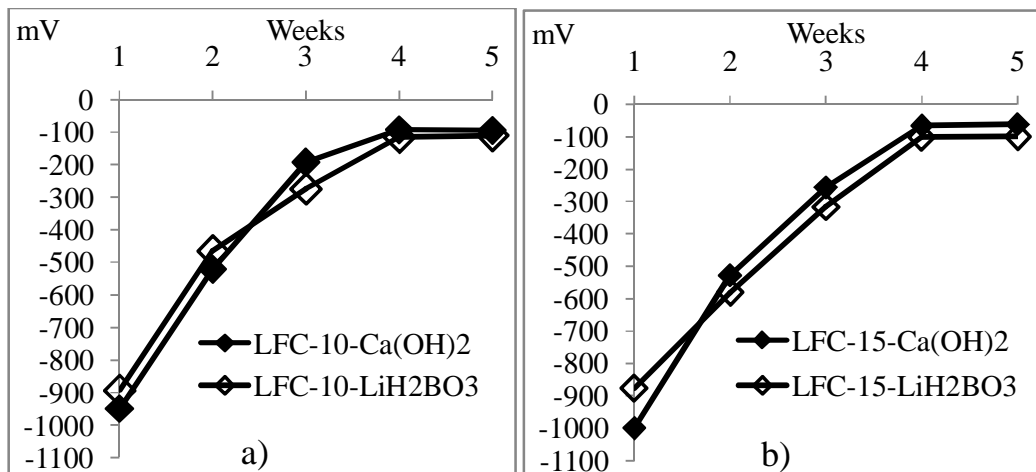


Figure 4.52: Half cell potential of reinforcing steel after stopped ECE treatment on limestone fly ash concrete with diameter a) 10cm b) 15cm

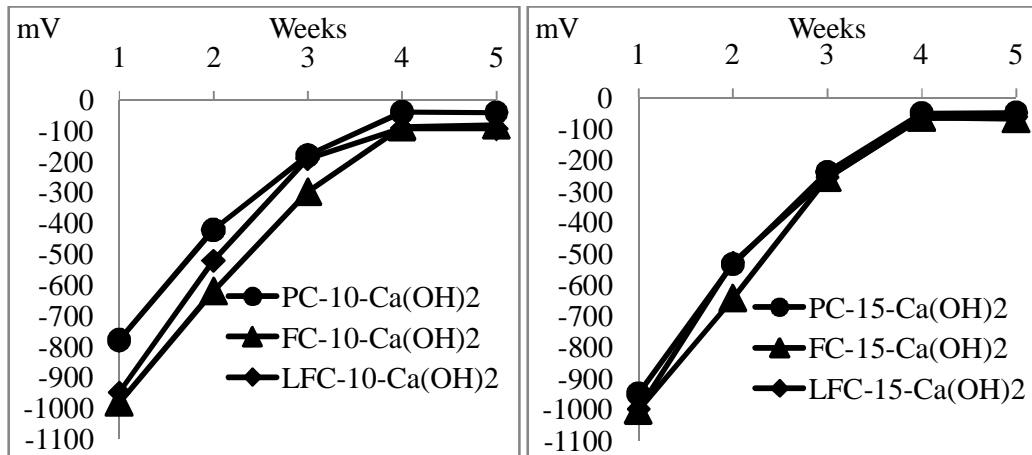


Figure 4.53: Influence of concrete type to half cell potential in case of saturated calcium hydroxide as electrolyte with diameter a) 10cm b) 15cm

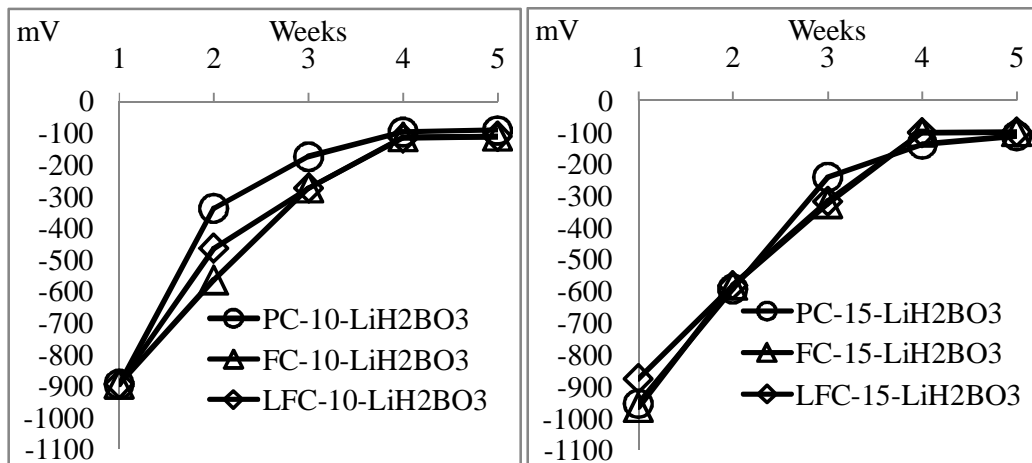


Figure 4.54: Influence of concrete type to half cell potential in case lithium borate buffer as electrolyte with diameter a) 10cm b) 15cm

CHAPTER 5

CONCLUSION AND RECOMMENDATION

5.1 Conclusion

Based on the result of both concrete microstructure and corrosion state of embedded steel, they indicated that electro-chemical chloride extraction could be considered as a rehabilitation method for reinforced concrete structure contaminated chloride with:

1. Condition of reinforced concrete structure need to be extracted have:
 - Acid soluble chloride content in concrete is less than 1.5% by mass of cement.
 - Corrosion state of embedded steel was specified on intermediate corrosion or at beginning of high corrosion by half cell potential monitoring.
 - Concrete composition could satisfy requirements for concrete using in marine environment, water/binder ratio 0.4 and minimum strength 35MPa. It can be plain concrete, fly ash concrete with 30% fly ash by mass of cement or limestone fly ash concrete with 25% fly ash and 5% limestone powder by mass of cement, respectively. Moreover concrete thickness can reach to 7cm.
2. Alternative mode on turning on power is more efficient mode to release chloride out of concrete than consecutive mode.
3. Impressed current density is 0.5A/m^2 with respect to concrete surface area.
4. Extracted chloride out of concrete is about 30% of initial acid soluble chloride content.

After extraction, reinforced concrete structure had:

1. Average acid soluble chloride content was still quite higher than threshold value; however, it reduced remarkable at interfacial zone, reached to threshold value or even lower.
2. Alkaline ions accumulated to alkali-rich crystal at the zone nearby steel/concrete interface. High content of Portlandite was observed at interface.
3. C-S-H was detected with lower C/S than before extraction, moreover, it contaminated a large amount of alkaline ions.

4. Ettringite was rarely to detect at interfacial zone.
5. Embedded steel can reach to passive state after halting extraction process within four weeks.

5.2 Recommendation

1. ECE could be a method for rehabilitation the concrete structure contaminated chloride with total contaminated chloride less than 1.5%.
2. The rate of decomposition/transformation of minerals in concrete during extracting need more study.
3. Although alternative mode of powering is better appropriate mode than consecutive mode, the appropriate time for turning-on and turning-off of power needs to study carefully to gain a suitable time and schedule for extraction process.
4. The morphology of mineral after extraction need to investigate carefully.
5. Saturated calcium hydroxide could be slightly more efficient than lithium borate buffer in releasing chloride.
6. Hydrated products of binder in fly ash concrete and limestone fly ash concrete seemed more stable in ECE than in plain concrete. However, the results from SEM showed an abnormal morphology of C-S-H. So, it needs more study to evaluate the effect of ECE on morphology of hydrated products of binder.
7. The evolution of hydrogen may reduce bonding strength steel and concrete. Simultaneously, it may embrittle embedded steel during extraction. It needs to investigate carefully.

REFERENCES

- American Society for Testing and Materials Standards. **ASTM Standard test Methods for chemical analysis of hydraulic cement: ASTM C114**. Philadelphia: ASTM Committee on Standards, 1997.
- American Society for Testing and Materials Standards. **ASTM Standard test Methods for Acid-Soluble chloride in mortar and concrete: ASTM C1152**. Philadelphia: ASTM Committee on Standards, 1997.
- Abdelaziz, G. E., Abdelalim, A. M. K., and Fawzy, Y. A. (2009) Evaluation of the short and long-term efficiencies of electro-chemical chloride extraction, **Cement and Concrete Research** **39**, 727-732.
- Aïtcin, P. C. (2003) The durability characteristics of high performance concrete: a review, **Cement and Concrete Composites** **25**, 409-420.
- Andrade, C., and Alonso, C. (2004) Test methods for on-site corrosion rate measurement of steel reinforcement in concrete by means of the polarization resistance method, **Materials and Structures** **37**, 623-643.
- Elsener, B. (2008) Long-term durability of electrochemical chloride extraction, **Materials and Corrosion** **59**, 91-97.
- Elsener, B., and Angst, U. (2007) Mechanism of electrochemical chloride removal, **Corrosion Science** **49**, 4504-4522.
- Fajardo, G., Escadeillas, G., and Arliguie, G. (2006) Electrochemical chloride extraction (ECE) from steel-reinforced concrete specimens contaminated by “artificial” sea-water, **Corrosion Science** **48**, 110-125.
- Gaidis, J. M. (2004) Chemistry of corrosion inhibitors, **Cement and Concrete Composites** **26**, 181-189.
- García Alcocel E., Garcés, P., and Chinchón, S. (2000) General study of alkaline hydrolysis in calcium aluminate cement mortars under a broad range of experimental conditions, **Cement and Concrete Research** **30**, 1689-1699.

- Ghods, P., Isgor, O., and Pour-Ghaz, M. (2008) Experimental verification and application of a practical corrosion model for uniformly depassivated steel in concrete, **Materials and Structures** **41**, 1211-1223.
- Glass, G. K., Page, C. L., Short, N. R., and Yu, S. W. (1993) An investigation of galvanostatic transient methods used to monitor the corrosion rate of steel in concrete, **Corrosion Science** **35**, 1585-1592.
- Gowripalan, N., Sirivivatnanon, V., and Lim, C. C. (2000) Chloride diffusivity of concrete cracked in flexure, **Cement and Concrete Research** **30**, 725-730.
- Green, W. K., Lyon, S. B., and Scantlebury, J. D. (1993) Electrochemical changes in chloride-contaminated reinforced concrete following cathodic polarisation, **Corrosion Science** **35**, 1627-1631.
- Irassar, E. F., Violini, D., Rahhal, V. F., Milanesi, C., Trezza, M. A., and Bonavetti, V. L. (2011) Influence of limestone content, gypsum content and fineness on early age properties of Portland limestone cement produced by inter-grinding, **Cement and Concrete Composites** **33**, 192-200.
- Ismail, M., and Muhammad, B. (2011) Electrochemical chloride extraction effect on blended cements, **Advances in Cement Research**, pp 241-248.
- Kadri, E., Aggoun, S., De Schutter, G., and Ezziane, K. (2010) Combined effect of chemical nature and fineness of mineral powders on Portland cement hydration, **Materials and Structures** **43**, 665-673.
- Lambert, P., Page, C., and Vassie, P. (1991) Investigations of reinforcement corrosion. 2. Electrochemical monitoring of steel in chloride-contaminated concrete, **Materials and Structures** **24**, 351-358.
- Luo, R., Cai, Y., Wang, C., and Huang, X. (2003) Study of chloride binding and diffusion in GGBS concrete, **Cement and Concrete Research** **33**, 1-7.
- Marcotte, T. D., Hansson, C. M., and Hope, B. B. (1999) The effect of the electrochemical chloride extraction treatment on steel-reinforced mortar Part I:

- Electrochemical measurements, **Cement and Concrete Research** **29**, 1555-1560.
- Marcotte, T. D., Hansson, C. M., and Hope, B. B. (1999) The effect of the electrochemical chloride extraction treatment on steel-reinforced mortar Part II: Microstructural characterization, **Cement and Concrete Research** **29**, 1561-1568.
- Montemor, M. F., Simões, A. M. P., and Ferreira, M. G. S. (2003) Chloride-induced corrosion on reinforcing steel: from the fundamentals to the monitoring techniques, **Cement and Concrete Composites** **25**, 491-502.
- Orellan, J. C., Escadeillas, G., and Arliguie, G. (2004) Electrochemical chloride extraction: efficiency and side effects, **Cement and Concrete Research** **34**, 227-234.
- Raupach, M. (1996) Investigations on the influence of oxygen on corrosion of steel in concrete—Part I, **Materials and Structures** **29**, 174-184.
- Redaelli, E., and Bertolini, L. (2011) Electrochemical repair techniques in carbonated concrete. Part I: electrochemical realkalisation, **Journal of Applied Electrochemistry** **41**, 817-827.
- Redaelli, E., and Bertolini, L. (2011) Electrochemical repair techniques in carbonated concrete. Part II: cathodic protection, **Journal of Applied Electrochemistry** **41**, 829-837.
- Sieglwart, M., Lyness, J. F., McFarland, B. J., and Doyle, G. (2005) The effect of electrochemical chloride extraction on pre-stressed concrete, **Construction and Building Materials** **19**, 585-594.
- Söylev, T. A., and Richardson, M. G. (2008) Corrosion inhibitors for steel in concrete: State-of-the-art report, **Construction and Building Materials** **22**, 609-622.
- Swamy, R. N., and McHugh, S. (2006) Effectiveness and structural implications of electrochemical chloride extraction from reinforced concrete beams, **Cement and Concrete Composites** **28**, 722-733.
- Tsivilis, S., Chaniotakis, E., Kakali, G., and Batis, G. (2002) An analysis of the properties of Portland limestone cements and concrete, **Cement and Concrete Composites** **24**, 371-378.

- Vennesland, Ø., Raupach, M., and Andrade, C. (2007) Recommendation of Rilem TC 154-EMC: “Electrochemical techniques for measuring corrosion in concrete”—measurements with embedded probes, **Materials and Structures** **40**, 745-758.
- Wang, X., Yu, Q., Deng, C., Wei, J., and Wen, Z. (2007) Change of electrochemical property of reinforced concrete after electrochemical chloride extraction, **Journal of Wuhan University of Technology--Materials Science Edition** **22**, 764-769.
- Yodsudjai, W., and Saelim, W. (2013) Influences of Electric Potential and Electrolyte on Electrochemical Chloride Removal in Reinforced Concrete, **Journal of Materials in Civil Engineering**, 10.1061/(ASCE)MT.1943-5533.0000777.

APPENDIX

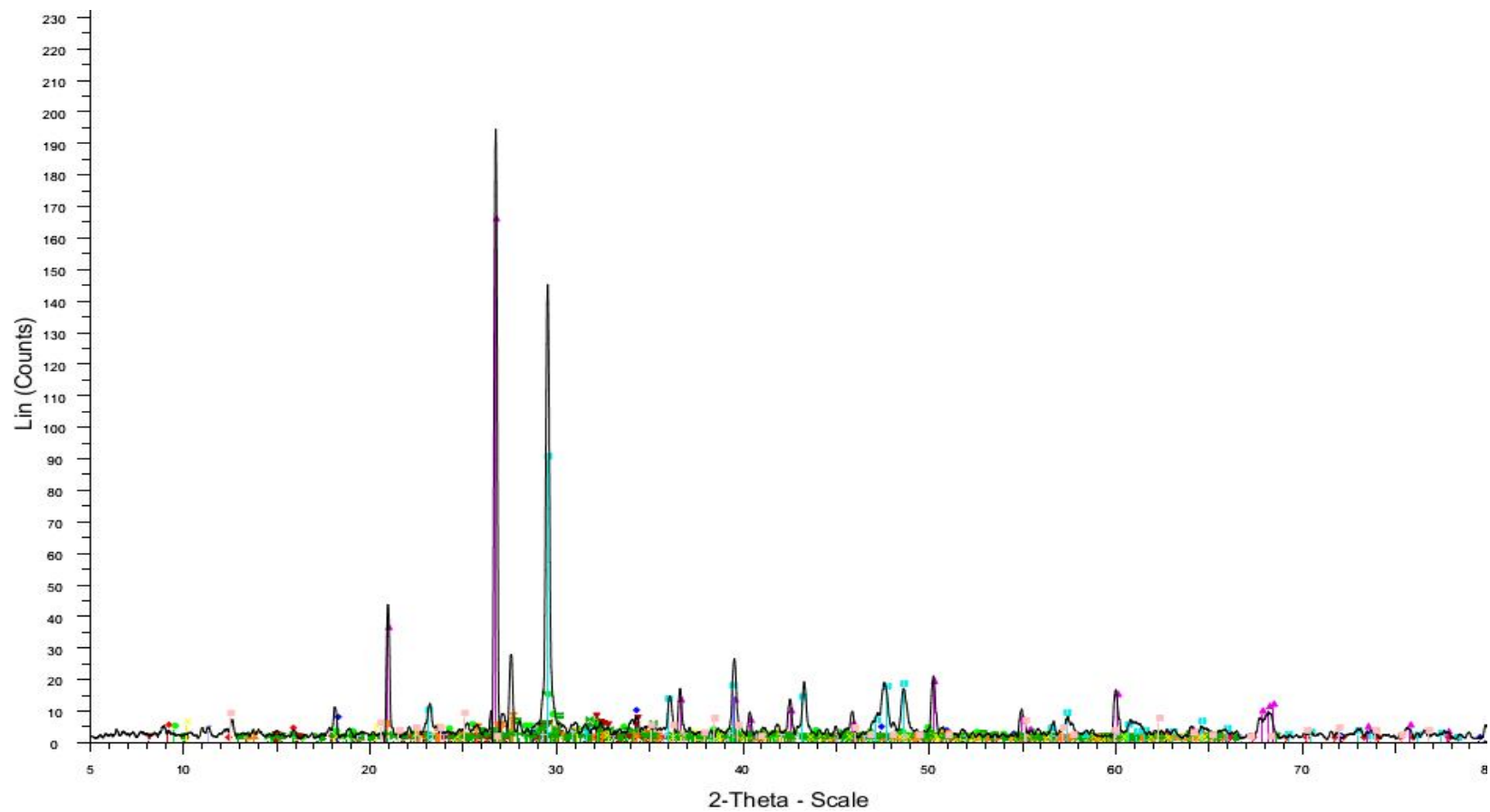


Figure 1: XRD result of PC 10cm before extraction

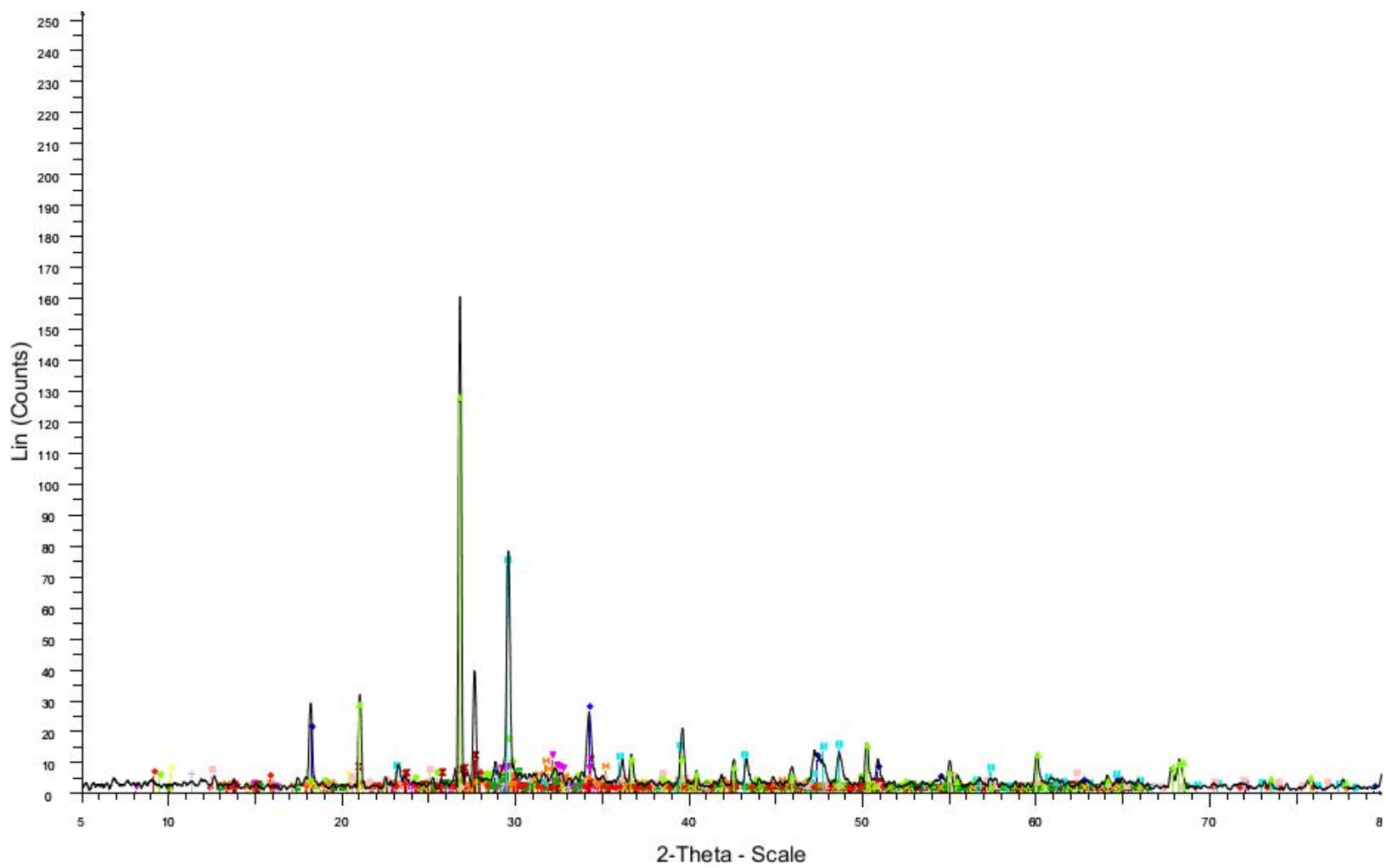


Figure 2: XRD result of PC 10cm after extraction in saturate calcium hydroxide

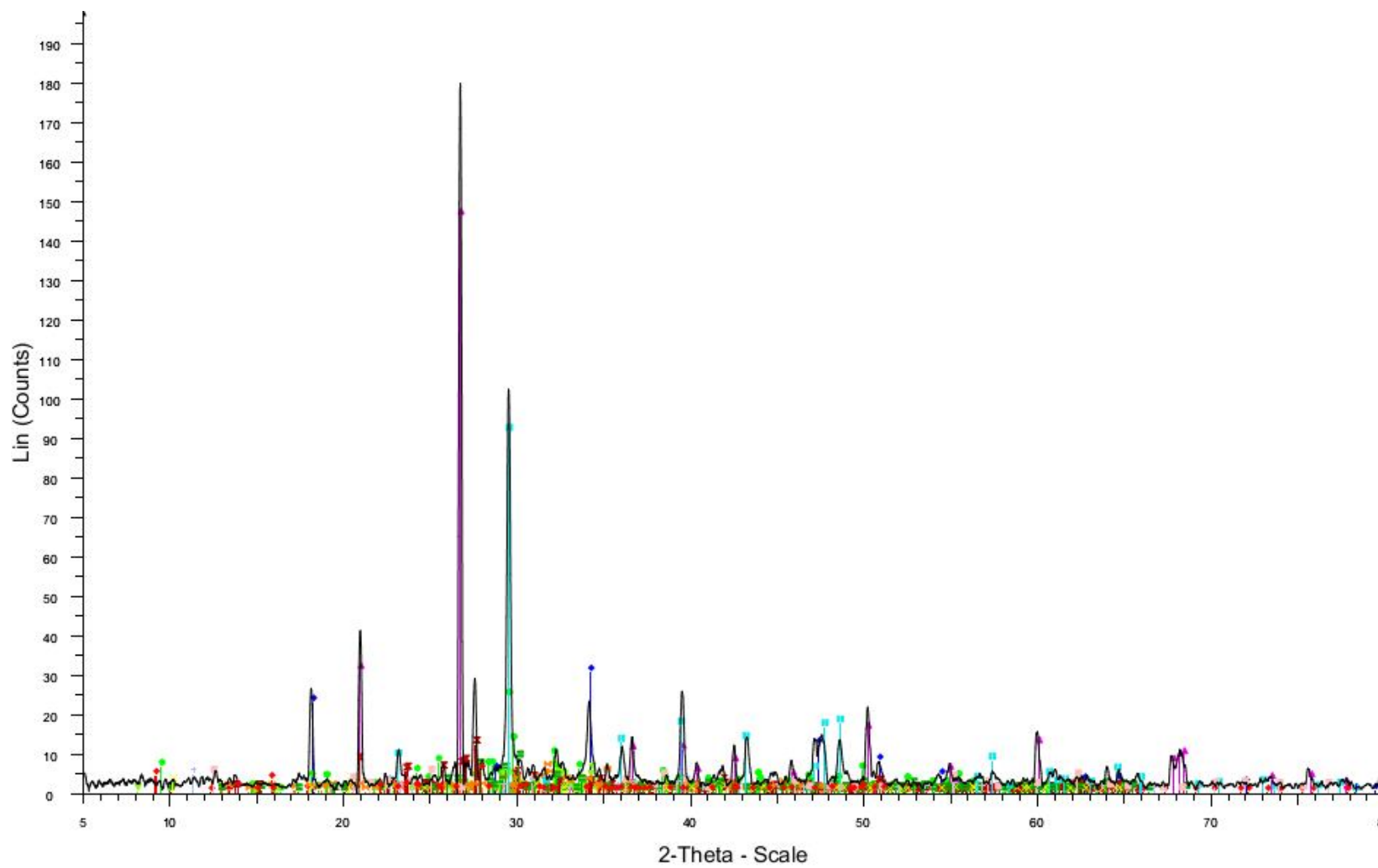


Figure 3: XRD result of PC 10cm after extraction in lithium borate buffer

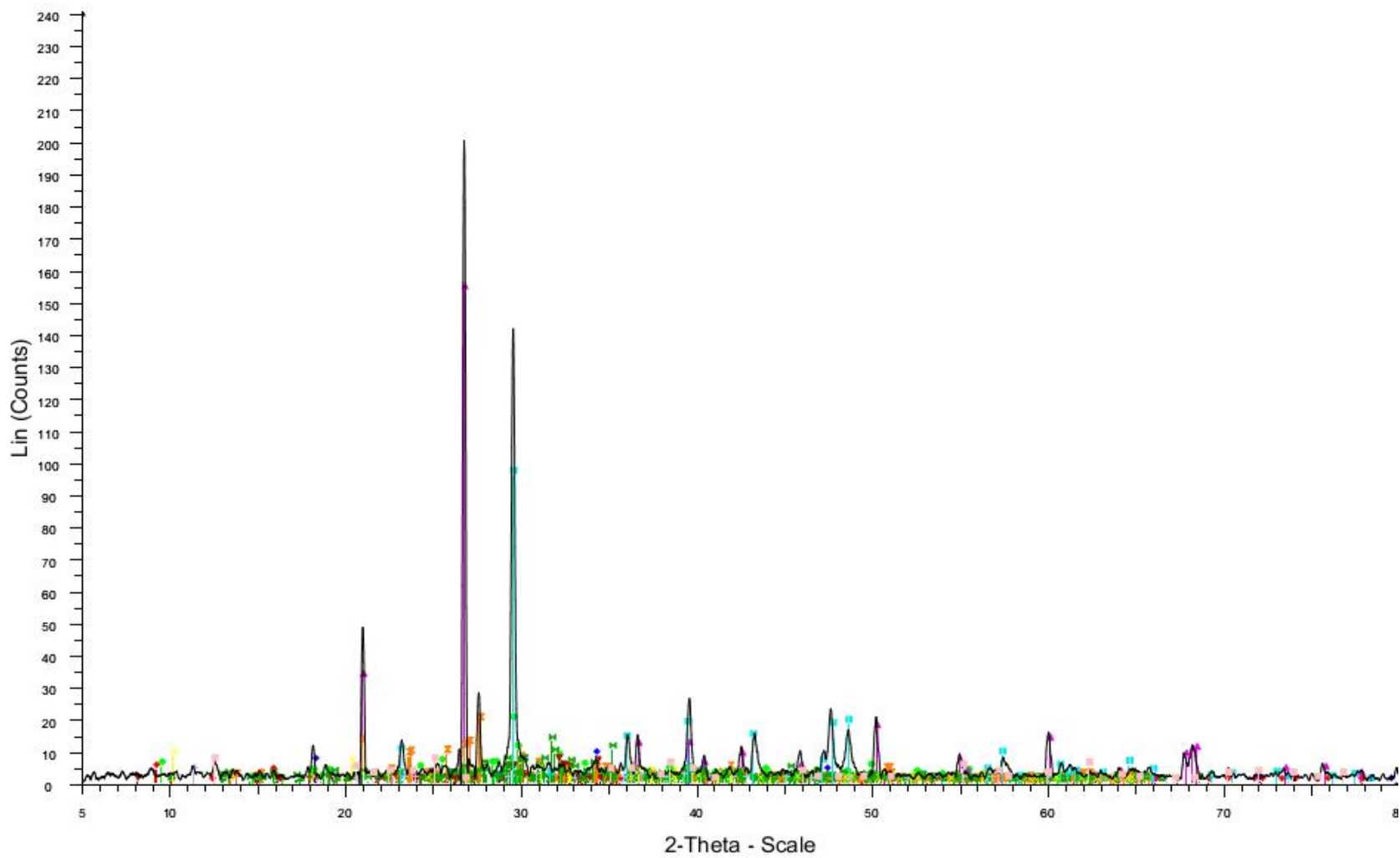


Figure 4: XRD result of FC 10cm before extraction

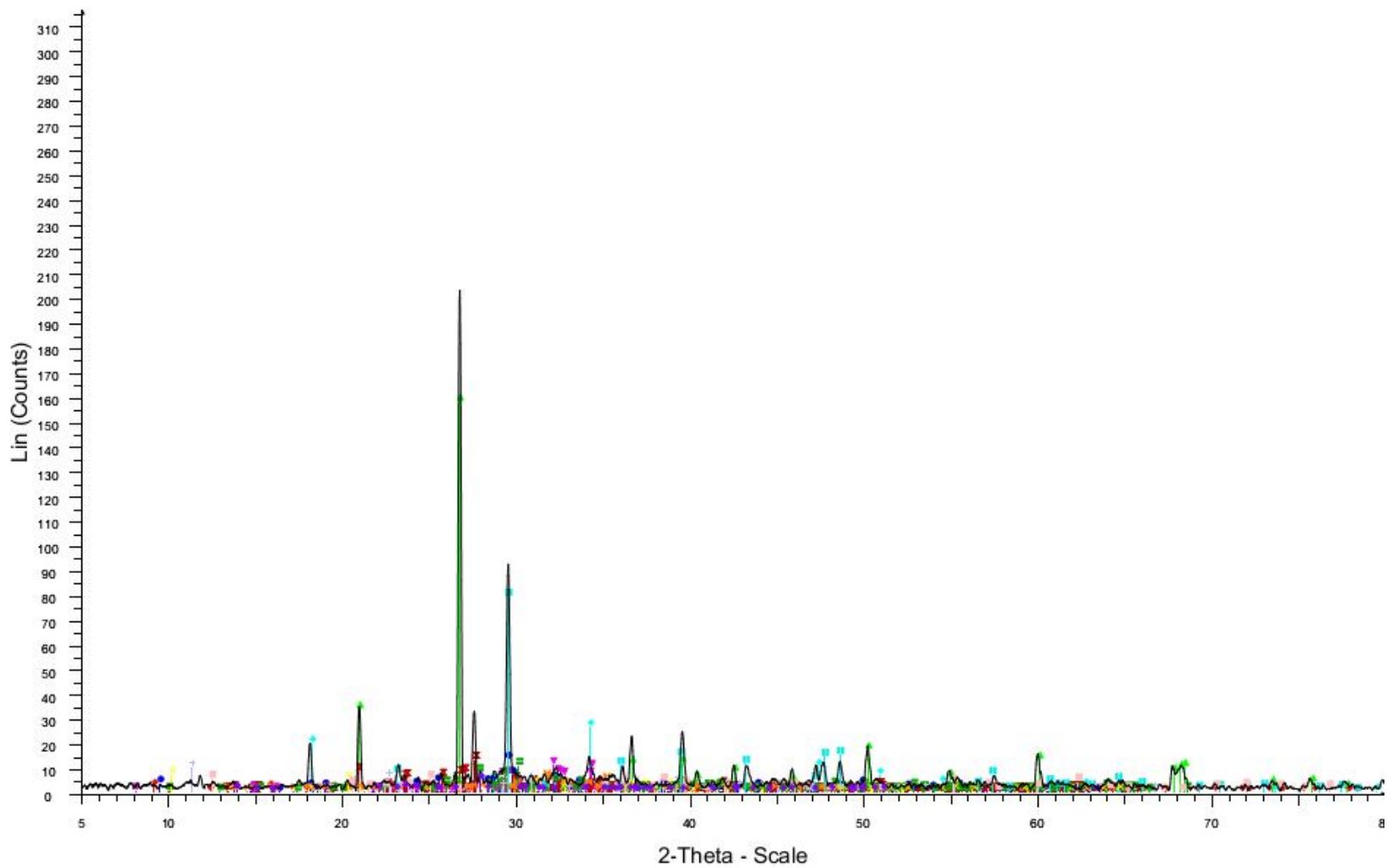


Figure 5: XRD result of FC 10cm after extraction in saturate calcium hydroxide

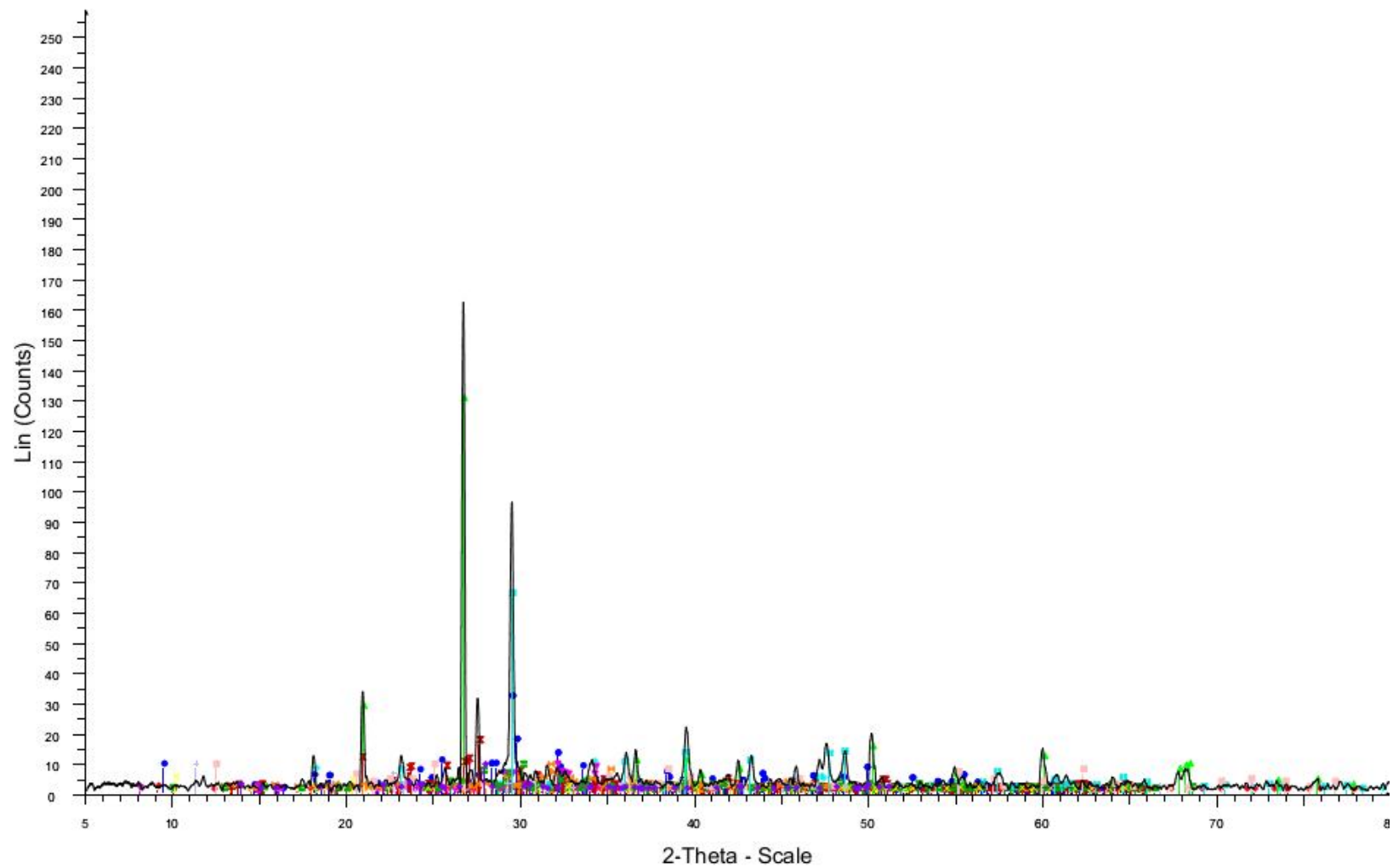


Figure 6: XRD result of FC 10cm after extraction in lithium borate buffer

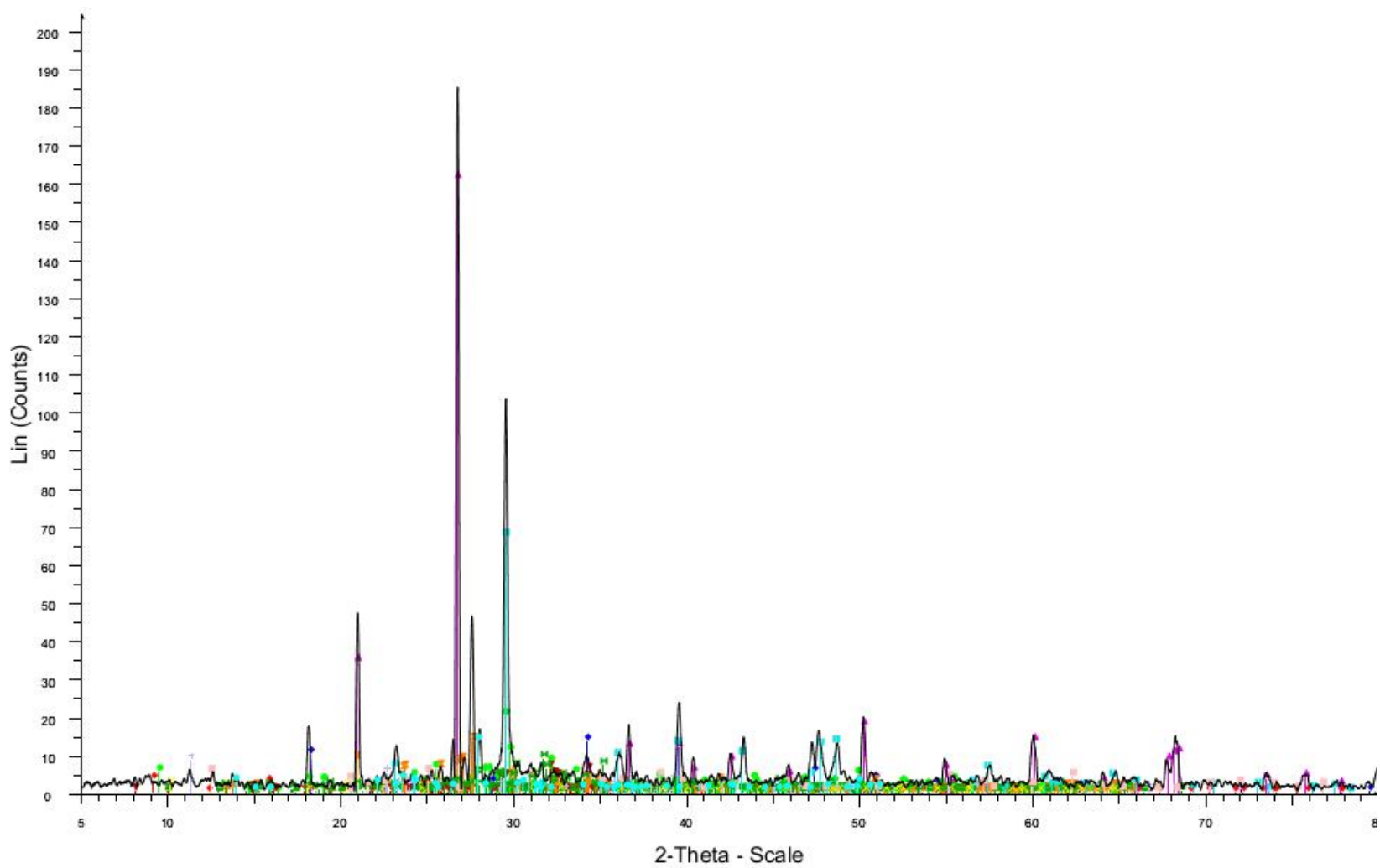


Figure 7: XRD result of LFC 10cm before extraction

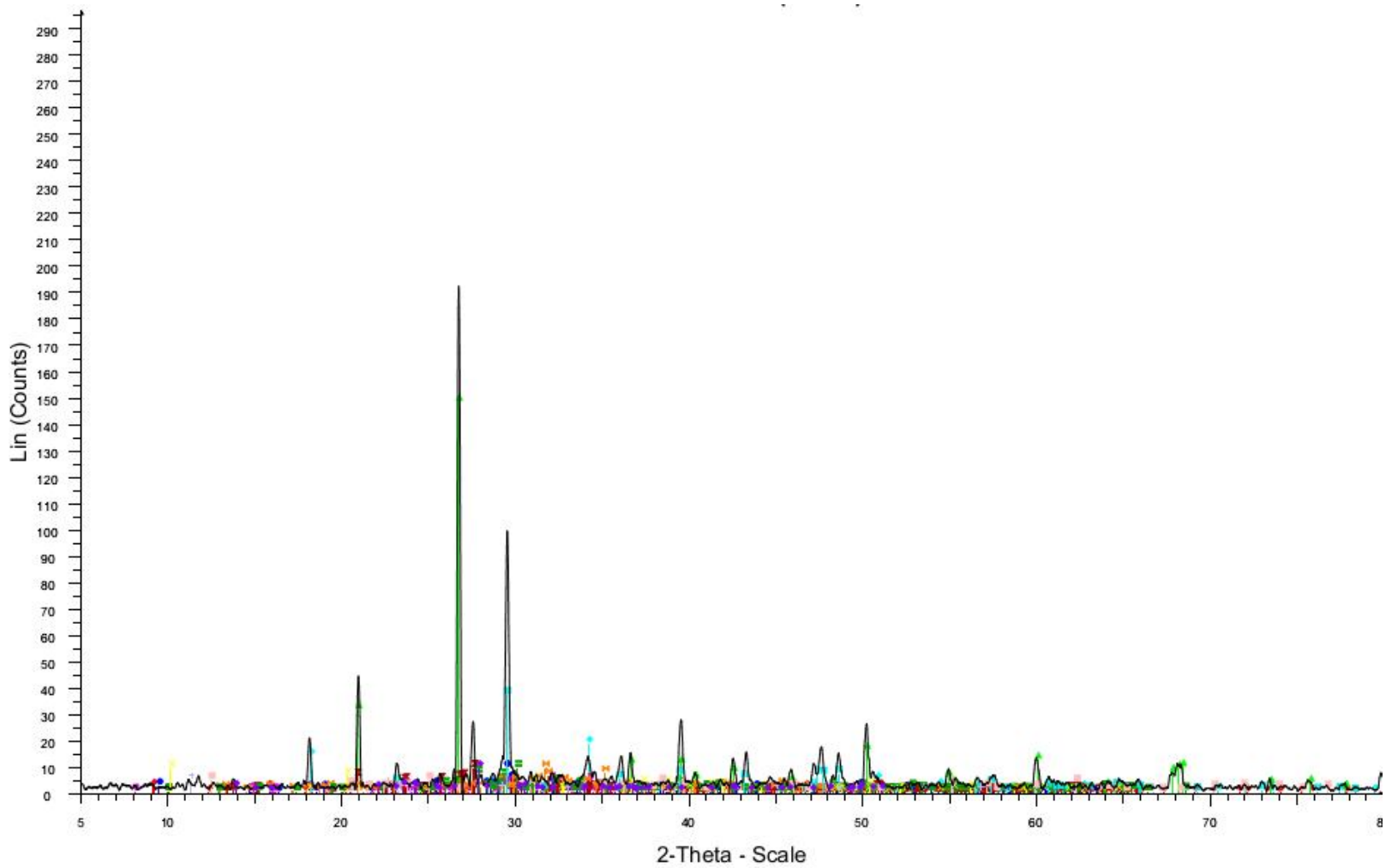


Figure 8: XRD result of LFC 10cm after extraction in saturated calcium hydroxide

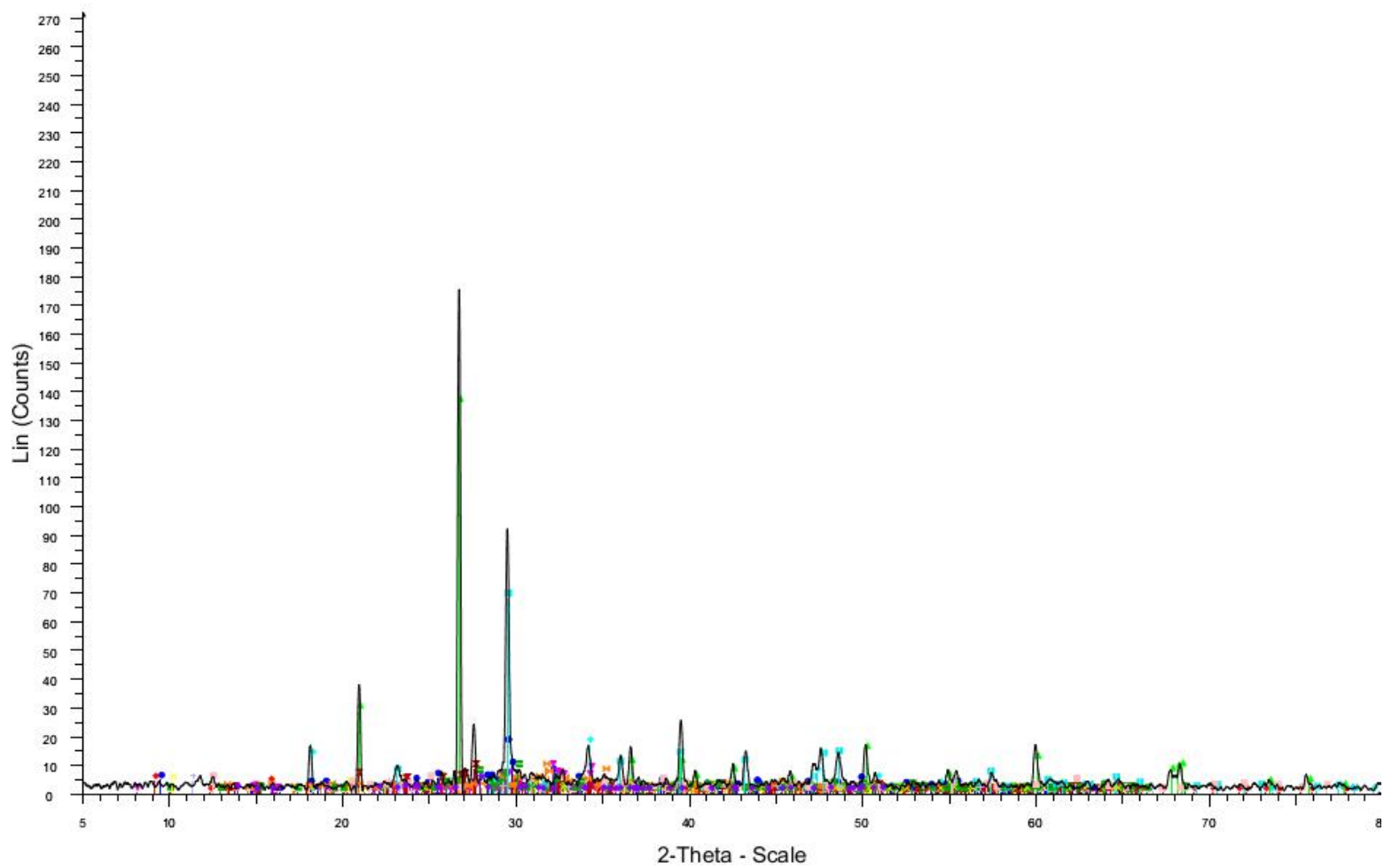


Figure 9: XRD result of LFC 10cm after extraction in lithium borate buffer

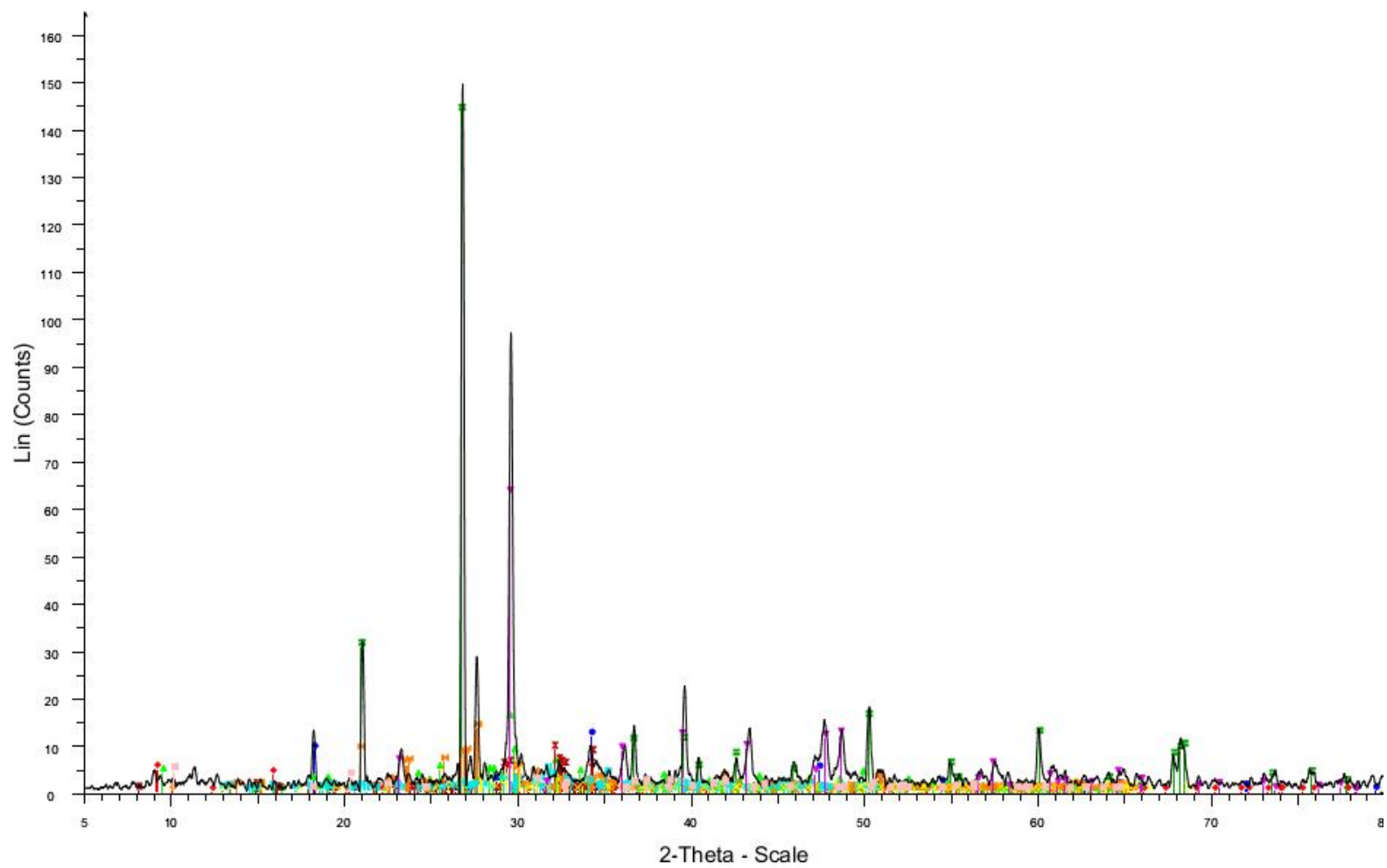


Figure 10: XRD result of PC 15cm before extraction

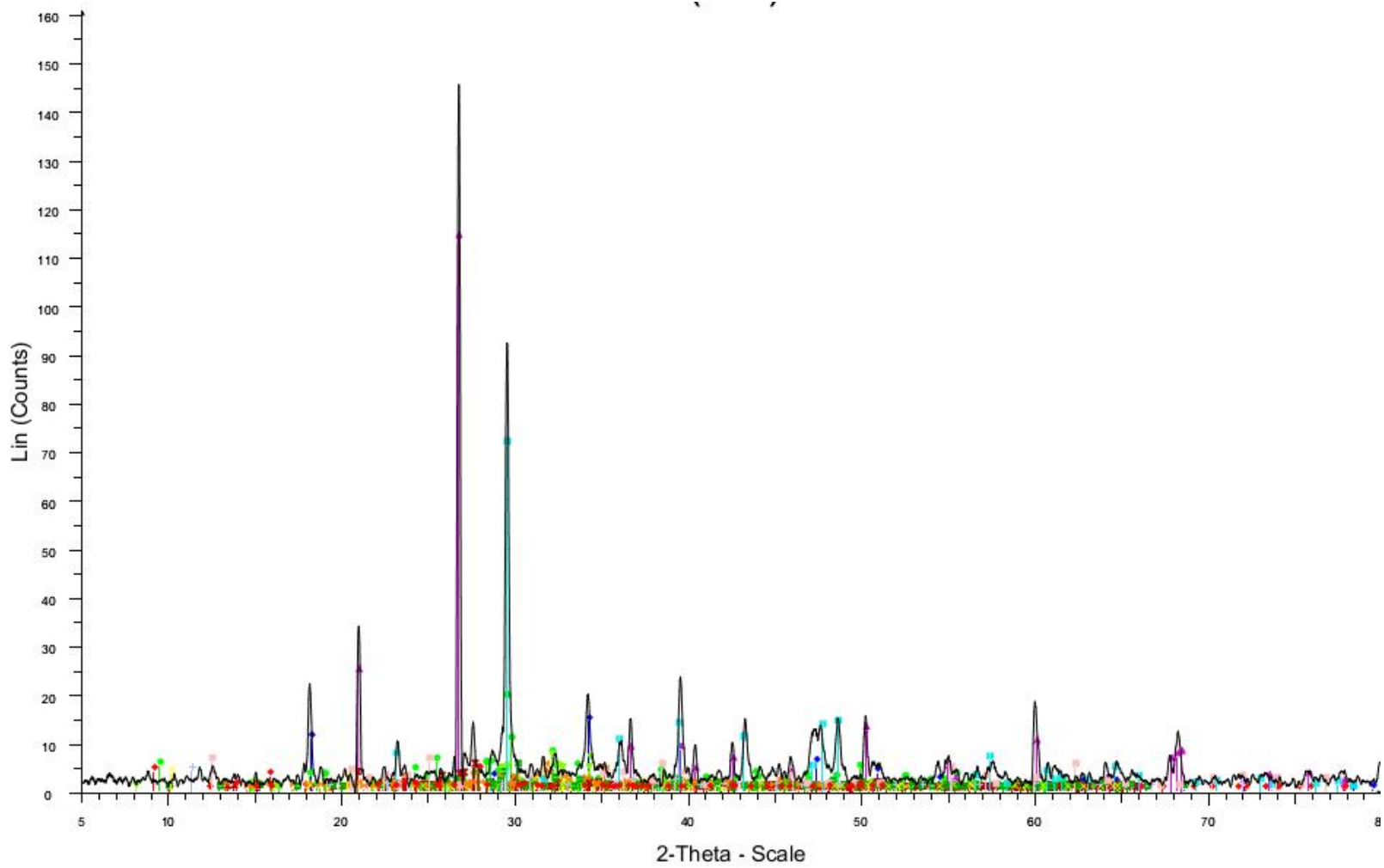


Figure 11: XRD result of PC 15cm after extraction in saturated calcium hydroxide

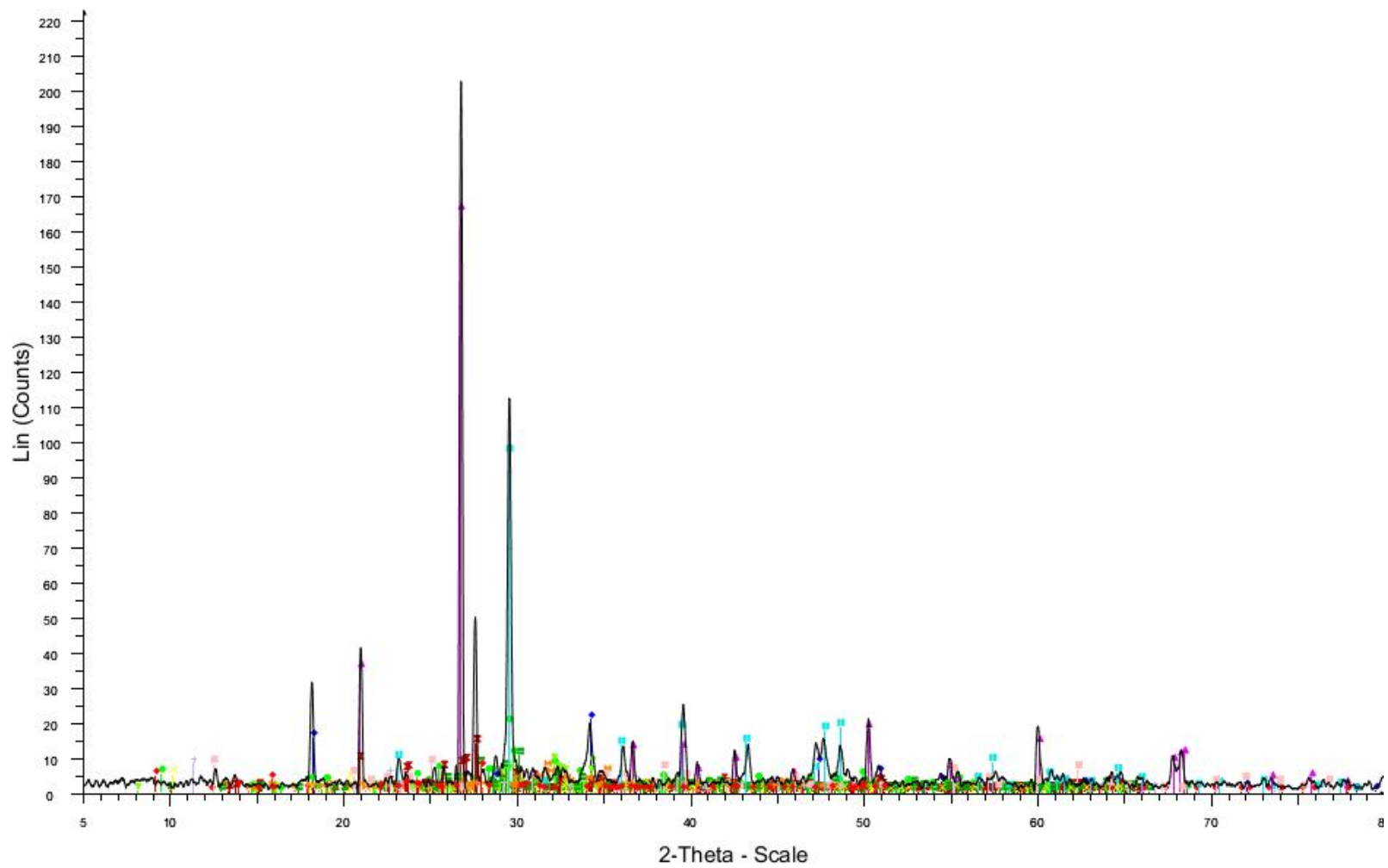


Figure 12: XRD result of PC 15cm after extraction in lithium borated buffer

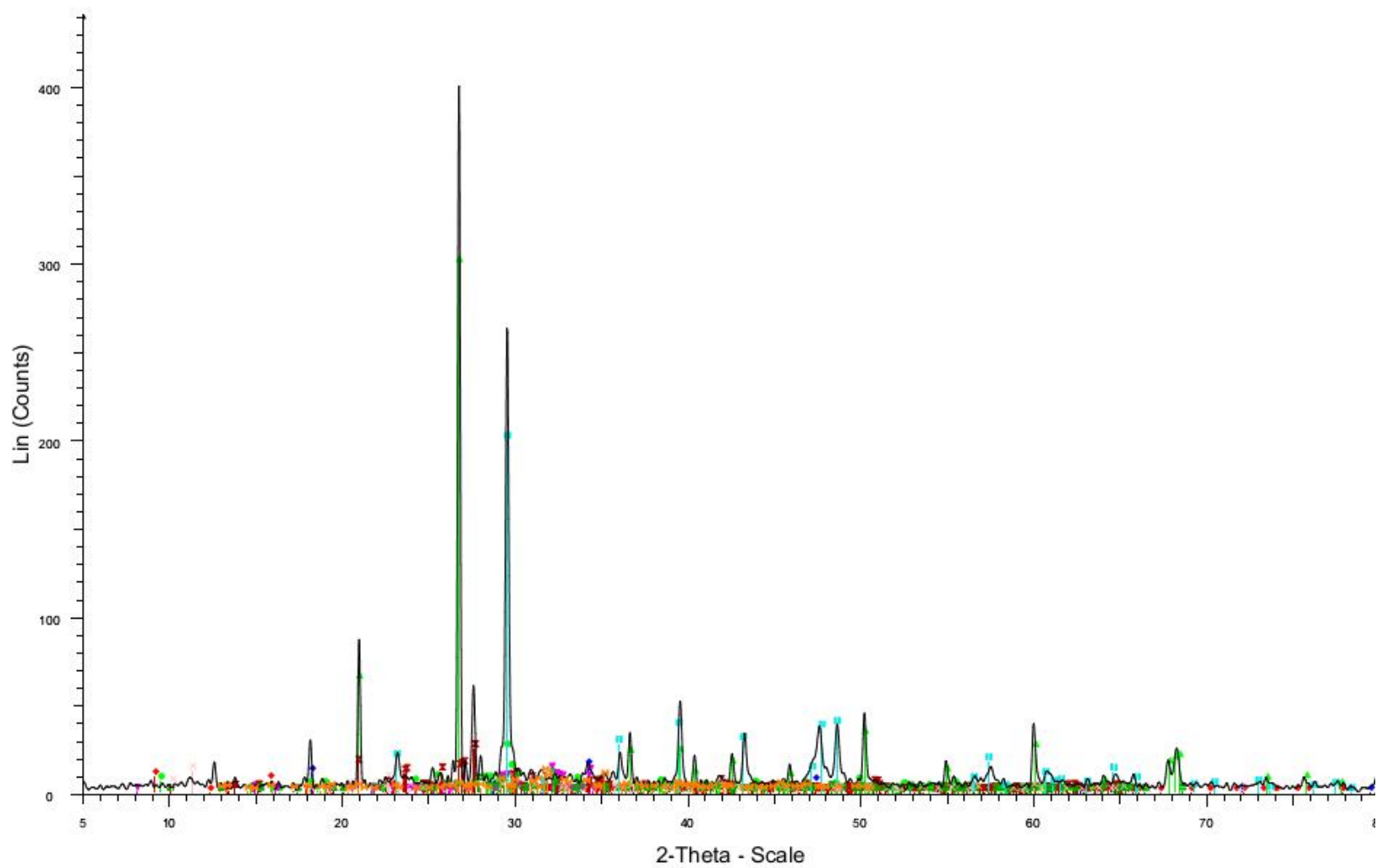


Figure 13: XRD result of FC 15cm before extraction

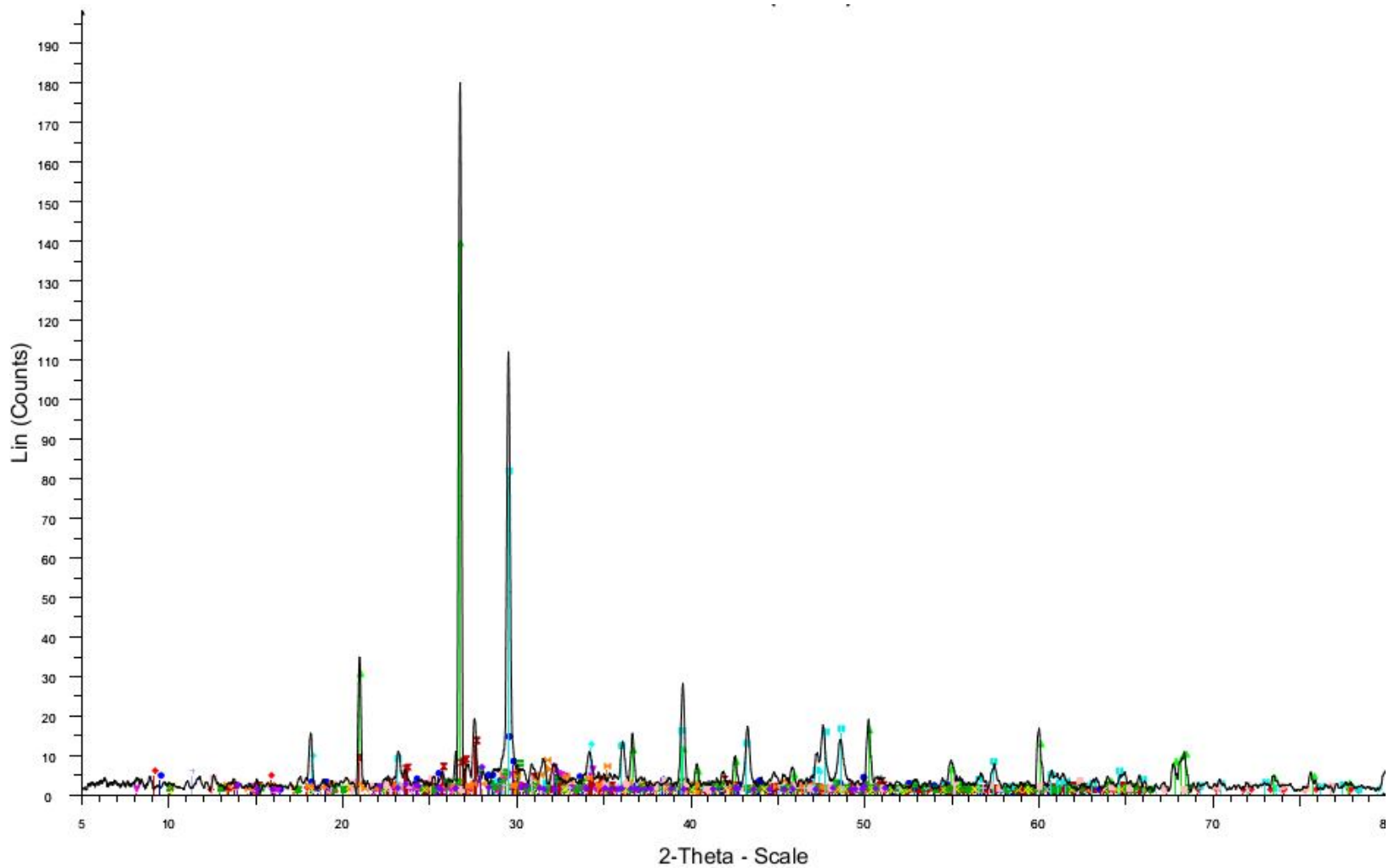


Figure 14: XRD result of FC 15cm after extraction in saturated calcium hydroxide

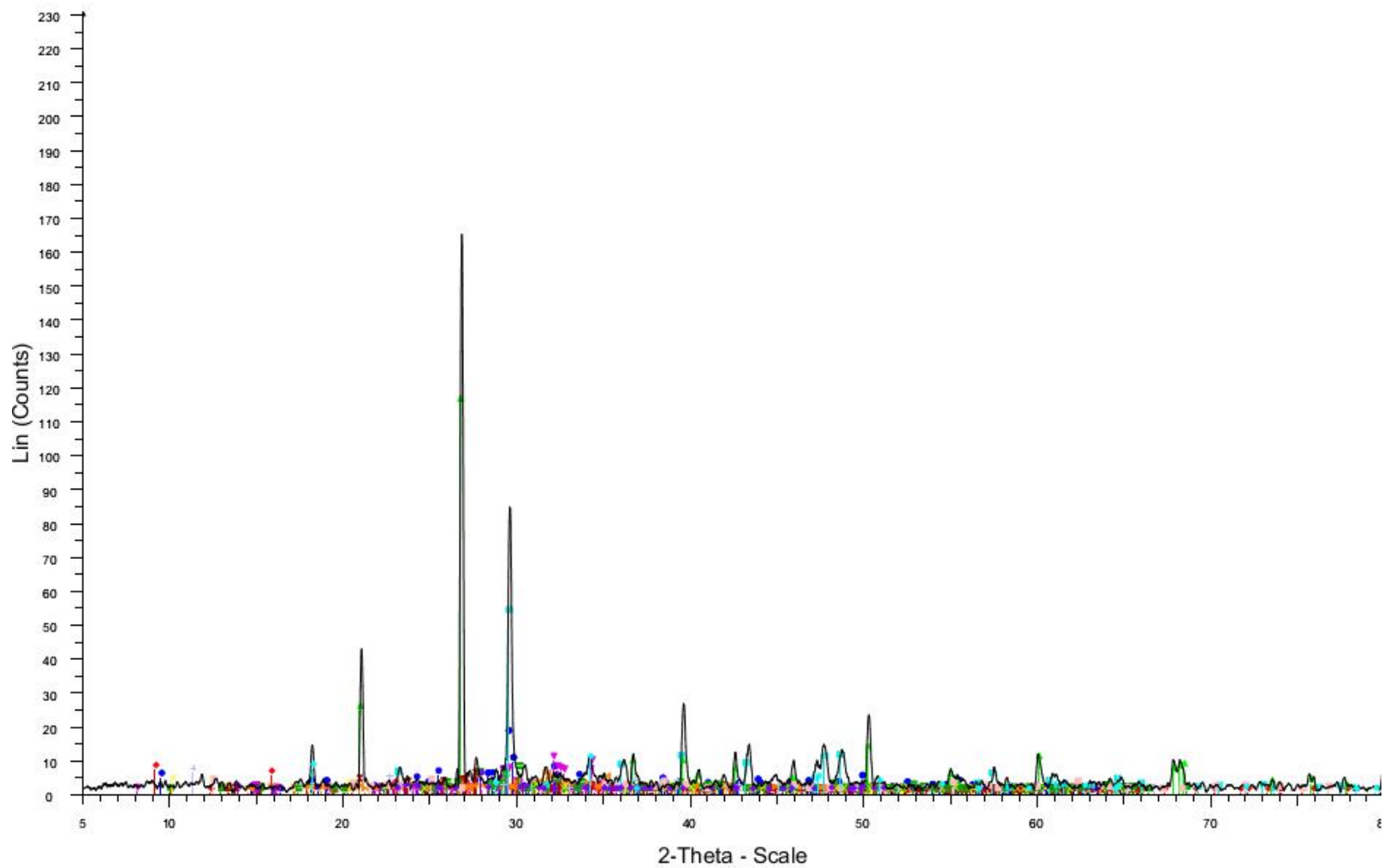


Figure 15: XRD result of FC 15cm after extraction in lithium borate buffer

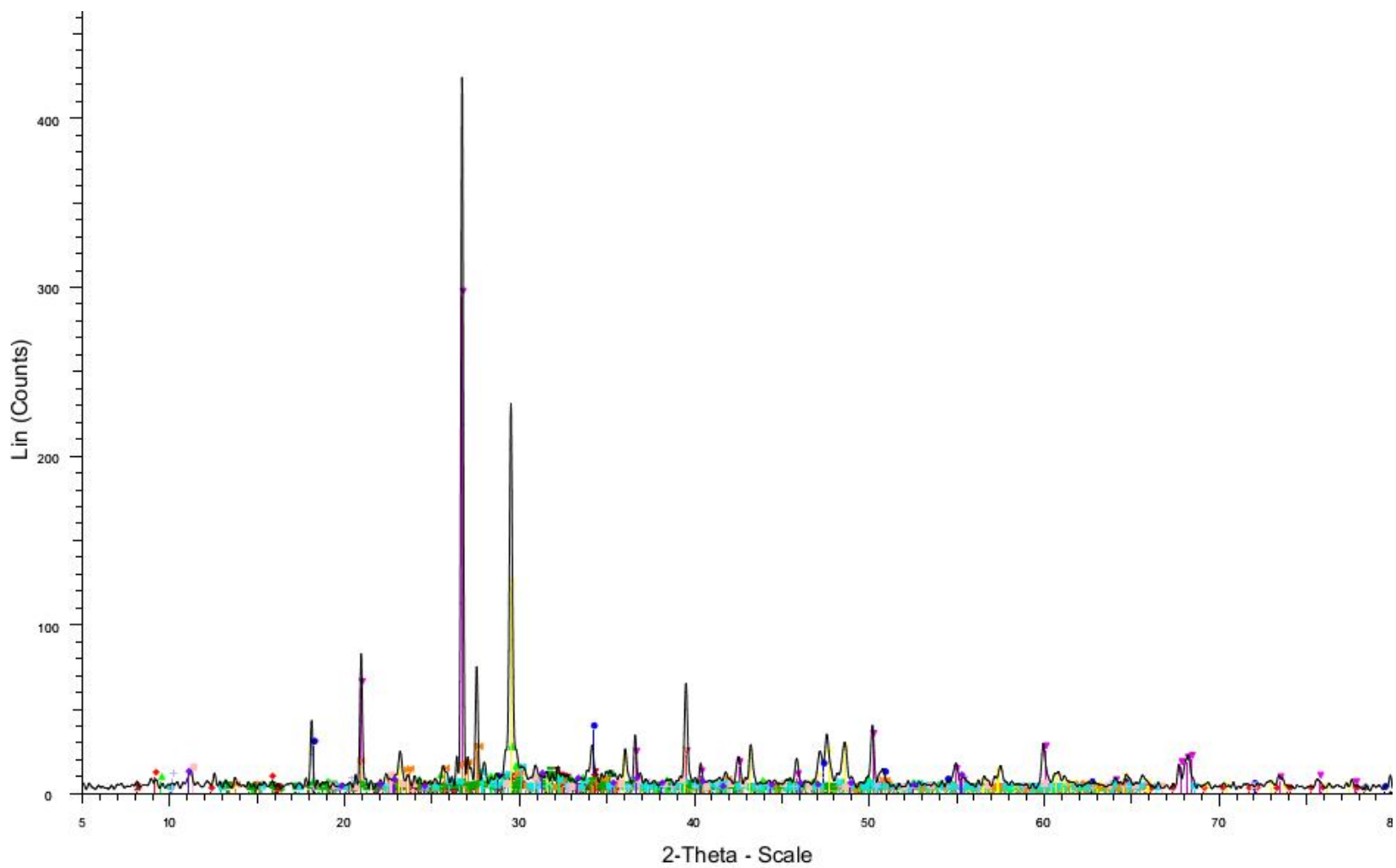


Figure 16: XRD result of LFC 15cm before extraction

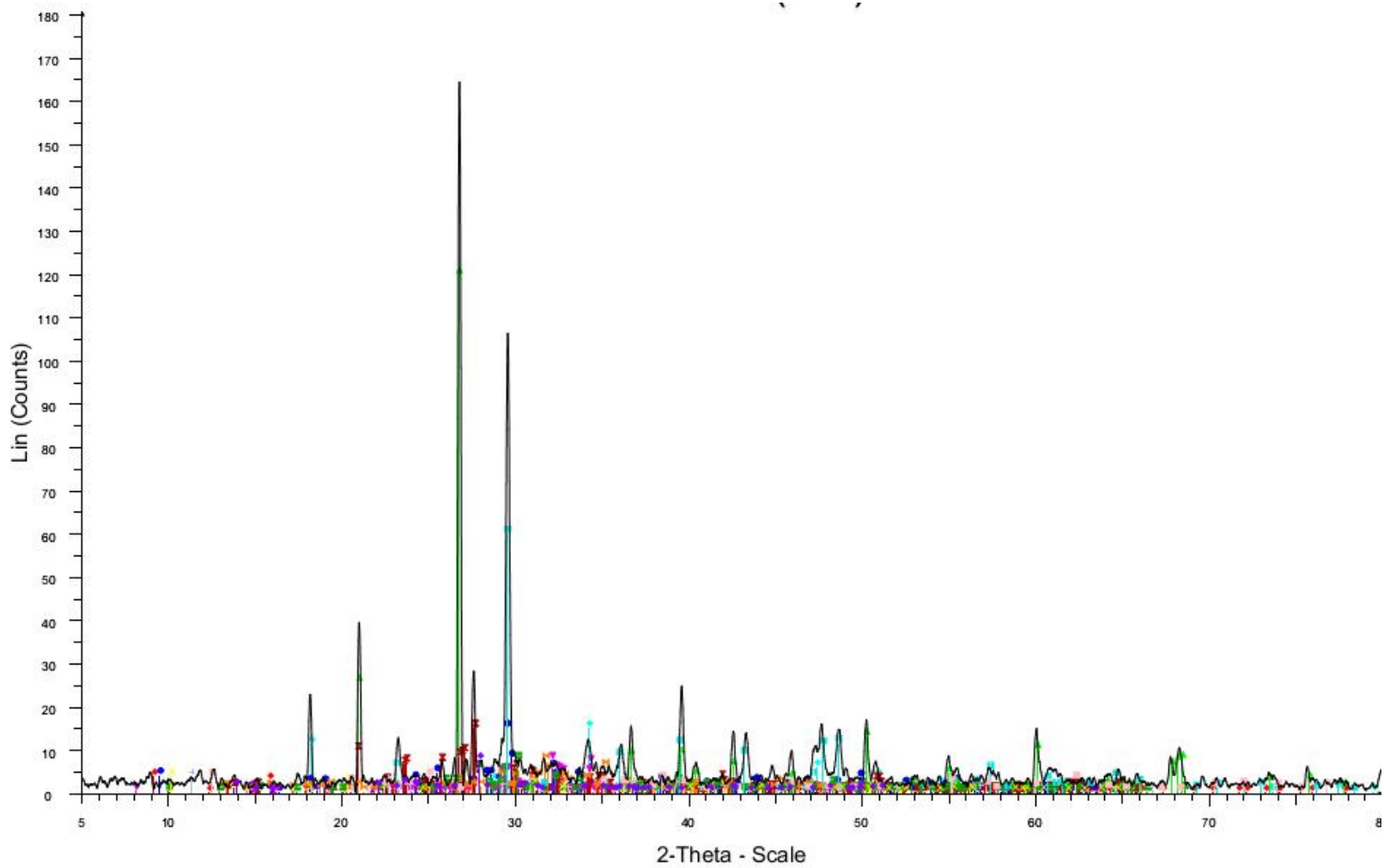


Figure 17: XRD result of LFC 15cm after extraction in saturated calcium hydroxide

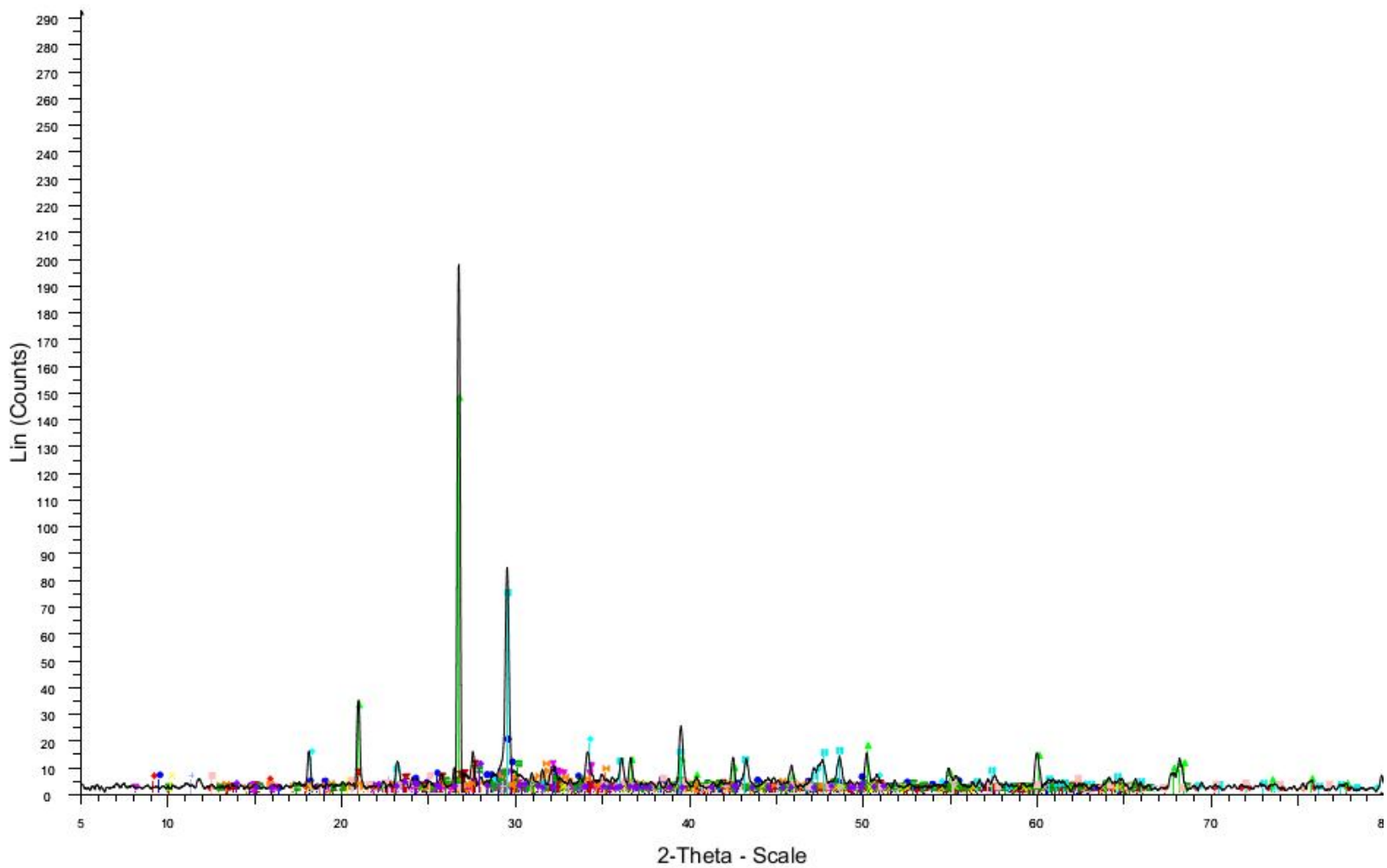


Figure 18: XRD result of LFC 15cm after extraction in lithium borate buffer

BIOGRAPHY

Name: Hai Yen Thi Nguyen

Date of birth: January 10, 1983

Place of birth: Binh Thuan, Vietnam

E-mail: haiyenvl06@gmail.com

| Education: | Year | University | Degree |
|------------|------|------------|------------------------------|
| | 2011 | HCMUT | Bachelor (Civil Engineering) |